Creep Estimation of Gas Turbine Rotor Discs at Different Ambient Conditions

A Thesis submitted
in the partial fulfillment of requirements for the degree of

Master of Technology

By

Ankita Sinha
(Roll No. 2K13/CDN/04)

Under the guidance of

A.K. Agrawal

Department of Mechanical Engineering,

Delhi Technological University

New Delhi-110042, India.

June-2015

Department of Mechanical Engineering
Delhi Technological University
New Delhi-110042
INDIA

CERTIFICATE

It is certified that the work contained in the thesis entitled "**Creep Estimation of Gas Turbine Rotor Discs at Different Ambient Conditions"** submitted by **Miss Ankita Sinha** to the Delhi Technological University for the award of the degree **Master of Technology** in Computational Design**,** has been carried out under my supervision in the Department of Mechanical Engineering, Delhi Technological University and she fulfills the requirement of the regulations of the degree. This work has not been submitted elsewhere for the award of any other degree or diploma.

Dr. A.K. Agrawal

(Supervisor)

Associate Professor

Department of Mechanical Engineering

Delhi Technological University

ACKNOWLEDGEMENT

It gives me immense pleasure to convey my profound sense of gratitude to my supervisor **Dr. A. K. Agrawal,** Department of Mechanical Engineering, DTU, for his continuous guidance, support, motivation and constant encouragement during the project work. I am thankful to him for providing the opportunity to do my project work in **Siemens Ltd**, Gurgaon.

I would like to thank Mr. Prashant kumar, Mr. Manish Kumar Purohit, and all colleagues in Siemens Ltd, Gurgaon, for their guidance and encouragement during the project work. I would like to thank Mr. Sunder Raman Mohan, Head of the Gas Turbine Department, Siemens Ltd, Gurgaon, for providing the opportunity and support during the project work.

I am very pleased to have this opportunity to thank to my family and friends for their guidance, support and encouragement.

Ankita Sinha

Delhi Technological University

ABSTRACT

This paper discusses the usage of several creep models in combination with ANSYS MECHANICAL APDL finite element software and analytical calculations to predict creep strain in terms of axial and radial distortion for the typical gas turbine rotor disc model. Creep analysis of gas turbine disc using different creep models at offset design condition is the main consideration of this work.

For many components of industrial gas turbine, the design for creep is conservative because of close control of dimensions required over the life, the maintenance of critical dimensions, such as clearance between rotating and static parts. Components operate for extensive periods of time under heavy loads in conditions of non-uniform temperature which go up to 535^0C during the process. The stress-strain state also changes over time due to creep phenomena. These conditions make difficult to simulate the actual body by other means like finite element analysis; it is essential to establish creep properties over all ranges of temperatures, stresses and durations of time for the reliable prediction of creep deformation and stress rupture in gas turbine components.

A typical gas turbine disc model is used in this present study to investigate the relationship between operating conditions and design parameters on the creep phenomena. Several ANSYS creep mathematical models are investigated to use for perfect fitting according to the conditions and available data. Time hardening and strain hardening creep model is further studied to analyze the creep of disk. While doing creep analysis, ambient temperature is set to standard 32^0C. But this standard process is not valid for every site of world so a different procedure has been set up to simulate the offset design conditions to capture site specific creep issues. Results show variations in axial and radial creep strain with respect to analysis done at constant average temperature for 160k hours. A good agreement is also found between the results obtained in this current study and the results available in the literature for strain hardening and time hardening model. It is found that stress relaxation after 160K hour using time hardening model is more than using strain hardening. Analysis with offset design condition shows that to capture the clearance correctly and more realistically, offset design condition needs to be simulated. Present work concludes that further study is required in the area of creep mathematical model and validation of simulated results with experimental data.

TABLE OF CONTENTS

LIST OF FIGURES

LIST OF TABLES

Abbreviations

GT	Gas Turbine
T_m	Melting Point of Material
T_{max}	Maximum Service Temp. of Material
ε	Creep Strain
$\dot{\varepsilon}$	Creep Strain Rate
t	Time
ε_{el}	Elastic Strain
T	Temperature in Kelvin
σ	Stress
G	Shear Modulus
k	Boltzmann Constant
GUI	Graphics User Interface
APDL	ANSYS Parametric Design Language
WB	Work Bench

Chapter 1

Introduction

Gas Turbine is an internal combustion rotary engine and it is required to operate under conditions of high temperature and mechanical loading. It consists of three major parts; compressor, combustion chamber and turbine. Ambient air is compressed in compressor and then the engine burns a lean mixture of fuel with compressed air in combustion chamber. The hot pressurized combustion gases expand through a series of rotating turbine wheel and blade assemblies. It results in shaft power output, propulsive thrust or a combination of two. A schematic diagram of gas turbine (fig. 1.1) is shown for the better understanding.

At these conditions, the components undergo various time dependent degradations that result in failure mechanisms such as low/high cycle fatigue, corrosion/oxidation and creep.

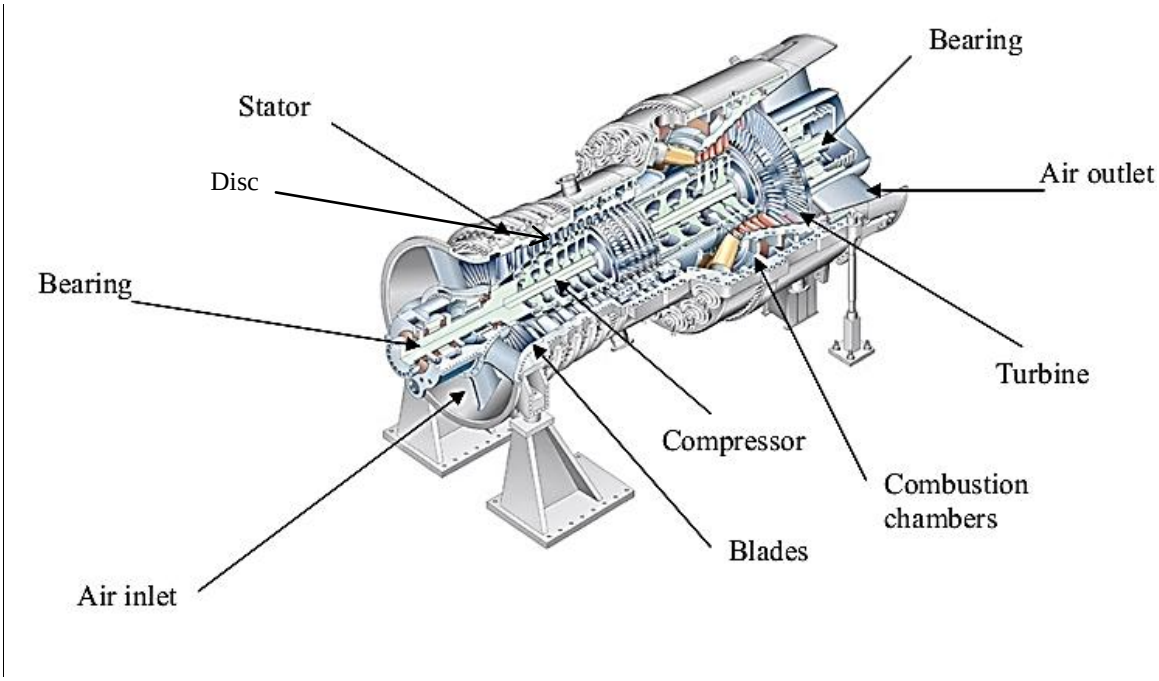

Fig. 1.1- Open Cycle Gas Turbine Schematic

(Source: www.siemensenergy.com)

Gas turbine discs (Fig. 1.2) are one of the most expensive components of the engine. These are incorporated with rotor parts of gas turbine. It consists of two types of disc; one is disc with blades and the other part is disc without blades. Main function of the disc is to accommodate

turbine blades and transform the energy to the shaft of the engine. To increase the thermal efficiency of gas turbine engines, there is an increase in operational temperature. Since discs work in the hot sections of the engine and heavily loaded due to mechanical and thermal loads, sudden failure can leads to a catastrophic damage to the entire engine. Hence, turbine discs are considered as most critical components of the engine.

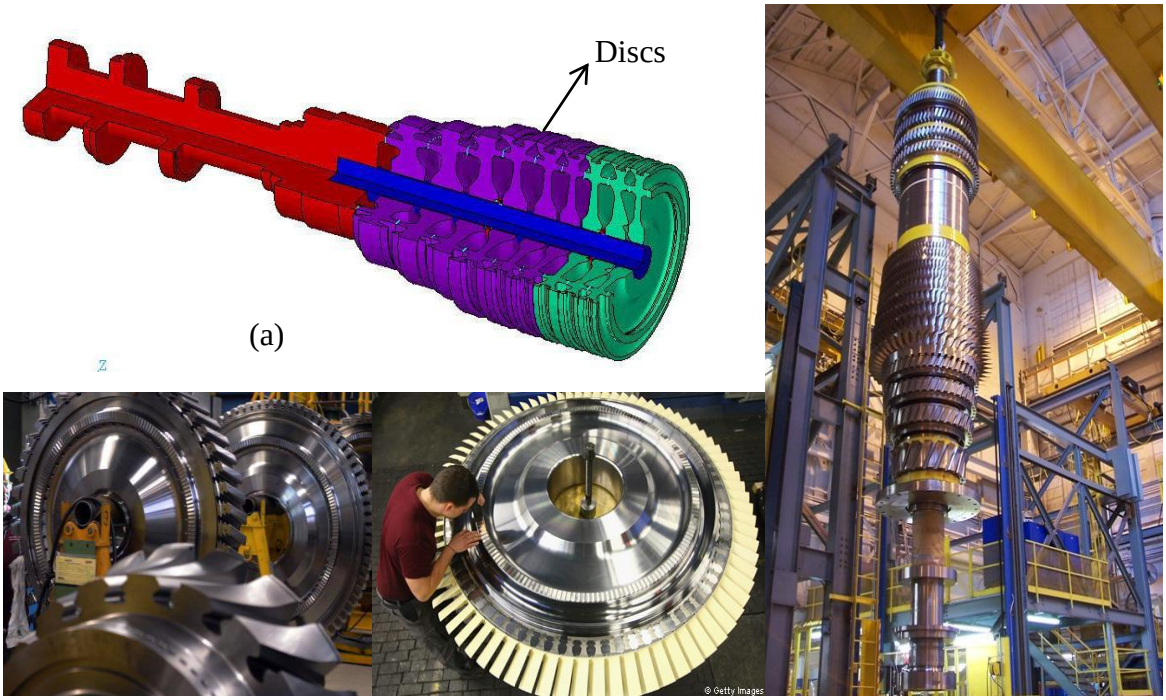

(a) (b) (c) (d)

Fig.1. 1- (a) Rotor cross-section gas turbine; (b) gas turbine disc; (c) Gas turbine disc with blades; (d) Assembled rotor gas turbine in vertical position

Metals subjected to a constant load at elevated temperatures will undergo 'creep', a time dependent increase in length. The terms 'high' and 'low' temperature in this context are to the absolute melting temperature of the metal. Since the development of the gas turbine in the 1940's successive designs have pushed this temperature up to typically 1300^0C. This will cause the disc Operating temperatures in applications like power plant, chemical plant and oil refineries sometimes exceeded 535^0C. Ni-based and Cr-based superalloys are the materials used for

applications at high temperatures such as in the manufacturing of hot gas path rotating turbine component. Developments in high temperature alloys with improved high temperature strength and oxidation resistance has to keep improving with these demands because applications like industrial turbines present greater problems.

Creep is the continuous accumulation of deformations and hence significantly reduces the component life of gas turbines. Most of the creep phenomena is irreversible, under constant loads at elevated temperatures maintained over a period of time, is a life limiting criterion for the design of the turbine discs. Creep resistance is one of the many requirements that must be met by the gas turbine components subjected to elevated temperatures. Precise information on the deformation is, therefore, required for the analysis and design of gas turbine components particularly the turbine discs and blades.

The creep life of a gas turbine depends on the design of the hot section components, duty cycle and the environment in which it operates. The design parameters of the hot section components are determined by both aerodynamic and structural characteristics. Keeping in mind to the possible interaction between these parameters and the intended operating conditions, it is necessary to consider the effect of creep on the life of the hot section components at the design stage.

The turbine disc operates for extensive periods of time under heavy loads in conditions of non-uniform heating. The disc stress strain state changes over time due to the creep phenomenon. It is essential to use correct mathematical models and nonlinear material properties for the reliable prediction of creep deformation and stress rupture in turbine components. A better understanding of the failure mechanisms will help designers in the trade-off between different design options and will also help operators to make informed maintenance decisions.

1.1 Problem Definition

In power-generation engine like gas turbine, the cycle is simpler with long periods of running at constant conditions between start and stop. At each segment of the cycle, the engine will run at high load in terms of mechanical (blade pull pre tension, speed etc.) and thermal load. For hot ambient condition gas turbine operations, creep deformation is one of the prime criteria for component design. For each set of conditions, a thermal analysis needs to be carried out, and the

results, together with nonlinear material properties data, will be used to for structural analysis of the component.

Although, creep calculation at different stresses, which generates because of rotational speed have been used since long before. Here, in literature not much study seems to have been carried out at different ambient temperature condition rather than at constant ambient temperature. In this present work the impact of different operating ambient conditions on creep life are investigated. The creep mathematical models are also investigated for better analysis.

This theses work has been carried out in ***Siemens Ltd***, Gurgaon. The organization is producing large gas turbines for power generation.

So, the aim of the present work is:

1. To find out a suitable ANSYS *creep mathematical model* coefficients from experimental data and analytical calculations.

2. To estimate creep strain of siemens gas turbine rotor disc at various ambient & operational offset temperature condition with different *creep mathematical models* using finite element software ANSYS'15.

3. Simulation of creep strain at variable ambient & operational offset temperature condition with strain hardening and time hardening *creep mathematical models* of siemens gas turbine rotor disc and comparison with the existing siemens methodology.

1.2 Methodology

In order to meet the objectives outlined in the proposed work, the following methodologies have been adopted.

1. First, on the basis of literature survey, a method to find coefficients of *creep mathematical model* from experimental data has been analyzed. These coefficients are calculated from the regression analysis in creep material curve fitting which is already

incorporated in the software used ANSYS'15. Analytical method is also used to calculate creep coefficients for other mathematical model.

2. The final one mathematical model named time hardening has been taken to solve benchmarking problems first. For this, one bar problem is taken and analyzed at different boundary conditions for basic understanding.

3. Finally, siemens gas turbine rotor disc of high alloy steel has been taken to analyze creep failure. Since a typical disc model has been taken in this study, as many as possible coefficients of *creep mathematical model* at various temperatures needed to obtain a better result. For this, a new data of coefficients for high alloy steel has been taken from ***Siemens Ltd.*** for a long range of temperatures.

4. Coefficient taken from the company is for "time hardening creep mathematical model". So, analytical calculations have been done for the coefficients of strain hardening mathematical model.

5. For the initial understanding, a constant average ambient temperature is assumed in analysis. The required numerical computations are done for stresses and creep response of the rotating disc.

6. In order to meet the objective of proposed work, offset temperature design condition is taken to analyze creep strain at variable ambient temperature. For this, a temperature data is taken from the web source in the analysis. **ANSYS'15** APDL coding will also be used in this work. The results obtained have been analyzed to draw salient conclusions.

Chapter 2

Literature Review

Creep is the progressive time-dependent inelastic deformation under load and temperature. Due to creep, a structural component undergoes time-dependent changes in the state of stress and strain such as progressive deformations, relaxation and redistribution of stresses, local reduction of material strength, change of material behavior from isotropic to anisotropic *etc*. Creep behavior also includes the phenomenon of relaxation, which is the reduction of stress in a structure with time while the total strain remains constant. Further, it also includes recovery, which is characterized by the reduction of inelastic strain with time after the stress has been removed. Ashby [1] and Frost [2], 1975 developed a convenient summary of the various active creep mechanisms as a function of stress and temperature in the form of deformation maps shown in Fig. 3.6. The deformation maps depend also on the microstructure of material. *Kraus, 1980* [3] pointed out that the creep behavior is a function of stress, temperature, time, stress history, temperature history and type of material.

To analyze creep in engineering structures and components, mathematical models of creep are needed. For this purpose, the data obtained from the tensile tests serve as the main source of information about creep. The very popular mathematical model used in creep calculation is Bailey-Norton's law. In its simplest form, a creep-hardening rule might be looked upon as a method of moving between constant stress and temperature creep curves as the stress and temperature change.

Two different hardening rules have been used with classical creep models: time hardening and strain hardening. When the creep rate equations are integrated for conditions of constant stress and temperature, both the hardening rules produce identical results, namely the uniaxial creep curve for that stress and temperature.

According to Rabotnov (1969), though both the laws are derived from the same equation, but it is observed that for varying stress, the time and strain hardening laws give different creep rates. Quite often the strain hardening models give more accurate predictions of experimental results for stepwise changes of stress. Unfortunately, strain hardening models do not always yield accurate predictions, particularly when several step changes in stress occur during the same test.

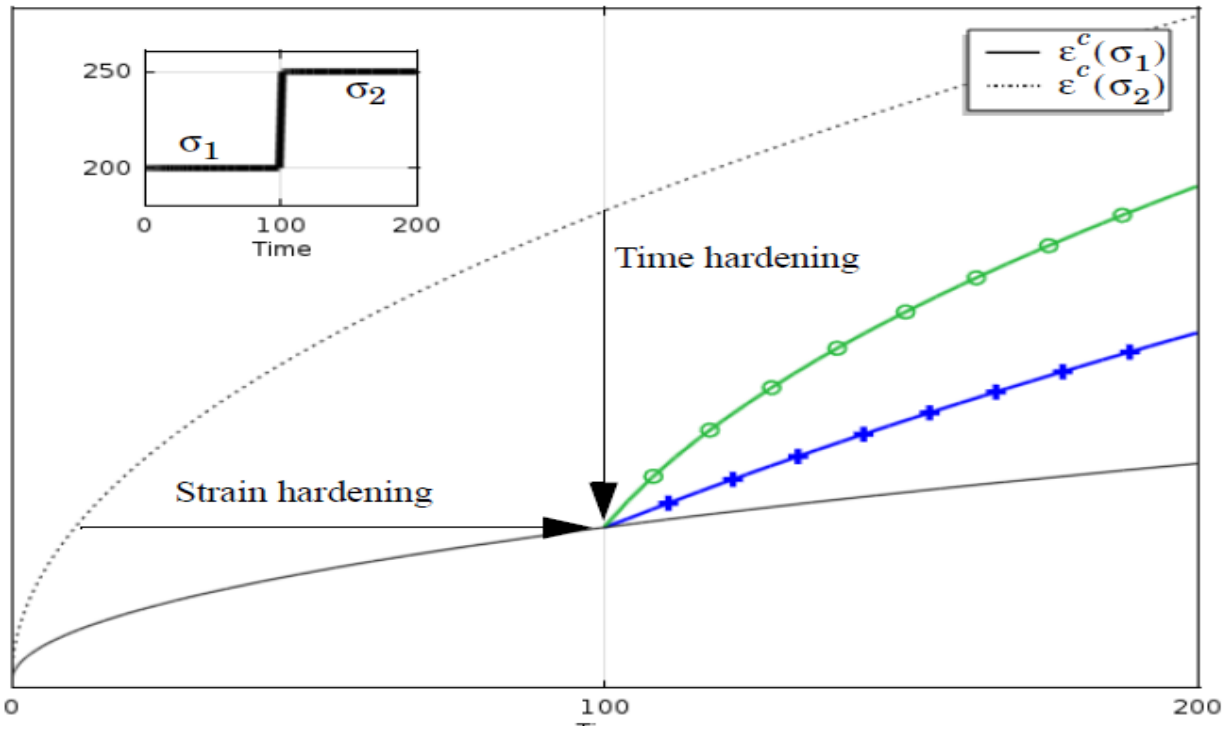

Fig. 2.1- Time hardening and strain hardening creep behavior with time

(Source: https://www.comsol.co.in/model/download/230301/models.nsm.variable_load_creep.pdf)

The time hardening formulation is easier to use, while the strain hardening is usually considered to be more accurate.

Pickel *et al* (1971) also noticed that the strain hardening model is unable to accurately predict the creep behavior resulting from structural instabilities. But for structurally stable materials, the predictions by strain hardening model are fairly reliable. However, in the case of gradually varying stress, both the laws give approximately similar predictions.

2.1 Literature Review on Rotating Disc

Rotating disc provides an area of research and studies due to their vast utilization in rotating machinery *viz.* steam and gas turbine rotors, turbo generators, pumps, compressors, flywheels, automotive braking systems, ship propellers and computer disc drives (Gupta *et al*, 2005; You *et al*, 2007; Hojjati and Hassani, 2008). In most of these applications, the disc has to operate at elevated temperature and is simultaneously subjected to high stresses originating due to disc

rotation at high speed (Farshi and Bidabadi, 2008). As a result of severe mechanical and thermal loadings, the material of the disc undergoes appreciable creep deformations, thereby affecting its performance (Laskaj *et al*, 1999; Farshi *et al*, 2004; Gupta *et al*, 2005). For example, in turbine rotor there is always a possibility that heat from the external surface is transmitted to the shaft and then to the bearings, which may adversely affect the functioning and efficiency of the rotor (Bayat *et al*, 2008).

Analysis pertaining to estimation of stresses and strain rates in thin rotating disc can be found in most of the standard text books and literature (Malkin, 1934; Finnie and Heller, 1959; Lubhan and Felger, 1961; Odqvist, 1974; Findely *et al*, 1976; Kraus, 1980; Boyle and Spence, 1983; Skrzypek and Hetnarski, 1993; Nabarro and Villiers, 1995; Penny and Mariott, 1995).

Wahl (1956) derived some formulas for calculating stress distributions in rotating discs having constant and variable thickness, undergoing steady-state creep at elevated temperature. The formulas were based on the Tresca's yield criterion and the associated flow rule and give reasonable results when compared with the available experimental data (Wahl *et al,* 1954)**.** Wahl (1957) utilized the formulas derived in their previous work (Wahl *et al*, 1954) to construct the design charts of stress distribution in constant thickness discs, undergoing steady state creep, for different values of stress exponent (*n*) and diameter ratios. In all the cases, the discs were subjected to a radial peripheral load to simulate the effect of blade loading. The steady state creep rate was expressed as a product of power function of stress multiplied by a function of time.

Bhatnagar *et al* (1986) carried out analysis of steady state creep in rotating discs. The creep stresses and strains were obtained for different cases by using Norton's power law creep model.
Singh (2000) investigated the effect of operating temperature on the steady state creep behavior of a rotating disc. It has assumed creep according to Norton's law. The creep parameters appearing in the creep law were extracted from the available experimental creep results reported by Pandey *et al* (1992).
Jahed and Bidabadi (2003) presented a method to analyze primary and secondary creep in axisymmetric rotating discs subjected to different types of loading, such as internal and external pressure, centrifugal loading and temperature gradient. Primary and secondary creep was

predicted and the results obtained were compared with those estimated by FEM technique. In all the cases, a good agreement is observed.

Gupta *et al* (2004) also made similar observations, however they used Sherby's law to describe the steady state creep behavior of the disc material.

Muhammad Naeem (2008) shows that under various operating condition, creep life consumption will be more. Because of significant variation of day temperature it causes deterioration of rotor disc and thus higher engine's life cycle cost.

Singh and Rattan (2010) analyzed steady state creep in a rotating disc by using isotropic Hoffman yield criterion. The results obtained were compared with those using von Mises yield criterion. It is observed that the distribution of stress in the disc is not too much affected in the presence of phase specific thermal residual stress. The presence of residual stress leads to increase the tangential strain rate, particularly in the region near the outer radius of the disc as compared to that observed in a similar disc but without residual stress.

Boris Vasilyev (2012) presented a method for obtaining creep information at all ranges of stress and temperatures using a limited amount of experimental data by using user defined creep model in ANSYS. He has also used modified time hardening creep model to analyze creep strain of turbine blades. To generalize from uniaxial to multiaxial creep data where multiaxial data do not exist, the author has used effective (Von Mises) stress.

Hosseini Kordkheili, Livani (2013) has taken the thermal and structural properties of the base metal as a function of temperature. It is noted that ignoring the temperature dependency of these properties caused up to 200% errors in the creep solution results. Also, results for the strain rates presented due to centrifugal force and thermal loadings for different disc cross section profiles as well as different boundary conditions. Results obtained within this solution are verified with those available in the literature for easier cases.

Raghavendra, Gurudath, Mallikarjunayya and Chandrashekhar (2014) have concluded that the process of evaluating the life of the aero gas turbine disc would be an underestimation, if the creep properties are ignored. He has evaluated material constants required for time hardening model using Larsen miller parameter (LMP) data for different values of accumulation of creep strain in the disc.

Chapter 3

Creep and Classification of Creep Models

3.1 Introduction and Definition of Creep

Creep is the occurrence of time dependent strain in material under constant stress, normally at elevated temperature. Creep occurs as a result of the competing processes of work hardening caused by the applied force (tensile or compressive stress) and of annealing due to high temperature. Creep usually attributed to vacancy migration in grains of bulk materials or along the grain boundaries in direction of applied stresses, (Nabarro-Herring, and Coble mechanisms), and causing grain boundary sliding and separation, and dislocation climb and cross-slip.

Creep deformation also continues until the material fails because of creep rupture. Creep occurs usually at high temperatures typically at 40-50% of the melting point of the material (T_m) in Kelvin. In crystalline materials the activation energy Q is approximately equal to the activation energy of the self-diffusion of the material. Diffusion of atoms and vacancies at grain boundaries and in grains in direction of applied tensile stress result in an elongation and in a decrease in cross section of materials in a creep experiment. Besides, since enthalpy of vacancy formation is correlated with the binding forces in the material and thus with the melting temperature, then the homologous temperature (T/T_m) is used as a parameter to characterize the creep properties.

High temperature materials have a large value of binding energy and so they need a large amount of energy to create and move vacancies. A general rule is the maximum service temperature of mechanically highly stressed materials with $T/T_m=0.5$. Approximate maximum service temperature T_{max} of several materials compared to their pure melting points Tm are given in Table 1. Exceptions to the rule are Ni-based super-alloys with higher service temperatures used in aero engines and industrial gas turbine.

Table 1: Approximate maximum service temperature T_{max} of several materials under high mechanical stresses compared to their pure melting points T_m

Material	T_m[K]	T_{max} [K]	T_{max}/T_m
Al-alloys	933	450	0.48
Mg-alloys	923	450	0.49
Ferritic steels	1811	875	0.48
Ti-alloys	1943	875	0.45
Al_2O_3	2323	1200	0.52
SiC	3110	1650	0.53
Ni-based superalloys	2304	1728	0.75

Creep tests are usually made by deformation of material as a function of time when material is under constant or variable stresses at a constant elevated temperature.
The standard practice for creep experiments of metallic materials is specified in ASTME 139, and the test may proceed for a fixed time and to a specified strain.

It is usually not practical to conduct full-life creep tests, because such a test takes a long time.

3.2 Creep Curve

The basic record of creep behavior is a plot of strain (ε) versus time (t). It is often useful to differentiate this data numerically to estimate the creep rate ($d\varepsilon/dt$) vs. time (t). The shape of the creep curve is determined by several competing mechanisms, including:-

1. **Strain Hardening:** With increasing strain, creep rate gradually decreases. This hardening transient is called "**primary creep**". Then the creep rate reaches a nearly constant value

known as the steady state creep rate or minimum creep rate ($\dot{\varepsilon}$). This value is usually used to characterize the creep resistance of materials and to identify the controlling mechanisms of the creep.

1. **Softening process:** While strain hardening decreases the creep rate the softening process increases the creep rate. So the balance between these factors and the damaging process determines the shape of the creep curves and results in a constantly increasing creep rate known as "secondary creep". This process includes processes like recovery, re-crystallization, strain softening and precipitate over-aging (in precipitation hardened materials). The extension of the steady state part (secondary creep) is material dependent. This part is longer for solid solution alloys and shorter in particle strengthening alloys.

2. **Damaging Processes:** As strain continues, micro-structural damages continue to accumulate and the creep rate continues to increase. This final stage, or "tertiary creep", results in final failure of the material (gradual or abrupt rupture of the specimen). This process includes cavitations (such as voids at grain boundaries), necking of the specimen and cracks in grains and grain boundaries.

Therefore, every creep curve is comprised of three different parts. These three parts with their stress and temperature dependencies are given in the following figure. Studying three parts of creep curve helps in understanding the whole process.

As the creep deformation begins to proceed in time, by applying a constant stress, the number of dislocations in material increases and the material get harder (hardening process).

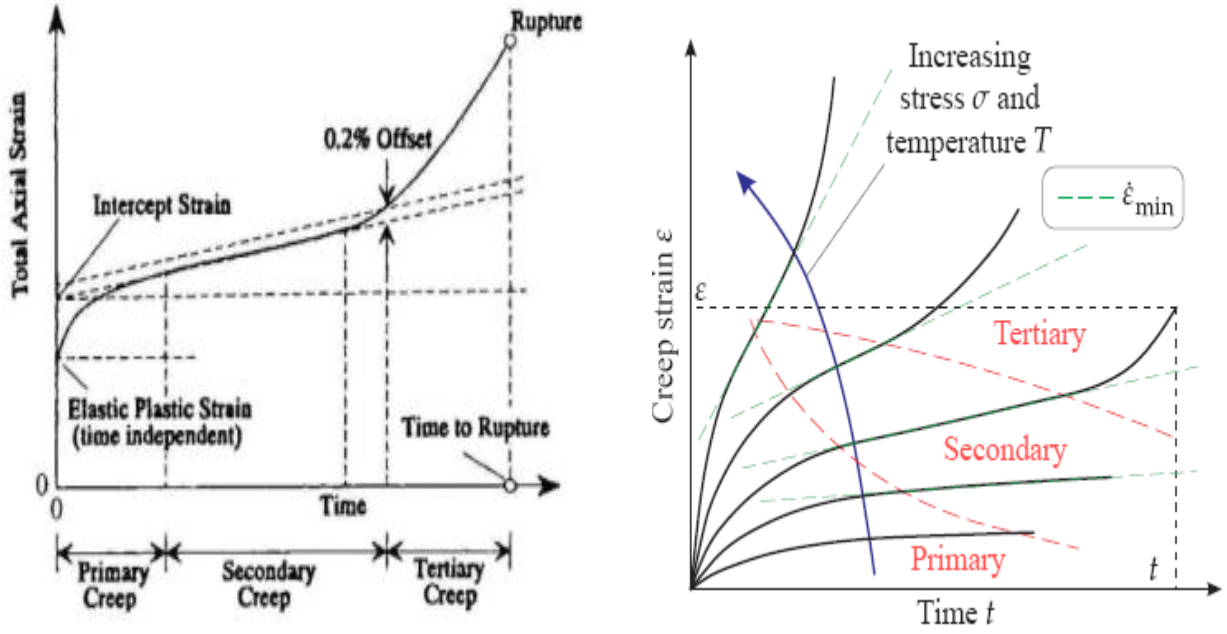

Fig. 3.1: Illustration of a typical creep curve showing three common regions of creep curve (left) and their stress and temperature dependencies (right) [24]

The increase of the dislocation density has a limit; as the result of keeping the material at an elevated temperature, the dislocations can change their places (by climbing) and re-arrange themselves in an energetically more favorable configuration or condition, called recovery. In other words, there is a competition between additional generation of dislocations (as the result of plastic deformation), and cancellation in the recovery process. Therefore, the creep rate becomes nearly constant as a result of such equilibrium and so the secondary part is built. In this part of the curve, local stress concentrations at grain boundaries help the formation of cavitations and pores.

In tertiary creep, the creep rate increases again as a result of massive structural damages. At high stresses, the material fails due to formation of micro-cracks and cavitations at grain boundaries or because of inter-crystalline fractures.

The secondary and tertiary parts of the creep curve are accompanied by a morphological change in materials. This morphological change starts from voids formation in the secondary parts; the aggregation of voids results in micro-cracks formation, which leads to complete rupture and fracture. Figure 3.2 shows these morphological changes for a steam generator schematically.

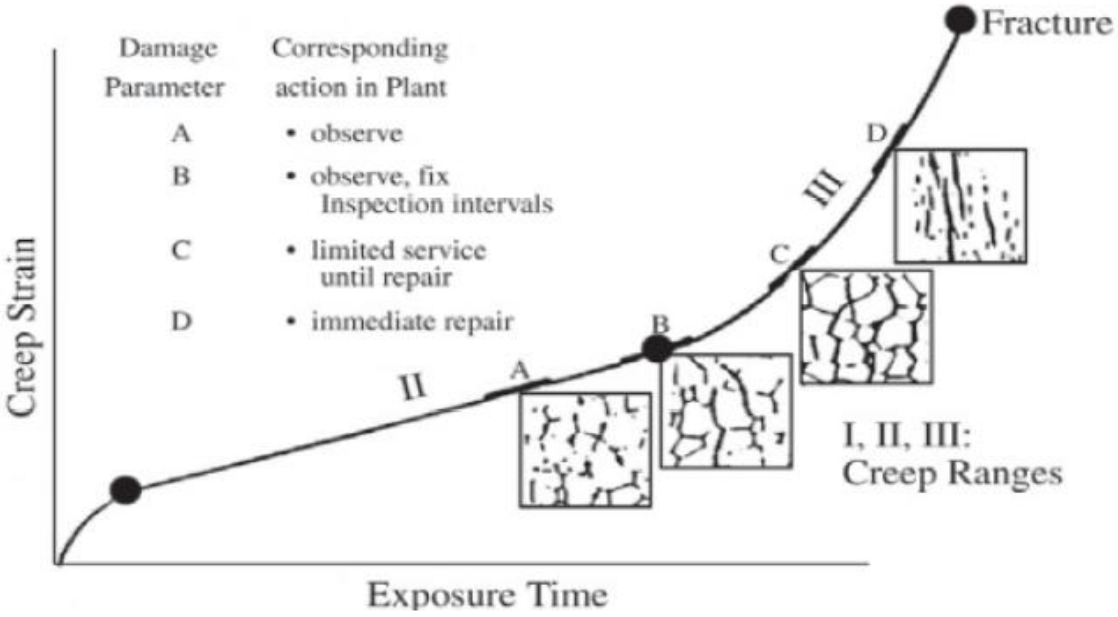

Fig. 3.2: Creep life assessment based on classification of creep damage from metallurgical point of view, formation of cavities at grain boundaries up to final creep fracture [24]

3.3. Comparison of Creep Curve with Cumulative Failure

A typical schematic plot of strain and strain-rate versus time for an ideal material is given in the left side of Figure 3.3. As it can be seen in Figure 3.3, the counterpart of creep strain versus time is the cumulative failures versus time in reliability. Besides, the counterpart of the strain-rate versus time in creep is the failure rate percentage versus time (Bath-tub curve) in reliability. Therefore, a cumulative degradation process can represent the creep experiment in time.

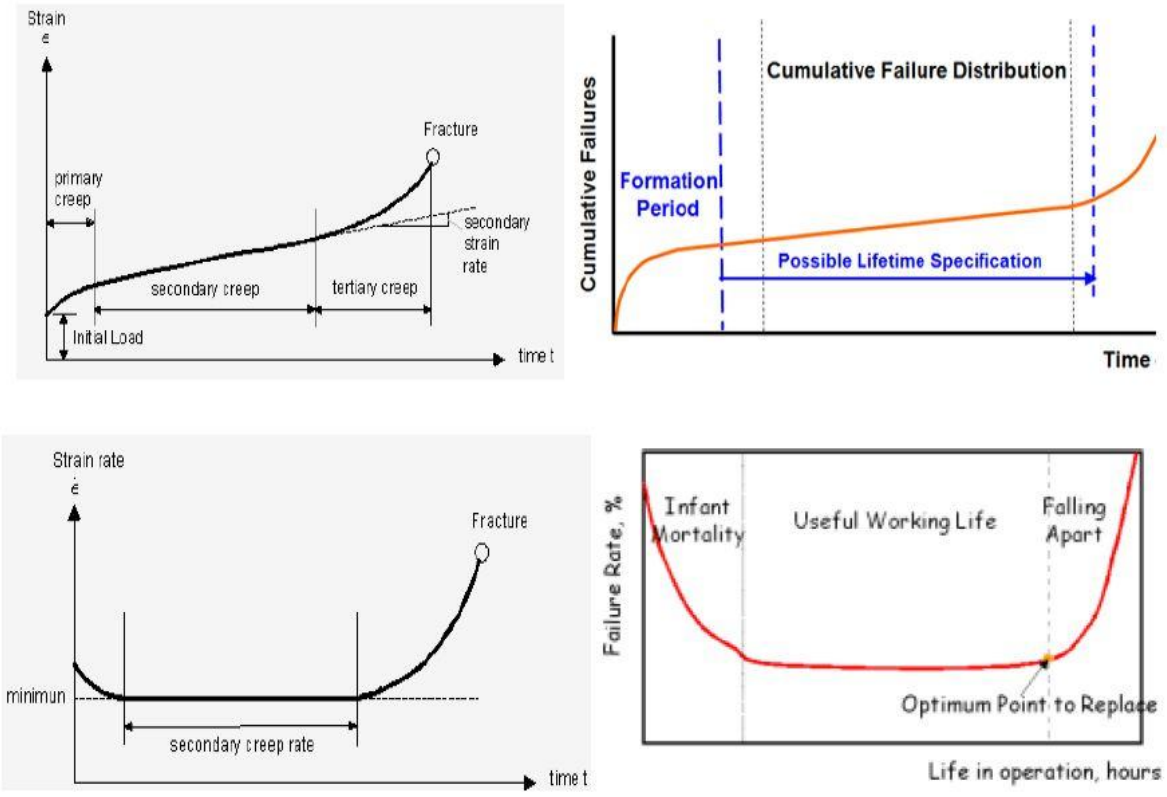

Fig. 3.3: Strain and strain-rate versus time of a typical creep experiment (left hand) compared with the cumulative failures and failure rate in percent versus time in reliability (right hand) [24, 28].

In the primary (transient) part of creep curve, strain (cumulative failure in reliability) increases, while the strain rate (failure rate) decreases continuously. In the secondary part, the strain increases nearly with a constant rate; this is also called the steady state creep, which can be compared with the constant failure rate part in reliability bathtub curve. In tertiary part, the creep rate strongly increases until the final fracture happens. This part is accompanied by a massive inter-structural damage of the material (comparable with the wear out of bathtub curve).

3.4. Creep Mechanisms in Metals

The response of a metallic body to mechanical stress σ below the yield stress of the metal results in an instantaneous elastic strain ε_{el}. The yield stress cannot be defined as a sharp limit. However, it can be stated that applied stress above the yield stress causes immediate plastic deformation. Creep in metals, i.e. the time-dependent plastic deformation of metals may occur at mechanical stress well below the yield stress. The creep strain rate $\dot{\varepsilon}$ is described and calculated as a function of temperature T, stress σ, structural parameters S_i (such as dislocation density and grain size) and material parameters M_j (such as diffusion constants or the atomic volume).

$$\dot{\varepsilon_t} = (T, \sigma, t, S_i , M_j)$$

There are three basic mechanisms that play significant role in both creep process and time-depending plastic deformation characterization; these three mechanisms are:

- Dislocation creep –(climb + glides)
- Diffusion creep: Nabarro Herring (volume diffusion- : interstitial and vacancy-diffusion)
- Diffusion creep: Coble (grain boundary diffusion

3.4.1. Dislocation Creep – (Climbs + Glides)

High stress below the yield stress causes creep by motion of dislocations, i.e. glide of dislocations. This motion of dislocations is hindered by the crystal structure itself (i.e. the crystal resistance). Further, discrete obstacles like single solute atoms, segregated particles or other dislocations block the motion of gliding dislocations. At high temperatures obstacle blocked dislocations can be released by dislocation climb. The diffusion of vacancies through the lattice or along the dislocation core into or out of the dislocation core drives the dislocation to change its slipping plane and to pass by the obstacle. Atoms diffuse into or out of dislocation core, lead to dislocation climb and dislocation climb-and-glide leads to creep. Dislocation mechanism, optical microscopic and TEM pictures are given in the Figure 3.4.

Dislocation rate of such a mechanism is given by:

$$\dot{\varepsilon_D} = A\frac{DGb}{KT}\left(\frac{\sigma}{G}\right)^n$$

where A is a material parameters, D is the diffusion coefficient, G is shear modulus, b is Burgers vector, σ is the applied stress, n is a material dependent constant, k is the Boltzmann constant, and T is the temperature given in Kelvin.

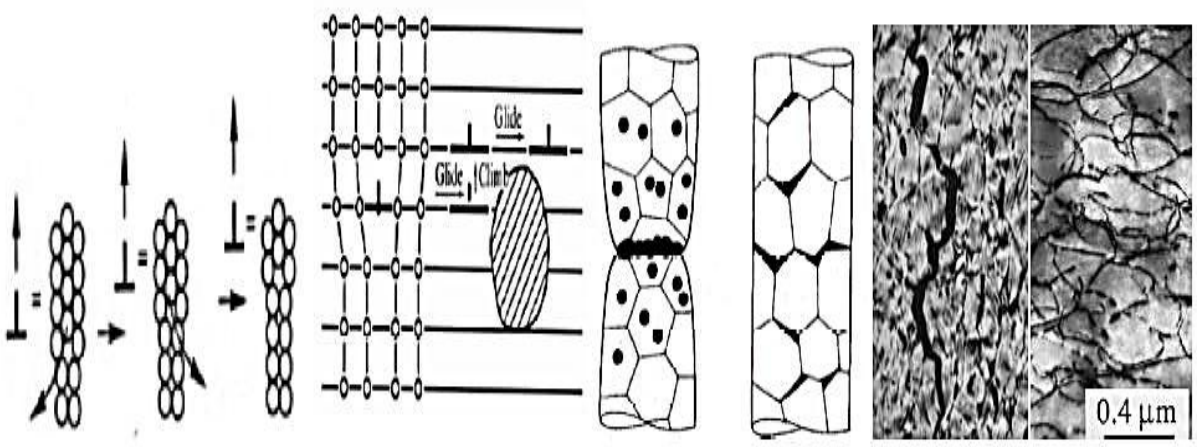

Fig. 3.4: Dislocation creep mechanisms, by vacancy climb and climb and glide over obstacle, optical micrographs showing longitudinal section near the fracture surface, and TEM Picture from dislocations on the fracture surfaces

3.4.2. Diffusion Creep

Diffusion creep is significant at low stress and high temperature. Under the driving force of the applied stress, atoms diffuse from the sides of the grains to the tops and bottoms. The grain becomes longer as the applied stress is applied, and the process will be faster at high temperatures due to presence of more vacancies. Atomic diffusion in one direction is the same as vacancy diffusion in the opposite direction. This mechanism is called Nabarro-Herring creep.

The jump frequency of atoms and vacancies are higher along the grain boundaries. This mechanism is called Coble creep. The rate controlling mechanisms in both cases are vacancy diffusion, or self-diffusion. These two mechanisms are shown in Figure 3.5.

Strain rate of these mechanisms are given by:

$$\dot{\varepsilon}_{NH} = A_{NH}\frac{D_V}{d^2}\frac{\sigma\Omega}{kT} \qquad \dot{\varepsilon}_C = A_C\frac{\delta D_{gb}}{d^3}\frac{\sigma\Omega}{kT}$$

Where, d is the grain diameter, Ω is the volume of a vacancy; δ is the grain boundary thickness, σ is the external stress, D_V is the diffusion coefficient for the self-diffusion through the bulk material, and D_{gb} is the diffusion coefficient for the self-diffusion along the grain boundary.

So it is possible to use these relationships to determine which mechanism is dominant in a material; varying the grain size and measuring how affect the strain rate.

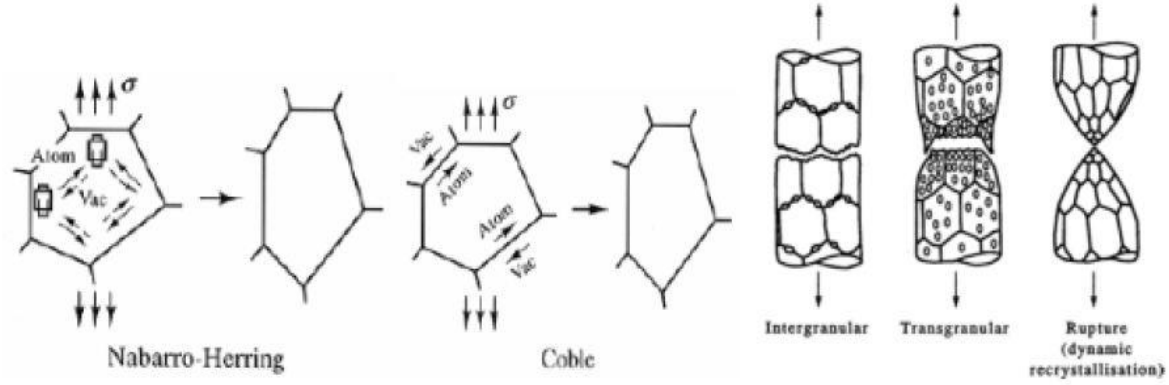

Fig. 3.5.: Different diffusional creep mechanisms (Nabarro-Herring and Coble), and grain growth, cavitation, inter-granular and trans-granular mode of rupture and rupture dynamic

3.5. Creep Deformation (Mechanisms) Map

Deformation and fracture mechanism map, developed by Ashby and Mohamed and Langdon, is a useful tool to characterize the type of deformation and the relevant fracture mechanisms. The deformation map helps to find the mode of fractures (inter-granular or trans-granular) of that special material. The maps of pure Aluminum (for 7075-T6 Aluminum), and iron (for X-70 carbon steel), used for experiments of this thesis, are given in Figure 3.6.

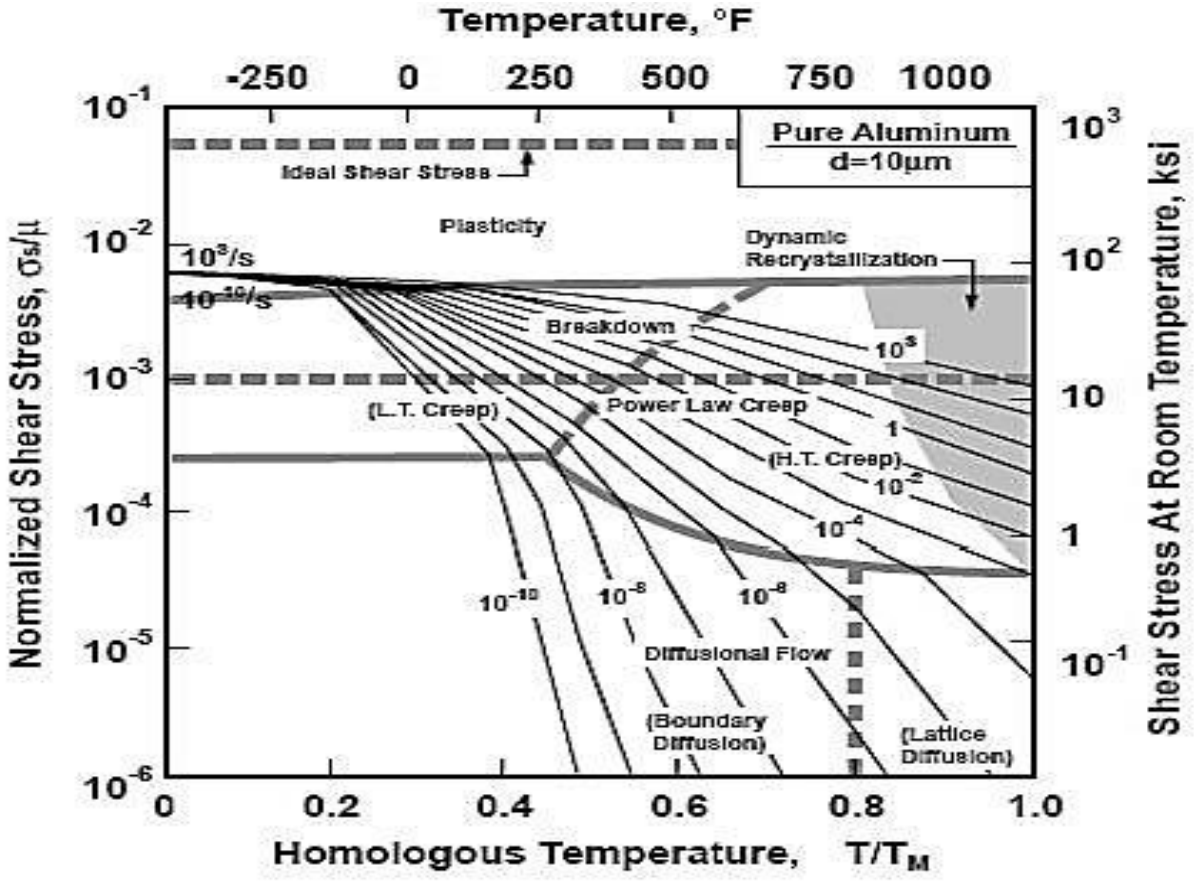

Fig. 3.6: Creep deformation map of pure Aluminum with given different fracture modes [24]

The phenomenon of creep is observed in most of the materials. The operating temperature in various industrial and structural applications is sufficiently high to cause significant creep as observed in chemical industries, nuclear power plants, missiles, aero engines, gas turbines *etc*.

The testing and estimation of creep in composite materials is tedious, costly as well as time consuming. Therefore, the prediction and analysis of creep is extremely important for estimating the life of components made of composite materials subjected to severe thermo-mechanical loadings. Accordingly, it is imperative to develop a thorough understanding of the methods for analyzing stresses and deformations in the components subjected to creep.

3.6 Creep Mathematical Model

Most of the models representing uniaxial creep of metals and alloys are empirical, established after years of experimentation. These models have been widely used and implemented as options in several finite element codes. The models express uniaxial creep strain or creep strain rate as a function of stress, time and temperature, and some models also use the accumulated creep strain to model strain hardening [52]. The mathematical form of these models is as given below,

$$\varepsilon = f\ (\sigma, T, t\ ) \qquad \text{..... (3.1)}$$

Where ε is the creep strain, σ is the applied stress, t is the time period and T is the temperature of application.

The Eqn. (2.9) can also be written in the following form,

$$\varepsilon = f_1(\sigma)\ f_2\ (T)\ f_3(t) \qquad \text{..... (3.2)}$$

If the temperature during creep test is constant, therefore, Eqn. 2.10 becomes,

$$\varepsilon =\ f_1\ (\sigma)\ f_2\ (t) \qquad \text{..... (3.3)}$$

Many empirical expressions, as a function of $f(\sigma)$ and $f(t)$, have been developed in the past. The most commonly used stress function law is Norton's law given as,

$$f_1\ (\sigma) = B\ \sigma^n \qquad \text{.....} \qquad \text{(3.4)}$$

Where *B* and *n* are the material constants. The approximation of a creep curve to a straight line is possible if secondary creep region is predominant, and elastic as well as primary creep is negligible. Under such conditions, it can be assumed that the creep strain rate depends upon stress function only. The time dependence of creep has been expressed in terms of Bailey's empirical law given by,

$$f_2(t) = At^m \qquad \text{..... (3.5)}$$

Where *A* and *m* are the material constants.

For practical applications creep does not usually occur at a fixed temperature and stress over the entire life of component. Therefore, it is not possible to compute the creep strain directly from a uniaxial creep equation. The rules of time hardening and strain hardening have been developed to extend the constant stress and temperature creep equations to time-varying stress and temperature histories. The creep strain is determined by integrating the creep strain rate equations for changing stress and temperature conditions. To compute the creep strain rate at a particular instant, the mechanical and thermal loads as well as the material history must be known. Hardening rules specify the state of material as a function of loading history. In its simplest form, a creep-hardening rule might be looked upon as a method of moving between constant stress and temperature creep curves as the stress and temperature change. Two different hardening rules have been used with classical creep models: time hardening and strain hardening. When the creep rate equations are integrated for conditions of constant stress and temperature, both the hardening rules produce identical results, namely the uniaxial creep curve for that stress and temperature.

The time hardening theory states that for a constant temperature and variable stress condition, creep rate ($\dot{\varepsilon}$) is a function of stress and time *i.e.*

$$\dot{\varepsilon} = f(\sigma, t) \qquad \text{..... (3.6)}$$

However, in case of strain hardening theory it is assumed that the creep rate is a function of stress and accumulated strain *i.e.*

$$\dot{\varepsilon} = f(\sigma, \varepsilon) \qquad \text{..... (3.7)}$$

The particular forms of these laws can be obtained by assuming that the creep curve can be represented by Bailey-Norton law, which is a common representation of creep in the primary and secondary creep ranges under isothermal conditions and is given below,

$$\varepsilon = C\sigma^n t^m \qquad \text{..... (3.8)}$$

where *C*, *m* and *n* are constants whose values depend upon the type of material. The constant *C*, and exponents *m* (>1) and *n* (<1), should be functions of temperature. The form of Bailey Norton given by Eqn. (3.7) could be used to describe creep in both tension and compression, but it would be reasonable to expect that the parameters would be different in tension and compression. Since the value of exponent $n < 1$, therefore the creep rate at $t = 0$ could not be defined.

Differentiating Eqn. (3.7) with respect to time, the ***time hardening law*** can be obtained as,

$$\dot{\varepsilon} = \frac{d\varepsilon}{dt} = Cm\sigma^n t^{m-1} \qquad \text{..... (3.9)}$$

From the above equation it can be seen that the creep rate decreases with time since $0 < m < 1$. Further, Eqn. (3.9) can also be written in the following form, independent of time *t*, by eliminating *t* between Eqs. (3.8) and (3.9)

$$\dot{\varepsilon} = \frac{mC^{1/m}\sigma^{n/m}}{\varepsilon^{1-m/m}} \qquad \text{..... (3.10)}$$

Eqn. (3.10) indicates that the creep strain rate decreases with increasing creep strain (ε) *i.e.* with the progression of creep strain the material hardens. This equation is known ***as strain hardening law***.

If this equation is written in right manner, it will become

$$\dot{\varepsilon} = mc^{m}\sigma^{n/m}\varepsilon^{m-1/m} \qquad \text{..... (3.11)}$$

Though, both the laws are derived from the same equation, but it is observed that for varying stress, the time and strain hardening laws give different creep rates. Quite often the strain hardening models give more accurate predictions of experimental results for stepwise changes of stress. However, in the case of constant applied stress, both the laws give approximately similar predictions.

Since time hardening model is a little easier to apply than strain hardening, the present study will use time hardening creep model for analysis. Later, the coefficients of strain hardening creep mathematical model is derived using analytical steps by using time hardening creep mathematical model. In the above derived equation, the creep strain is in terms of percentage in Norton- Bailey equation while in time hardening and strain hardening equation creeps are in the form of strain rates.

3.7 Summary of Theoretical Background

All the theoretical background required to understand creep mechanism is explained. This includes basic concepts of creep mechanics, mathematical models and different methods to calculate creep strain with terminology. Calculations have also made for strain hardening creep law with help of Norton-Bailey equation and time hardening equation. Both of the creep coefficients are to calculate creep strain. But the benchmarking study is involve with only time hardening law because of understanding the method to solve creep strain with the required software. Next, comparison between different results is presented. Next chapter contains numerical analysis of bench marking problems.

Chapter4

Finite Element Analysis and Benchmarking Results

4.1 General Overview

The finite element method is a numerical analysis technique for obtaining the approximate solutions to a wide variety of engineering problems. Because of its diversity and flexibility as an analysis tool, it is receiving much attention in almost every industry. In more and more engineering situation today, we find that it is necessary to obtain approximate solution to problem rather than exact closed form solutions. Though, exact analytical mathematical solution may possible for simple problem but it is not possible for many engineering complex problems. An analytical solution is a mathematical expression that gives the value of a desire unknown quantity at any location in the body and it is applicable for infinite number of location within the body. For problems involving complex materials properties and boundary conditions, the engineer has used numerical methods which involve approximate but exact solution.

ANSYS is a vast numerical technique to integrate differential equations. This software uses Newton- Raphson numerical method for nonlinear solutions. Sparse solver use to calculate creep strain and PCG solver uses to calculate initial value at creep rate off.

4.2 Procedure for ANSYS Analysis

Static analysis in ANSYS is used to determine displacements, stresses, strains and forces for structures and different types of components which do not produce inertia or damping effects. Static analysis can be done for linear as well as nonlinear solutions. Since we are analyzing creep which is a nonlinear material property as discussed in previous chapter, we have considered static nonlinear analysis in our present work.

The procedure of benchmarking analysis has considered three main steps:

a) Preprocessor
b) Solution phase
c) Postprocessor.

4.3 Preprocessing

Preprocessing includes different stages of work which can be concluded as different parts. This process is available in GUI and macro which is also called as ANSYS APDL command.

1. Regression analysis for creep mathematical model coefficients.
2. Building the geometrical model.
3. Material properties.
4. Mesh generation.
5. Apply all boundary conditions.

4.3.1 Regression Analysis for Creep Mathematical Model Coefficients

We can calculate the coefficients of *creep mathematical model by* creep material curve fitting process in ANSYS. These coefficients are used for further creep analysis for the different problems. ANSYS does a regression analysis to calculate creep coefficients. Thirteen creep models are available in ANSYS'15 version, along with the tools to generate and fit derived coefficients to our experimental data.

To understand the Creep Material Curve-Fitting Process, the detailed information's are according to the given steps below in the table.

Flow Chart 1: Creep curve fitting procedure to calculate the coefficients of creep mathematical model

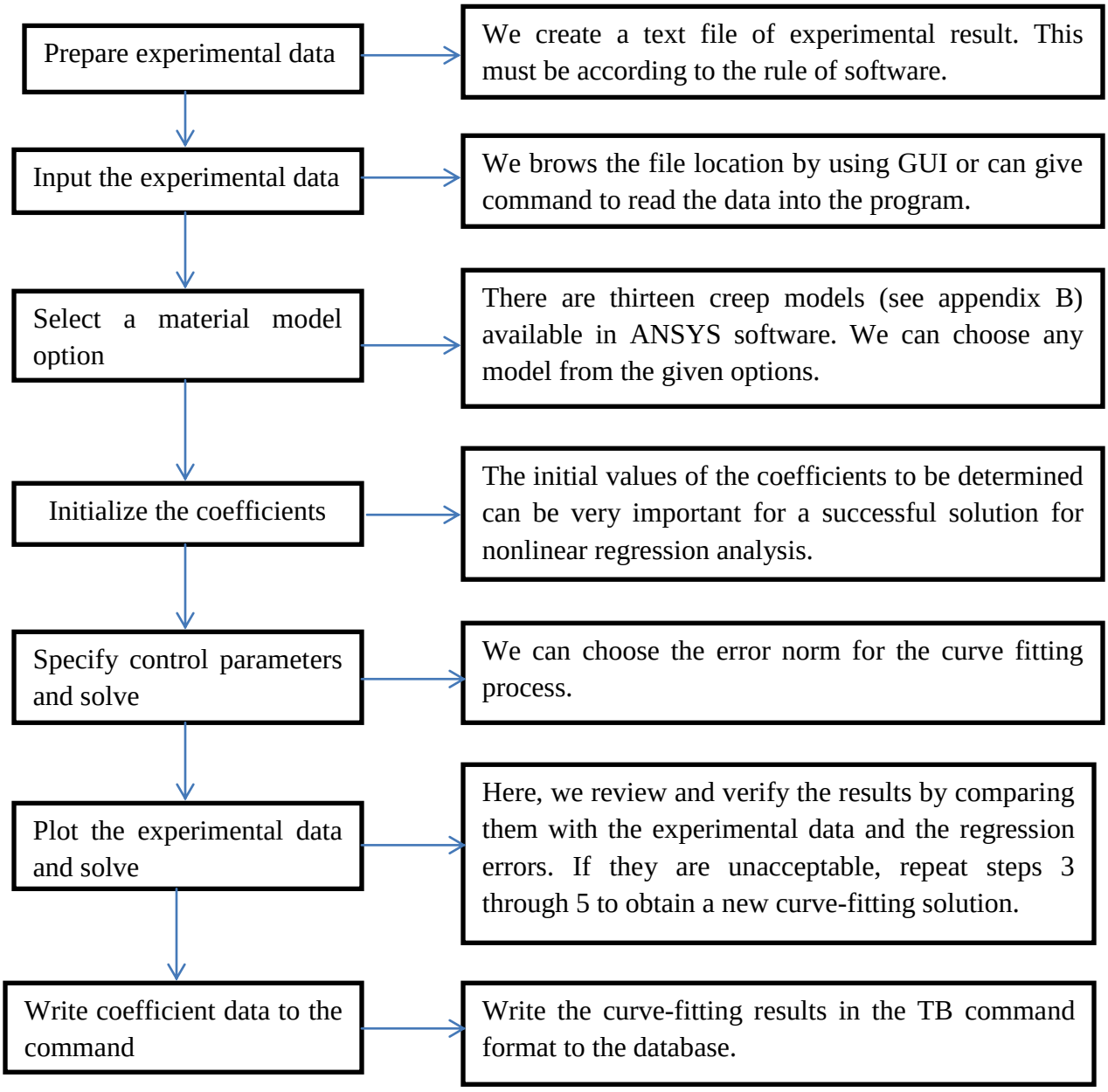

Experimental values have taken form the paper reference [19]. Text files of the experimental results are given in appendix A.2. After follow every steps, we reach to the point that the experimental results which we have taken for analysis is only for secondary region creep.

The regression analysis result the best coefficients for combined time hardening creep model because of limited experimental results. The validation of creep material curve fitting is shown in the graph and coefficients at different temperature as also given in the table.

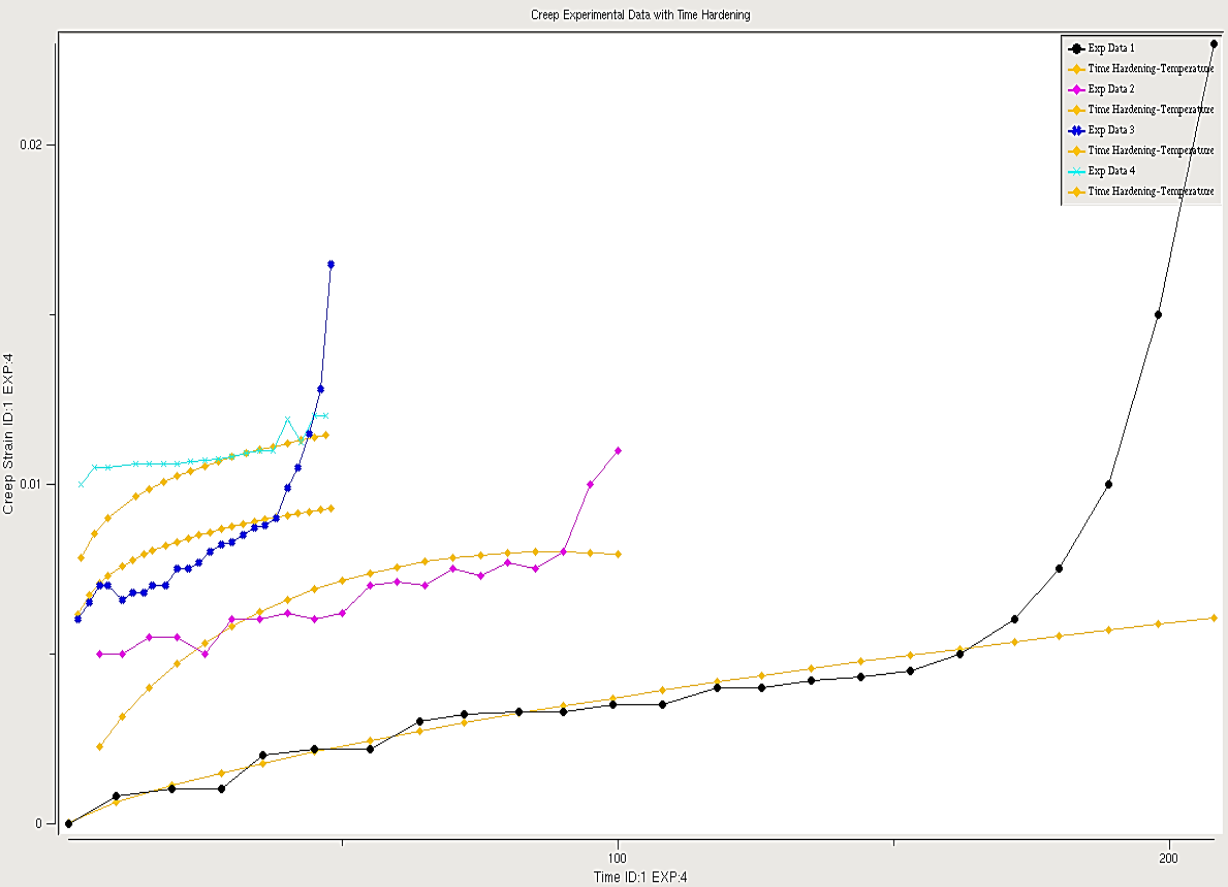

Fig. 4.1: Validation of creep material curve fitting

In figure 4.1, the yellow curves are showing the creep curve fitting data and all rest of the curves are showing experimental data at different temperatures.

Table 2: Results of Combined Time Hardening Creep Coefficients

Coefficient	C1	C2	C3	C4	C5	C6	
Values	1.104e-23	7.009	-0.86633	0	0.0001	-5.3	0

This work is added into this thesis work just to show that how we can find the creep coefficients from the regression analysis of creep material curve fitting process. However the analysis needs many creep coefficient valves at different temperatures.

In gas turbine rotor disc, we are highly concerned about the primary region creep followed by secondary region. Apart from this, when we are analyzing the live gas turbine rotor part, we have to take as much coefficients as possible at different temperatures for better and accurate results.

So after analyzing these steps, we have decided to do further analysis with the data taken from the material laboratory department of ***siemens ltd*** for *time hardening material model* which are listed in appendix.

4.3.2 Building of Preprocessing

In ANSYS, we can build the model with the help of *modeling* option present in preprocessor. Here all the entities are independent of other and have unique identification labels. Since all boundary conditions and loads can be possible to define in 2-Dimensional geometrical model, we have generated a 2D bar model for simple calculation. The cross-section is rectangular for easy consideration. The benchmarking model have taken in this present work is as shown below.

For this problem, we have taken plane 77 for thermal analysis and plane 183 for structural analysis as element type. All the material properties needed in this calculation are given in the table. For nonlinear creep analysis, the coefficients of creep mathematical model are also fed to the program from the table.

In the finite element analysis, the basic concept is to analyze the model, which is the assemblage of discrete piece called element. These elements are connected together at a finite number of points called nodes. A network of these elements is known as mesh. The element shape in this work has taken as quadrilateral and the dimension has taken as 2.5×2.5 mm. After completion of the finite element modeling and meshing, it has to constrain which is also called boundary conditions and load has to apply. A user can define boundary conditions and load in various ways.

Table 3: Material Property of Nickel Based Alloy (*Source: Siemens Ltd.*)

Temperature	Young's Modulus	Poisson's Ratio	Density	Thermal Conductivity	Mean Coeff. of Linear Therm. Exp. (L-LT)
(^{0}C)	(MPa)		(kg/dm^3)	(W/m-K)	(10^-6/K)
20	212900	0.285	7.824	23.1	10.59
50	210900	0.286	7.816	23.7	11.07
100	209900	0.287	7.803	24.6	11.4
150	208300	0.288	7.789	25.3	11.63
200	205300	0.29	7.775	25.8	11.79
250	201800	0.292	7.761	26.2	11.9
300	198100	0.294	7.746	26.6	12
350	194200	0.297	7.732	26.9	12.09
400	190300	0.299	7.717	27.3	12.18
450	186400	0.302	7.702	27.8	12.29
500	182200	0.305	7.687	28.4	12.4
550	176800	0.308	7.672	29.1	12.52
600	169100	0.311	7.656	30	12.62
650	156900	0.316	7.641	31.1	12.69

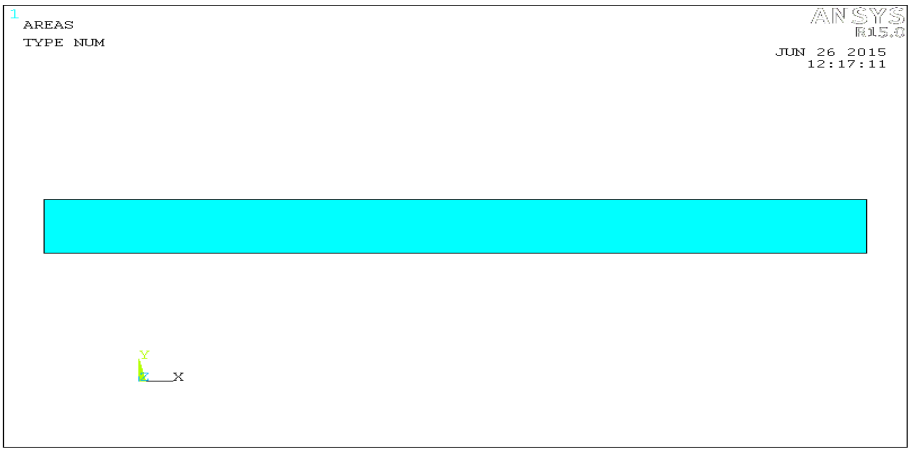

Figure 4.2: 2-D Bar model geometrical representation

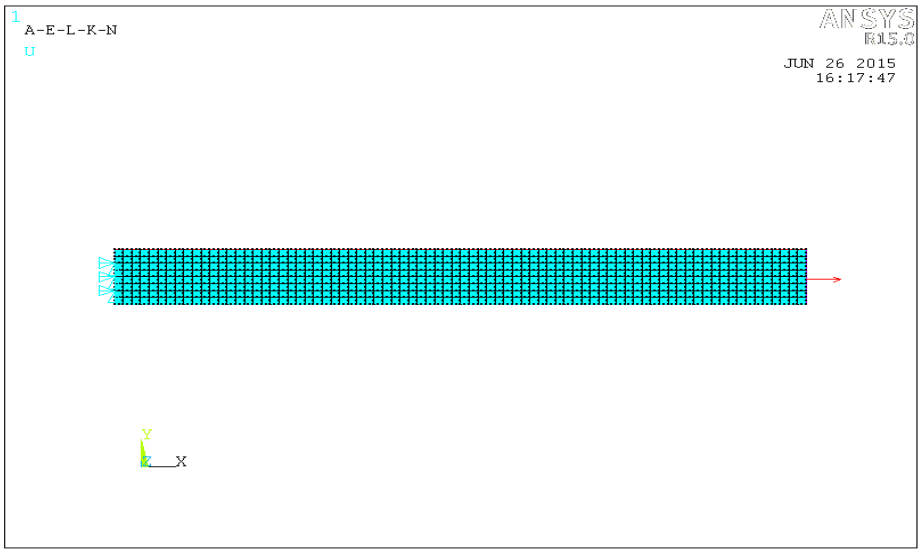

Fig. 4.3: Meshed bar with boundary conditions and loads

4.4 Solution Phase

The solution phase deals with the solution of the problem according to the problem definition. All the tedious work of formulating and assembling of matrices are done by the computer and finally displacements, stress and strain values are given as output. Some of the capabilities of ANSYS are linear static and dynamic analysis, nonlinear static and dynamic analysis. In the present work, the nonlinear static solution has been done for creep analysis. The program has

solved the nonlinear matrices by Newton- Raphson method. After the completion of nonlinear solution, the convergence graph will come on the screen of the computer which shows the solution has completed.

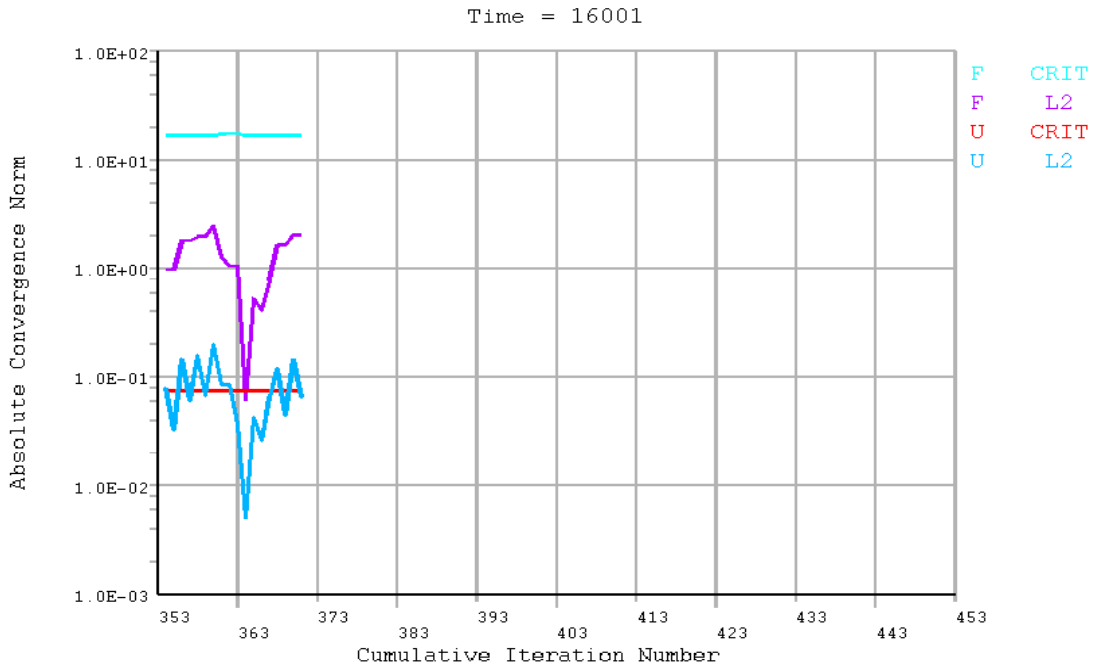

Fig. 4.4: Nonlinear convergence solution graph

4.5 Post-Processing

ANSYS is a powerful user-friendly post-processing program using interactive colour graphics. It has extensive plotting features to see the results obtained from the finite element analysis. The entire range of the post-processing data of different types of analysis can be accessed through the command mode or through GUI.

Various results of benchmarking problems are as follows.

4.5.1 Creep Estimation at Uniform Temperature 400^0c

a) Stresses:

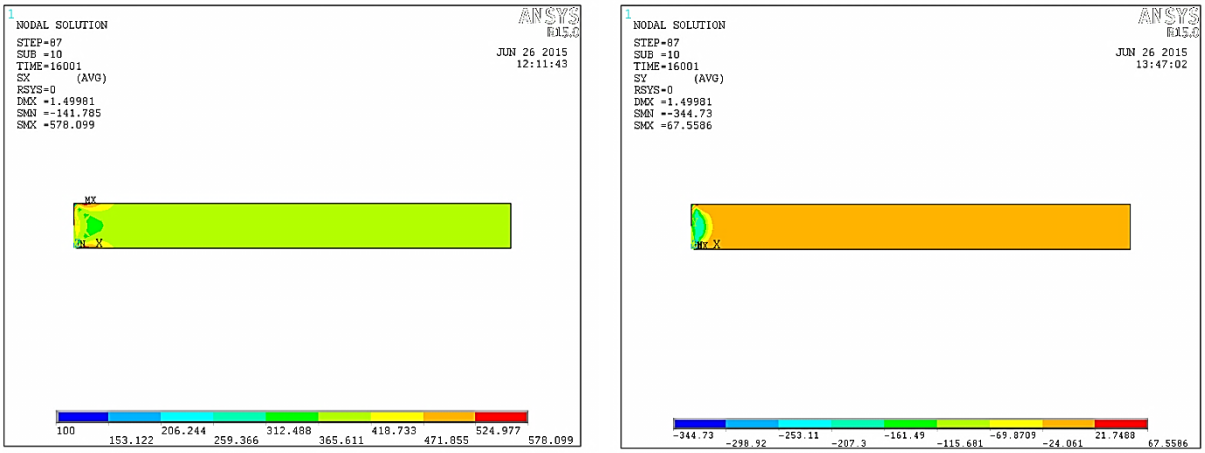

(a) (b)

Fig. 4.5: (a) Stress in x direction (b) Stress in y direction

As shown in the above figure, it is clear that the stress generated in y direction is very low compare to stress generated in x direction. So this stress will be a less interest of matter and we can ignore this graph for further analysis.

b) Creep strain

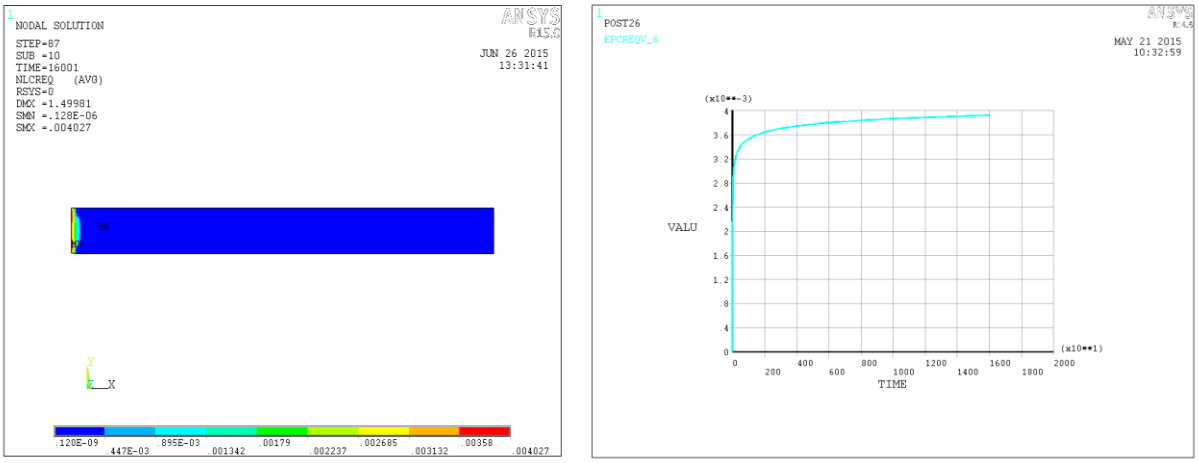

Fig. 4.6: Equivalent creep strain at uniform temperature

c) Displacement

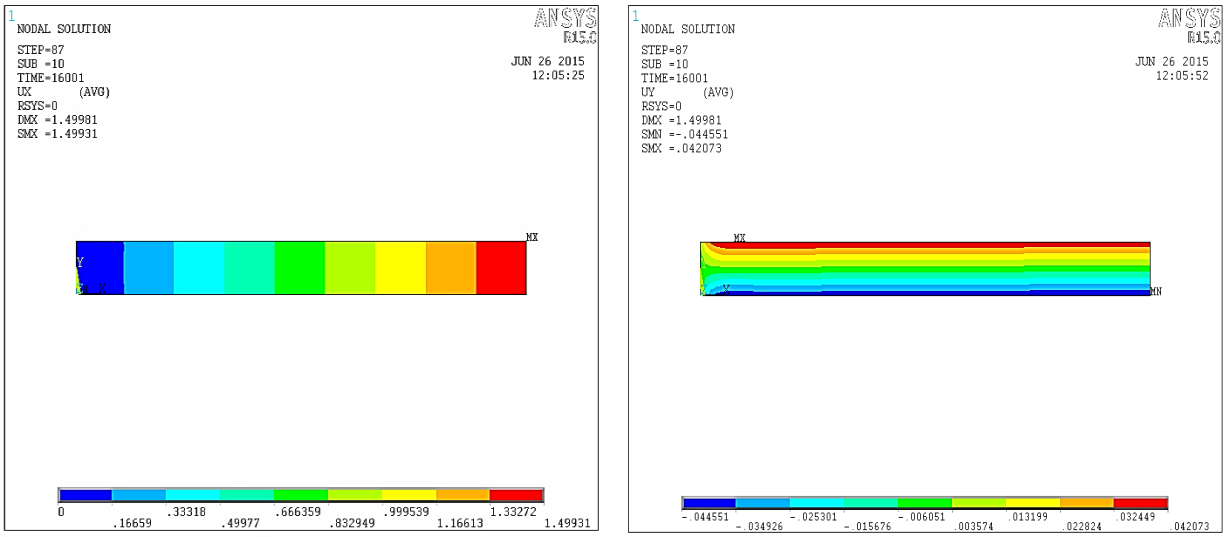

Fig. 4.7: displacement of bar in x and y direction

4.5.2 Creep Estimation at Temperature 400^0c at Fixed End and 450^0c at Right End

For the analysis of creep at variable temperature profile, first we have to perform two different thermal and structural analyses. First we feed material conductivity at different temperature in material property section and perform thermal analysis. Doing this, ANSYS will create an *.rst* file in the working directory. This result file obtained will be further used for structural analysis as an input. The all boundary conditions and load are defined and clearly shown in the figure.

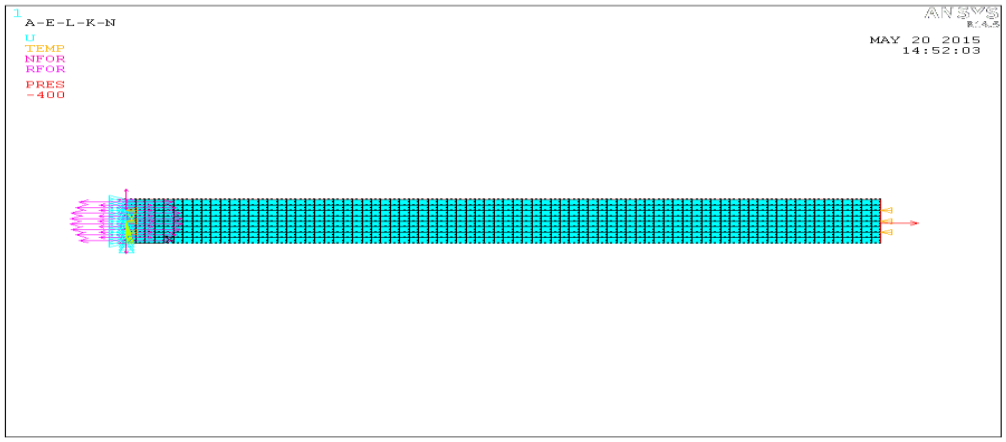

Fig. 4.8: Loads and boundary conditions for bar with different temperature at both of the end

a) Thermal Analysis

The temperature profile along the length after thermal analysis is as shown.

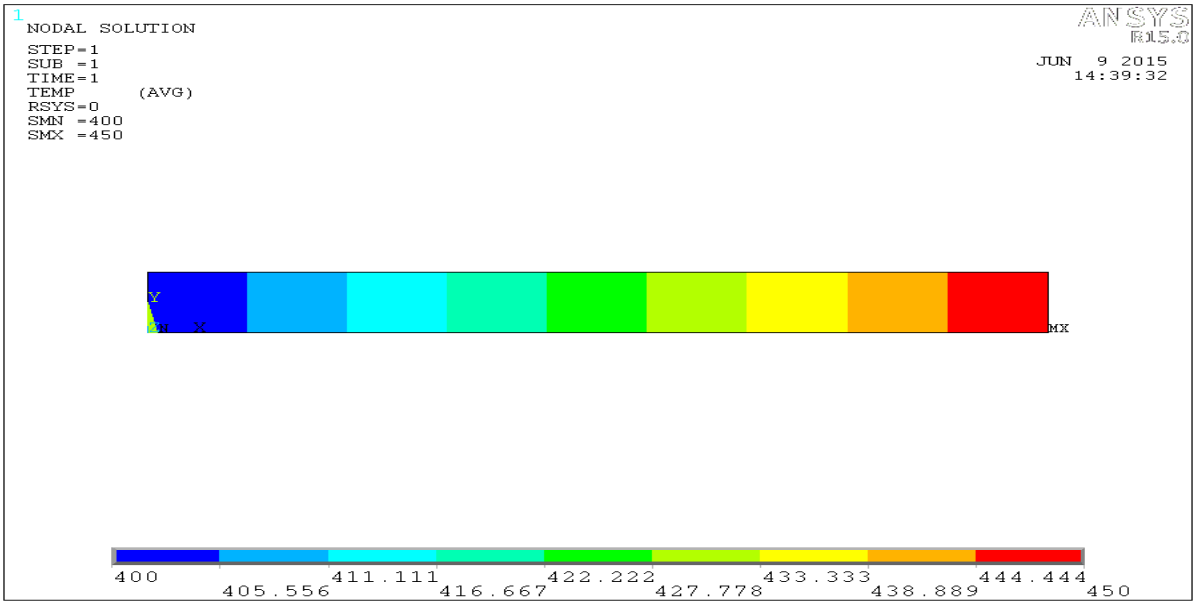

Fig. 4.9: Temperature profile of bar at different temp. at both of the side

b) Structural Analysis

i. Stress

The stress in longitudinal direction i.e. in x direction will come with a considerable value and stress in y direction will be very less. This value can also be validating with the theoretical calculation. The result graphs of all stresses are as listed below.

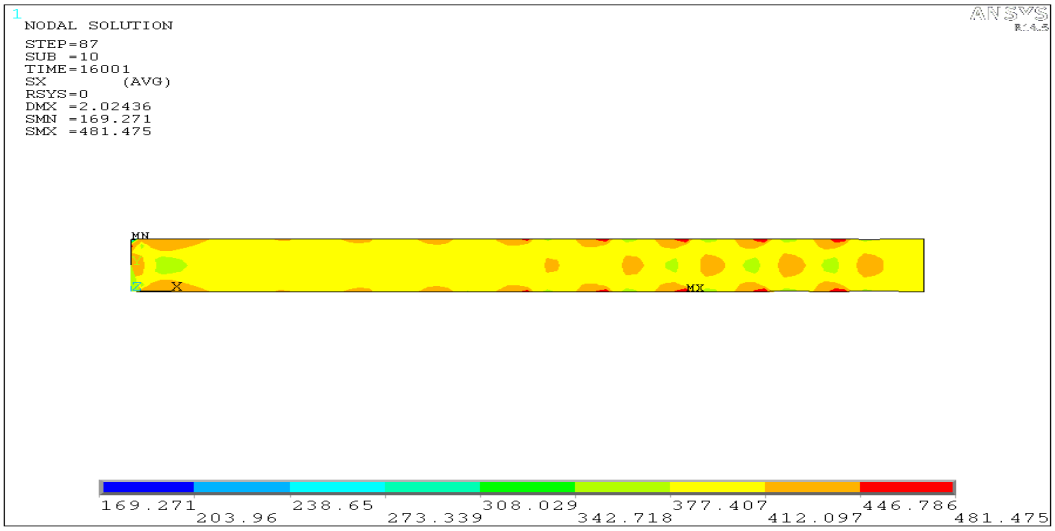

Figure 4.10: Stress in x direction of bar at different temp. profile

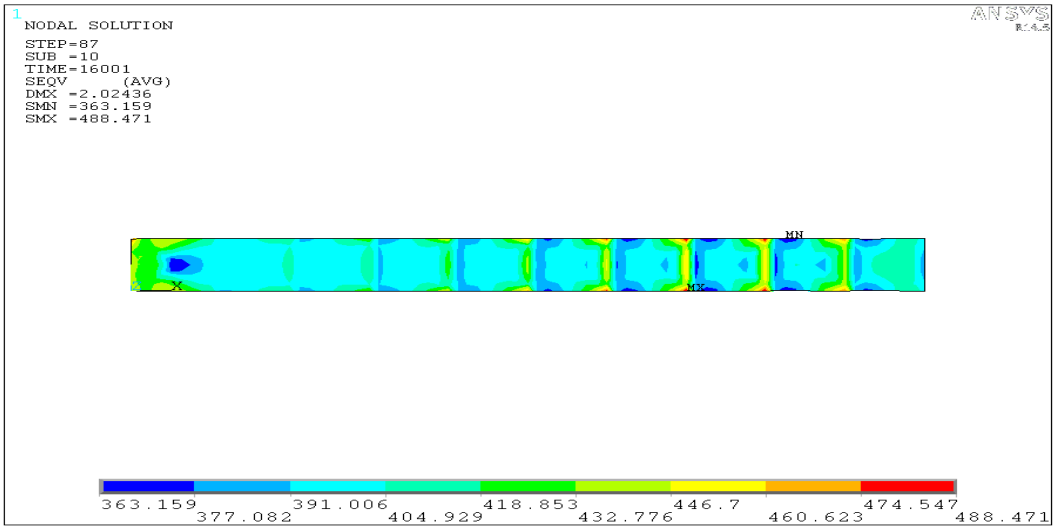

Figure 4.11: Von mises stress distribution of bar at different temp. profile

ii. Equivalent creep strain

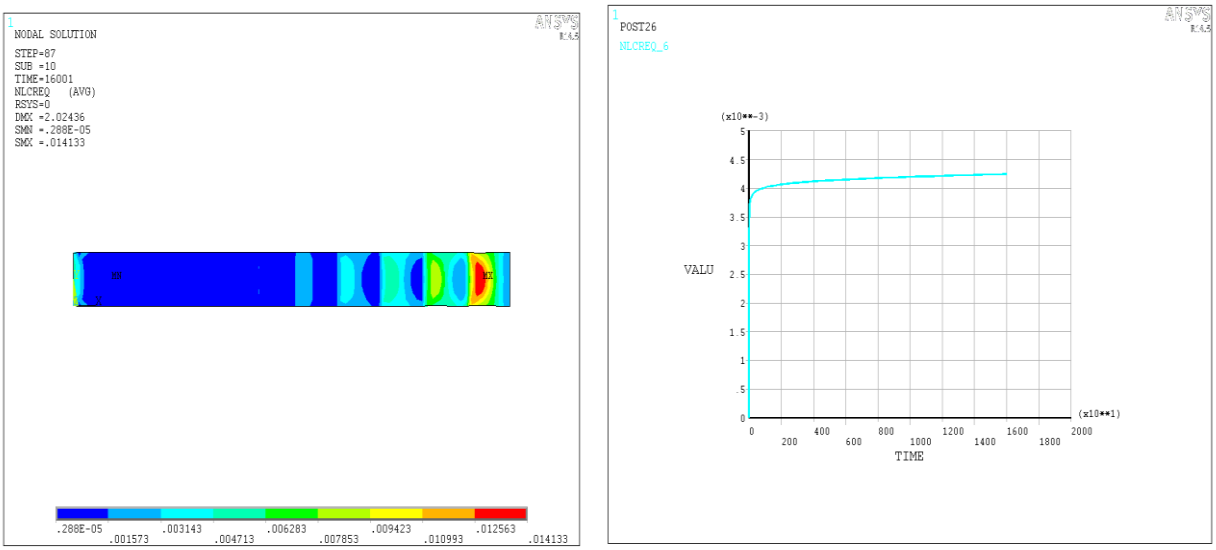

Fig. 4.12: Equivalent creep strain of bar at different temp. profile

iii. Displacement in x direction

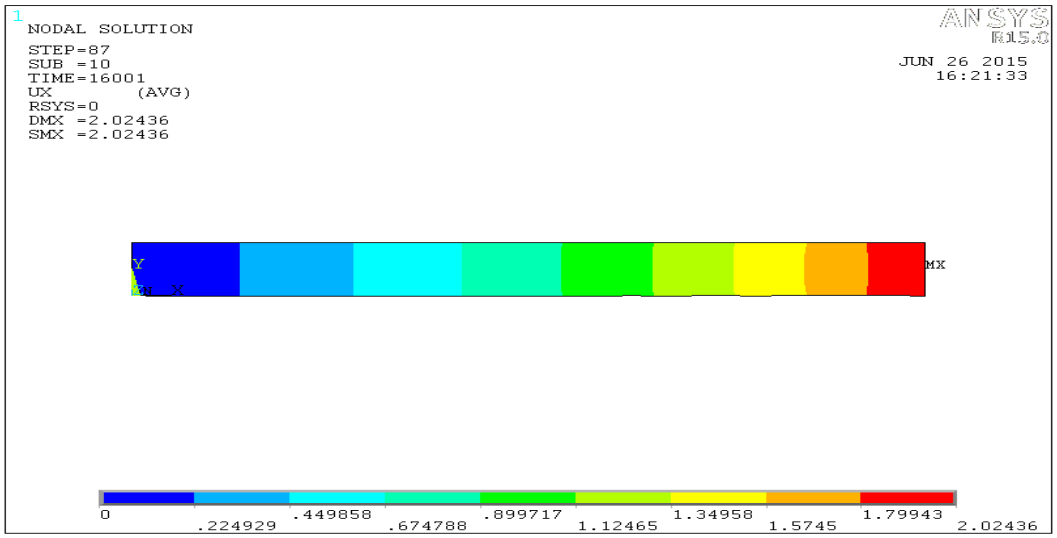

Fig. 4.13: Displacement in x direction of bar

4.6 Comparison between Uniform Temperature Analysis and with Temperature Profile Analysis

The analysis done with different temperature profile is more realistic than the uniform temperature analysis because when we come into a live situation, the temperature will vary according to length in almost every industry or power sector.

This benchmarking problem we discussed is the pillar of the next analysis.

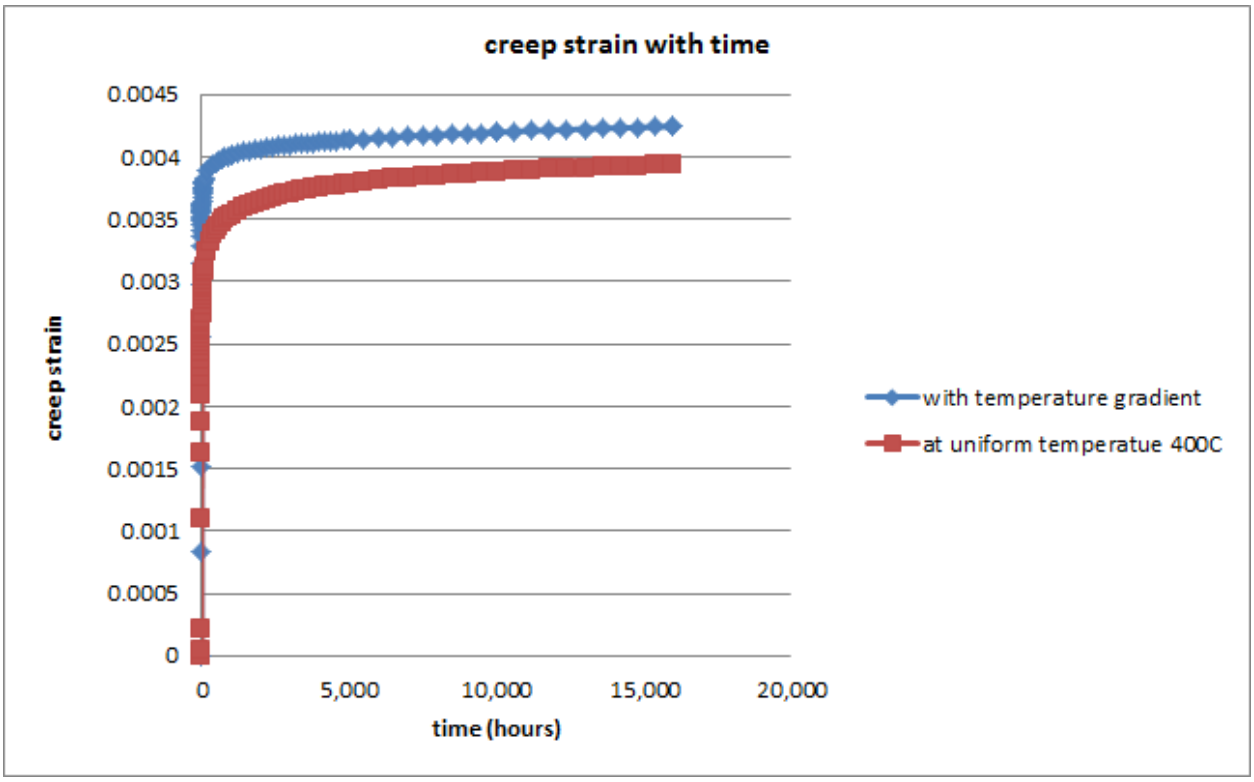

Fig. 4.14: Comparison of creep data at uniform temperature and variable temperature gradient

In the above graph shown, it is clear that the creep strain calculated for uniform temperature is less than with the temperature gradient.

4.7 Summary of Benchmarking Results

Benchmarking analysis required for the actual calculations on discs which will be performed in next chapter. First, the creep strain is calculated for a bar at uniform temperature and then the same model is taken for temperature gradient along the length in finite element analysis. Since there is no creep experimental data available in the literature for primary region of creep strain at higher temperature for long duration of time, these results are compared with the analytical calculation mentioned in the previous chapter.

Also, we have seen that creep strain at constant temperature will differ with almost 13% comparison to creep strain calculated for temperature gradient. It states that thermal analysis is important step in gas turbine disc calculation before analyzing structural analysis.

The *creep mathematical model* coefficients are the major role in the calculation of creep strain. We can calculate coefficients for any mathematical model incorporated in ANSYS through regression analysis if we have sufficient relevant experimental data. ANSYS also allow generating coefficients at different temperature as well as temperature dependent coefficient. For extrapolation of the experimental data, *Larson Miller parameter* method is the best method according to the literature survey. Unfortunately the lack of experimental data did not give a chance to use this parameter for further study.

The lack of experimental data available for primary region creep, coefficients at different temperatures have taken from the material laboratory department of *Siemens Ltd* for *time hardening creep mathematical model*.

The entire benchmarking model is created and analyzed in ANSYS APDL which is a classical platform. Apart from this, ANSYS WB is also available that we can use for analysis but ANSYS APDL is more accurate numerical platform than WB.

This completes the benchmarking process. Knowledge acquired form benchmarking problems applied in next chapter which contains creep strain estimation of actual gas turbine disc at constant ambient temperature and variable ambient operating temperature.

Chapter 5

Creep Estimation of Gas Turbine Disc

This chapter contains details of creep calculations in gas turbine disc. Since disc is one of the important components of gas turbine rotor, it is chosen for creep analysis. The disc part present just below the combustion chamber contains the highest temperature in gas turbine rotor. Disc temperature varies radially with time during the operation. The typical gas turbine rotor disc is shown in figure 5.1.

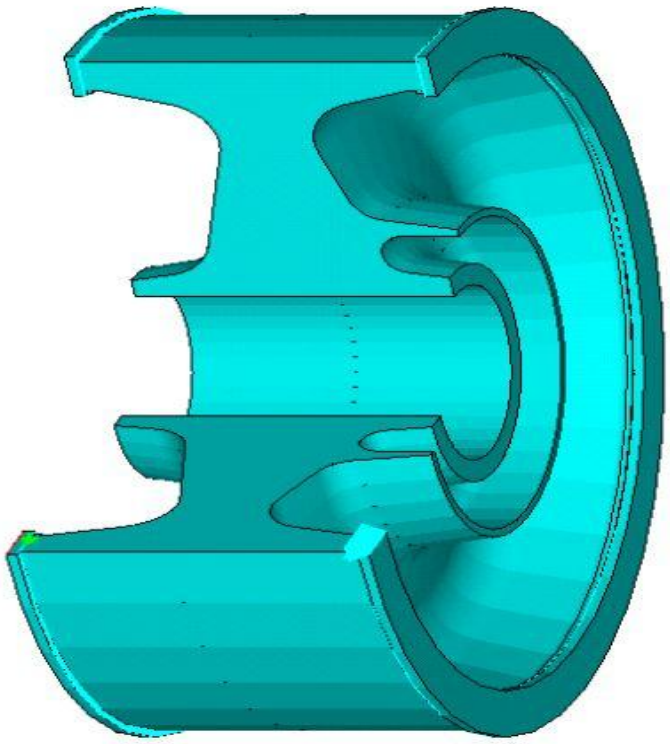

Fig. 5.1 – GT rotor disc without detailed features

Generally power industries calculate creep at constant ambient condition. Though, ambient condition varies with respect to time. As we all know because of the geographical reason, ambient temperature varies throughout the year and place to place. Here in this study, constant ambient temperature condition and monthly varying ambient condition both are considered and effect of these two conditions on discs creep calculation are detailed here.

5.1 Aim of the Present Chapter

The goal of this chapter includes various studies and numerical mathematical calculations which are presented in previous chapters. Considering all previous study, aims of the present chapter are as follows:

1. First creep estimation has been done by assuming constant average temperature as 32^0c. This average temperature is calculated by taking data of temperatures across the glove. Creep estimations of disc have calculated with *time hardening creep mathematical model*. Now the calculations have been done with the *strain hardening creep mathematical model* at constant temperature. Both of the estimated results have also compared.

2. Next, creep is calculated at variable temperature for hot ambient condition. To achieve this goal, one hot temperature condition data which varies monthly of city Abu Halifa (Kuwait) has been captured for getting the real calculation results. These calculations have also been done for time hardening and strain hardening *creep mathematical models*. Results are also compared with the constant ambient temperature condition for both of the mathematical models.

5.2 Analysis of Disc

Thermal analysis and structural analysis are performed on disc one after another. Disc is meshed with fine density. A typical disc geometry sector model and meshed model are shown in the below figure 5.2 and 5.3.

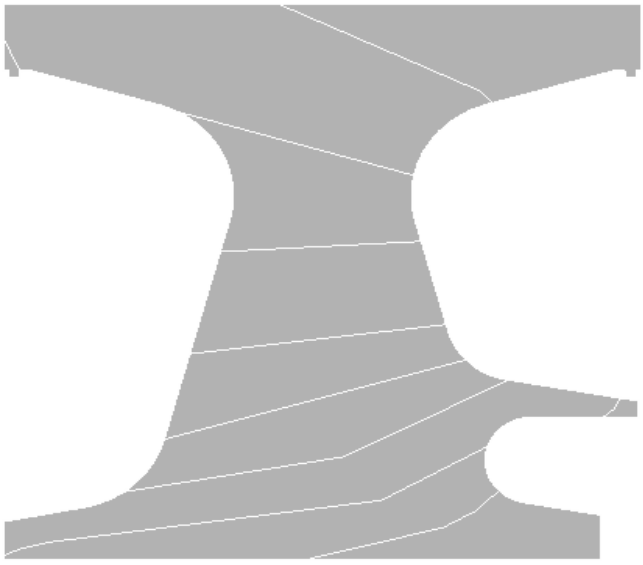

Fig. 5.2 - Sector model of GT rotor disc

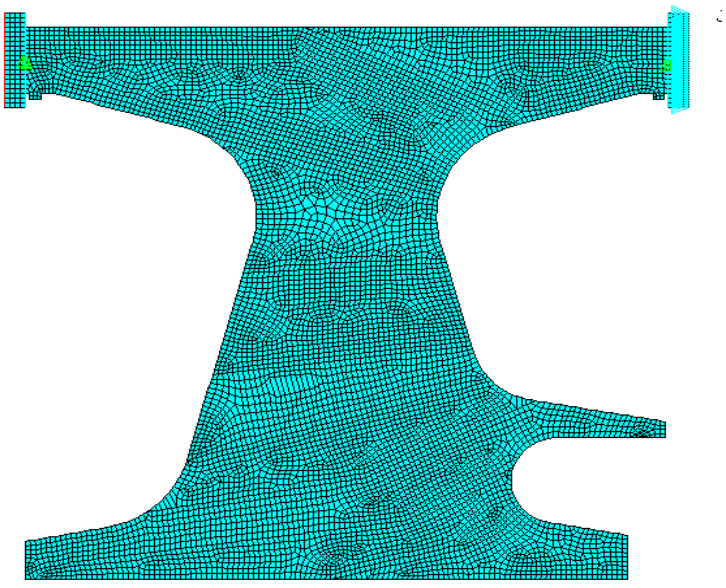

Fig. 5.3 - Meshed view of GT rotor disc

5.2.1 Thermal Analysis of Disc

Typical thermal distribution in disc at steady state are shown in below figures. To obtain that required temperature distribution in disc, model is divided into several number of areas in ANSYS WB design modeller as shown in Fig. 5.2. Model is free meshed with quadrilateral and plane 183 elements as shown in Fig. 5.3. Next, respective temperatures are applied on cut lines and thermal analysis is performed in ANSYS APDL to get nodel temperature distribution as shown in the figure in Fig. 5.4. In bore location, temperature is around 325^0c and in the disc circumferencial area, it is around 522^0c. This analysis is done only for constant ambient temperature.

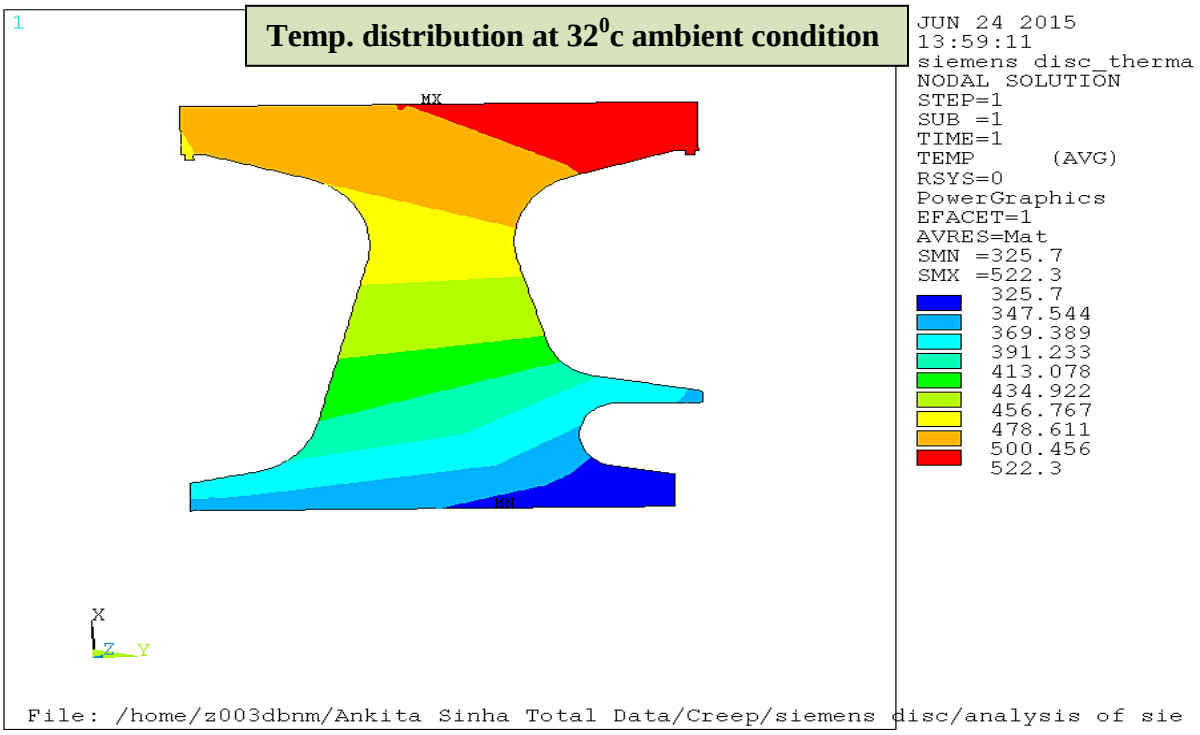

Fig. 5.4- Nodal temp. distribution after thermal analysis at constant ambiant temp. 32^0C.

For variable ambient temperature condition, the disc temperature profile along the radial direction is varied monthly with time along the year which is shown in figure 5.5. Twelve thermal distribution has been done for every month to capture mothly varition of temperature in order to simlate offset desing condition, while it is assumed that disc temperature varies linearly

with ambient tempearture in the case of montly variation. Only the highest and lowest nodal temperature distributions are shown during the year in figure 5.6 and 5.7.

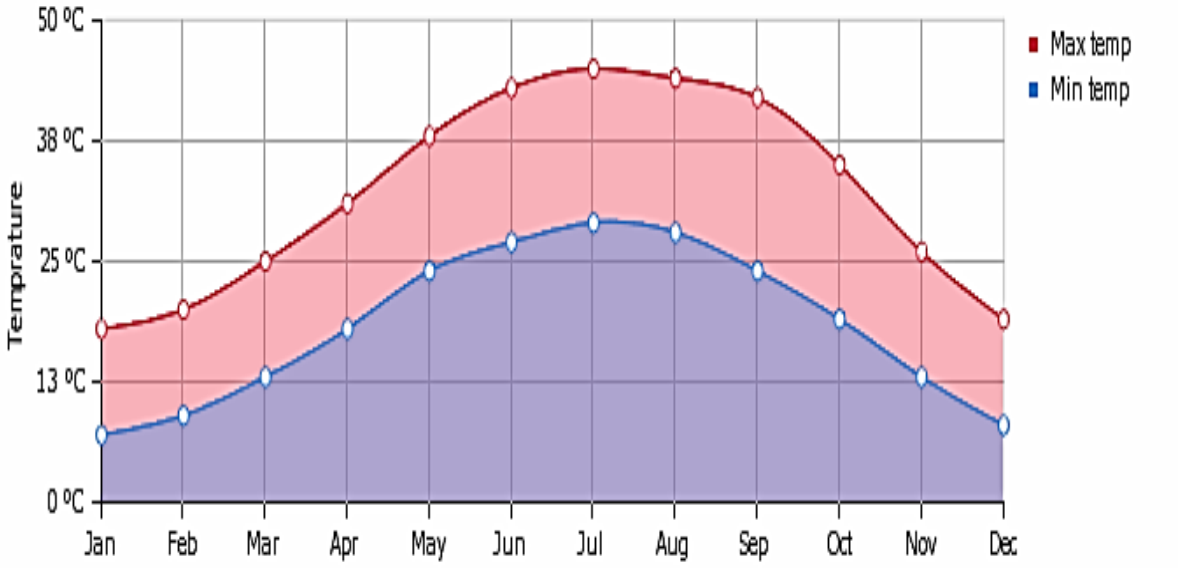

Figure 5.5: Average minimum and maximum temperature over the year of city Abu Halifa (Kuwait)

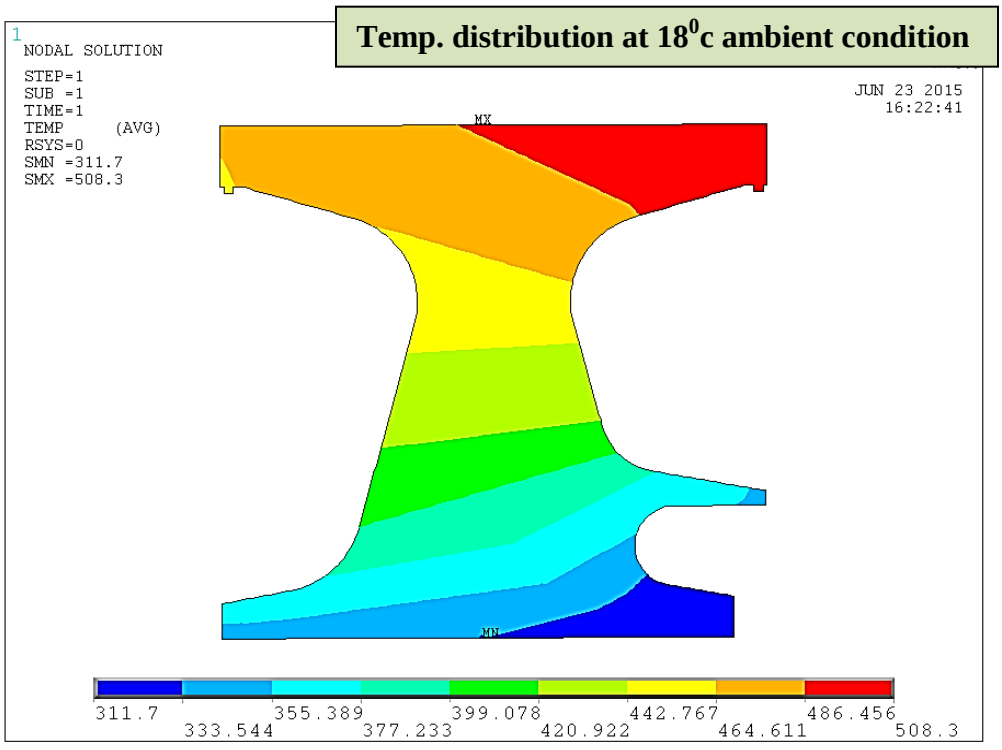

Fig. 5.6 - Nodal temp. distribution after thermal analysis at temp. offset by -14^{0}C

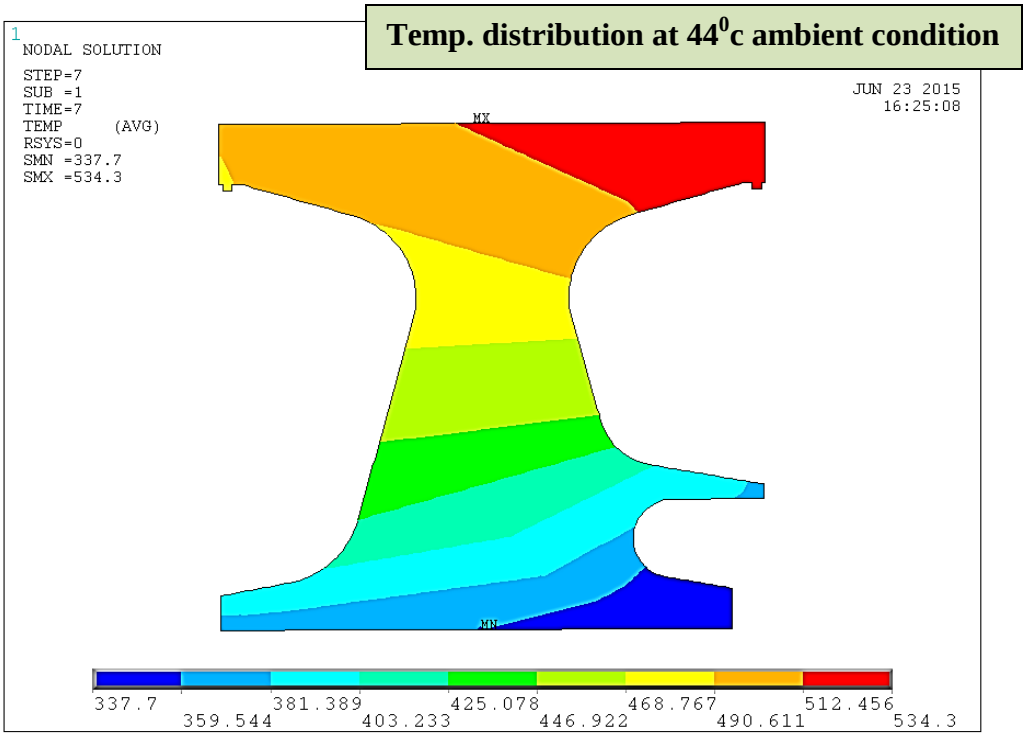

Fig. 5.7 - Nodal temp. distribution after thermal analysis at temp. offset by 12^0C

5.2.2 Structural Analysis of Disc

After thermal analysis, structural analysis with the following loads and boundary conditions is performed on disc. Typical elastic, thermal and creep material properties i.e. youngs modulus, poissons ratio, density, coefficient of thermal expansion, creep coefficients at different temperatures for time hardening model are shown in Fig. 5.9, 5.10 and table 4. Model is meshed as same as in thermal analysis. Axial Pressure at steady state = 52.46 MPa; Rotational speed N = 3000 rpm; since the model is taken as axis symmetry, constraints are kept in axial direction to cut surfaces in sector model. Displacement in axial direction is restricted as shown in Fig. 5.8 on the right hand side while pressure is applied on the left hand side. Two auxilary cylinders are made on both of the side on disc axially to capture correct behavior of disc. Tepmerature distributions are clearly shown at each sliced line of the disc in figure. Nodal temperatures are imported from the results file of thermal analysis.

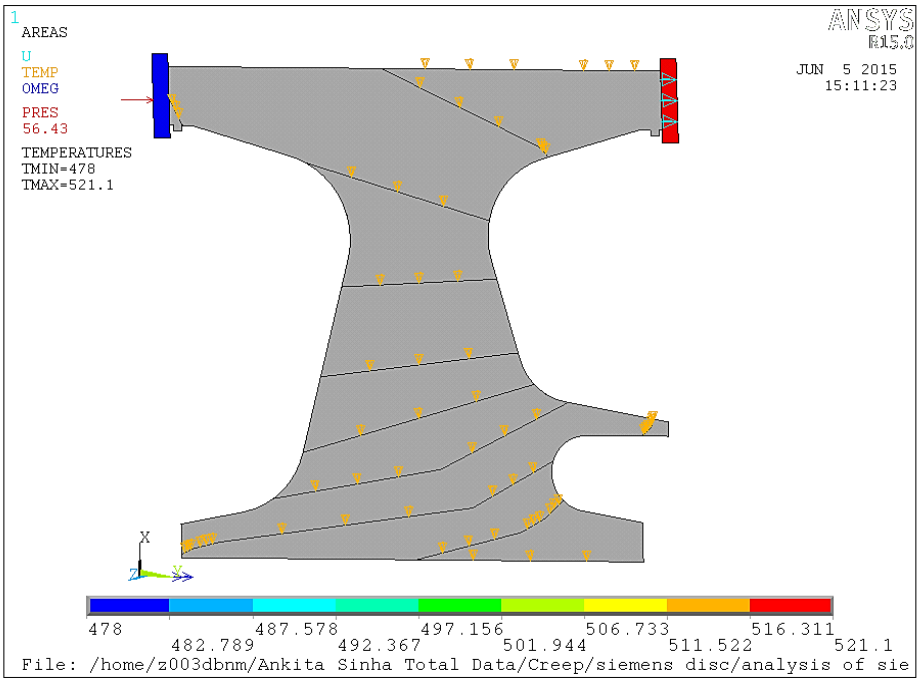

Fig. 5.8 - Boundary conditions and load of axisymmetric disc model including temperature profile.

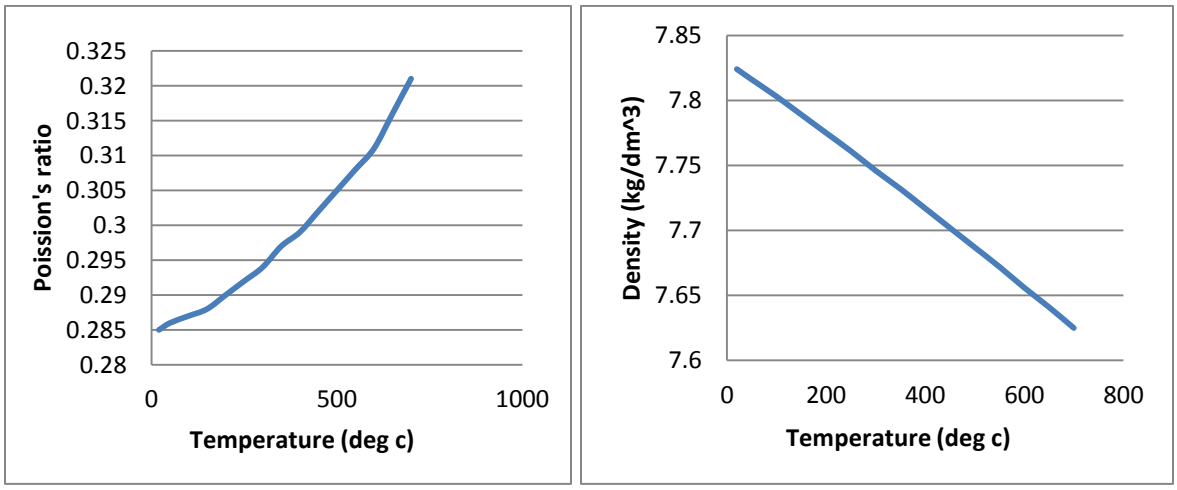

(a) (b)

Fig. 5.9 - Material properties of disc (a) Poisons Ratio (b) Density

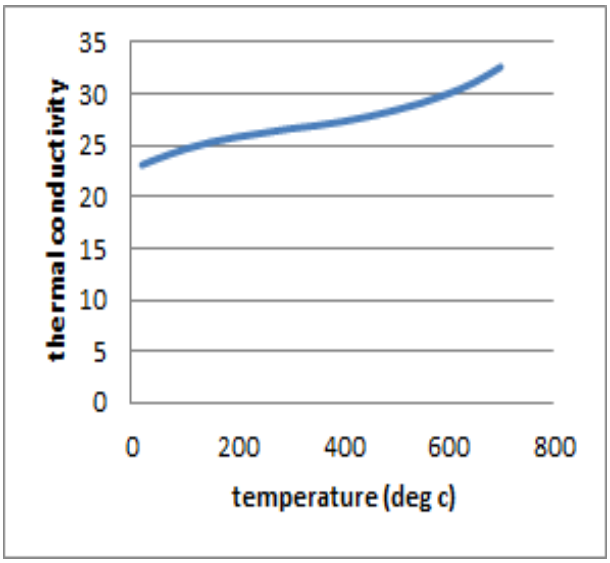

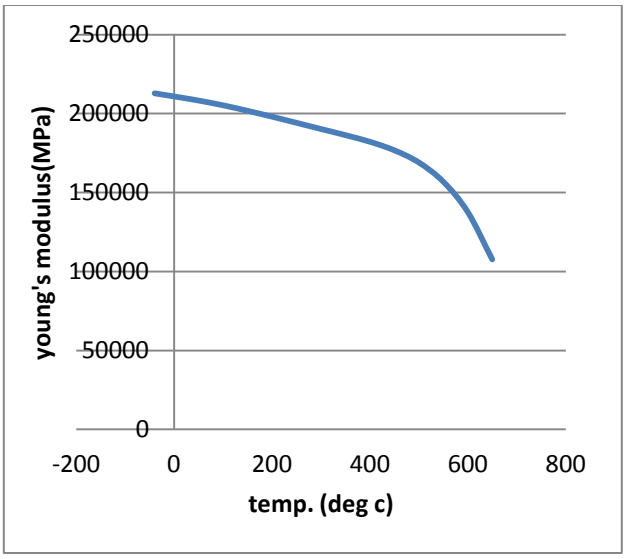

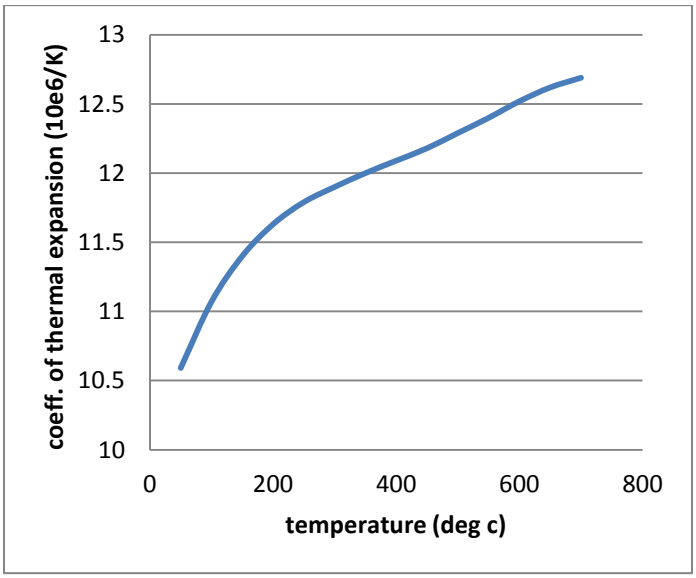

Fig. 5.10 - Material properties of disc Thermal Conductivity, Young's Modulus and Coefficient of Thermal Expansion, w.r.t. Temperature

Table 4: Time Hardening Creep Coefficients for Nickel Based Superalloy

Time Hardening Coefficient				
Temperature	C1	C2	C3	C4
(Deg C)				
350	2.21E-40	12.78399	-0.70426	0
355	1.56E-39	12.50582	-0.70521	0
360	1.09E-38	12.22843	-0.70617	0
365	7.51E-38	11.95181	-0.70715	0
370	5.14E-37	11.67596	-0.70814	0
375	3.48E-36	11.40088	-0.70915	0
380	2.33E-35	11.12657	-0.71016	0
385	1.54E-34	10.85303	-0.7112	0
390	1.01E-33	10.58026	-0.71224	0
395	6.56E-33	10.30826	-0.71331	0
400	4.21E-32	10.03704	-0.71438	0
405	2.68E-31	9.766587	-0.71547	0
410	1.68E-30	9.496904	-0.71657	0
415	1.05E-29	9.227993	-0.71769	0
420	6.45E-29	8.959854	-0.71882	0
425	3.93E-28	8.692485	-0.71996	0
430	2.37E-27	8.425888	-0.72112	0
435	1.41E-26	8.160061	-0.72229	0
440	8.35E-26	7.895006	-0.72347	0
445	4.88E-25	7.630723	-0.72467	0
450	2.82E-24	7.36721	-0.72588	0
455	1.61E-23	7.104469	-0.72711	0
460	9.13E-23	6.842498	-0.72835	0
465	5.12E-22	6.581299	-0.7296	0
470	2.84E-21	6.320872	-0.73087	0
475	1.56E-20	6.061215	-0.73215	0
480	8.45E-20	5.80233	-0.73345	0
485	4.54E-19	5.544215	-0.73476	0
490	2.41E-18	5.286872	-0.73608	0
495	1.27E-17	5.030301	-0.73742	0
500	6.6E-17	4.7745	-0.73877	0

(Source: *Siemens Ltd.*)

Table 5: Calculated Strain Hardening Creep Coefficients for Nickel Based Superalloy by Analytical Method (Appendix A.3)

Strain Hardening Coefficient				
Temperature	C1	C2	C3	C4
(Deg C)				
350	1.48E-133	43.226	-2.381	0
355	4.23E-131	42.422	-2.392	0
360	1.19E-128	41.617	-2.403	0
365	3.32E-126	40.812	-2.414	0
370	9.12E-124	40.005	-2.426	0
375	2.48E-121	39.197	-2.438	0
380	6.69E-119	38.389	-2.450	0
385	1.78E-116	37.579	-2.462	0
390	4.74E-114	36.768	-2.475	0
395	1.24E-111	35.955	-2.488	0
400	3.25E-109	35.142	-2.501	0
405	8.42E-107	34.325	-2.514	0
410	2.16E-104	33.507	-2.528	0
415	5.562E-102	32.687	-2.542	0
420	1.421E-099	31.864	-2.556	0
425	3.61E-097	31.040	-2.571	0
430	9.17E-095	30.213	-2.586	0
435	2.32E-092	29.383	-2.6008	0
440	5.88E-090	28.551	-2.616	0
445	1.489E-087	27.715	-2.632	0
450	3.77E-085	26.876	-2.648	0
455	9.56E-083	26.034	-2.664	0
460	2.43E-080	25.188	-2.681	0
465	6.19E-078	24.339	-2.698	0
470	1.58E-075	23.486	-2.715	0
475	4.08E-073	22.629	-2.733	0
480	1.05E-070	21.768	-2.751	0
485	2.75E-068	20.902	-2.770	0
490	7.23E-066	20.032	-2.789	0
495	1.92E-063	19.157	-2.808	0
500	5.13E-061	18.28	-2.828	0

5.3 Validation of experimental data with ANSYS

We have discussed in previous chapters that the cumulative creep strain i.e. equivalent creep strain in time hardening and strain hardening give same results at constant stress and temperature condition experimentally and analytically [17, 51]. Here, the analysis is done at constant stress and ambient condition with the help of ANSYS numerical method with strain hardening model and time hardening model. Temperature is taken as constant during the analysis. ANSYS has given good agreement as shown in fig. 5.11 and validates previous research papers.

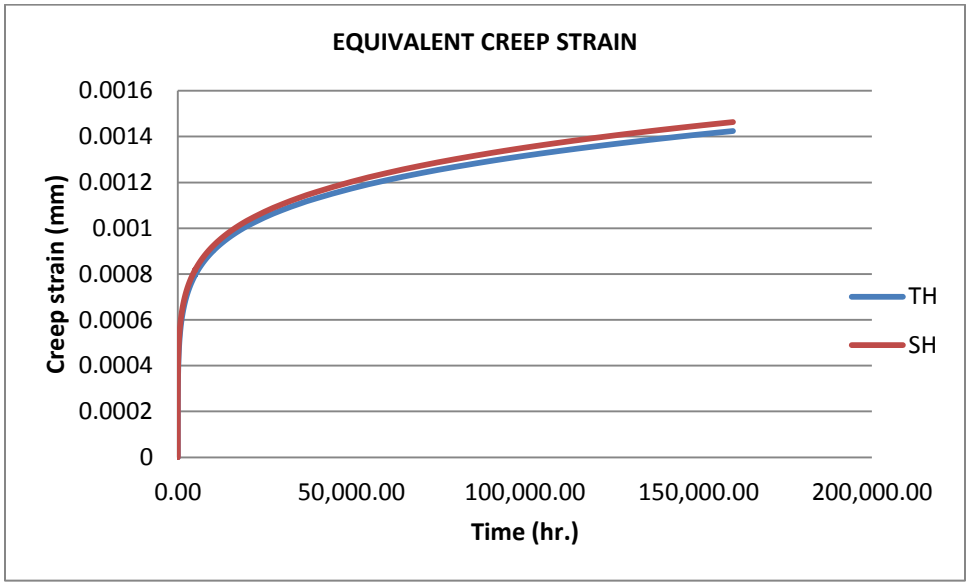

Fig. 5.11: Comparison of creep curve of disc at constant stress and temperature with time hardening and strain hardening

This present work is done at constant and variable temperature with time hardening mathematical model as well as strain hardening mathematical model. Analysis has also been done with variable pressure for both of the models since strain hardening gives better results than time hardening at variable applied pressure.

5.4 Estimated Results

5.4.1 Creep of Disc at Constant Ambient Condition

Creep estimation of disc at constant ambient temperature i.e. 32^0c has been calculated in this section. The result will analyse the time hardening model as well as strain hardening model at constant temperature.

5.4.1.1 Stress Distribution

The axial, hoop and radial stresses are shown in the below figures.The analysis proves the theoretical results as well that the hoop stress is maximum at the bore of the disc, the radial stress is maximum in between the disc in radial direction while axial stress is maximum at the top region of applied axial load.

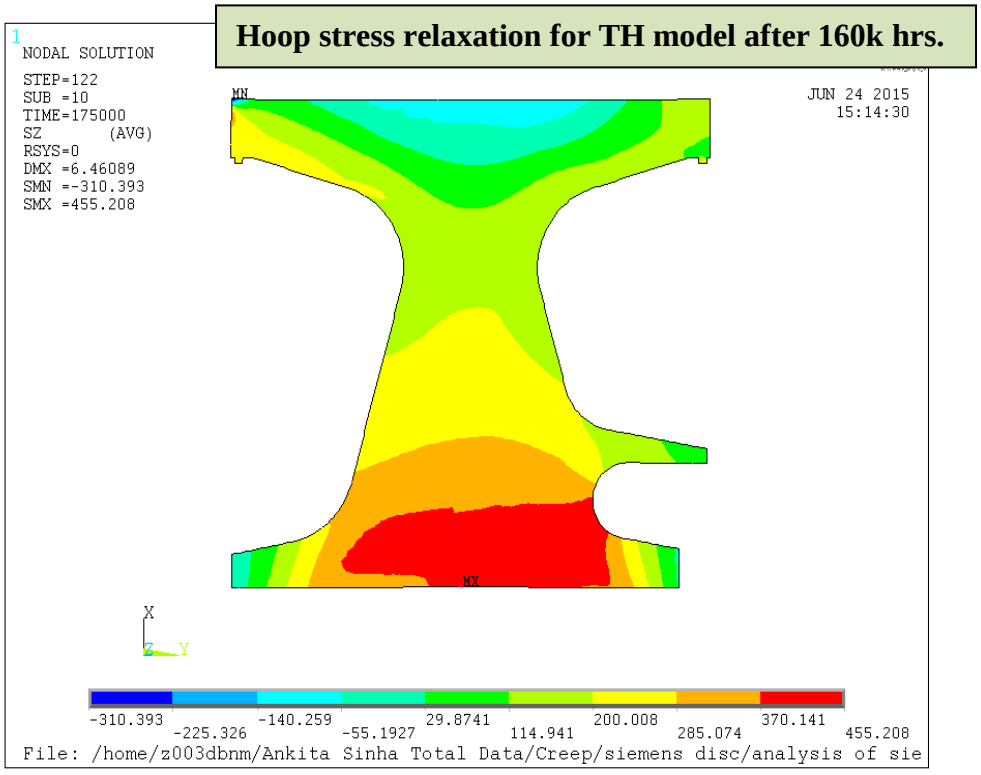

Figure 5.12 : Hoop stress distribution model at constant temp. for time hardening model after 160k hours.

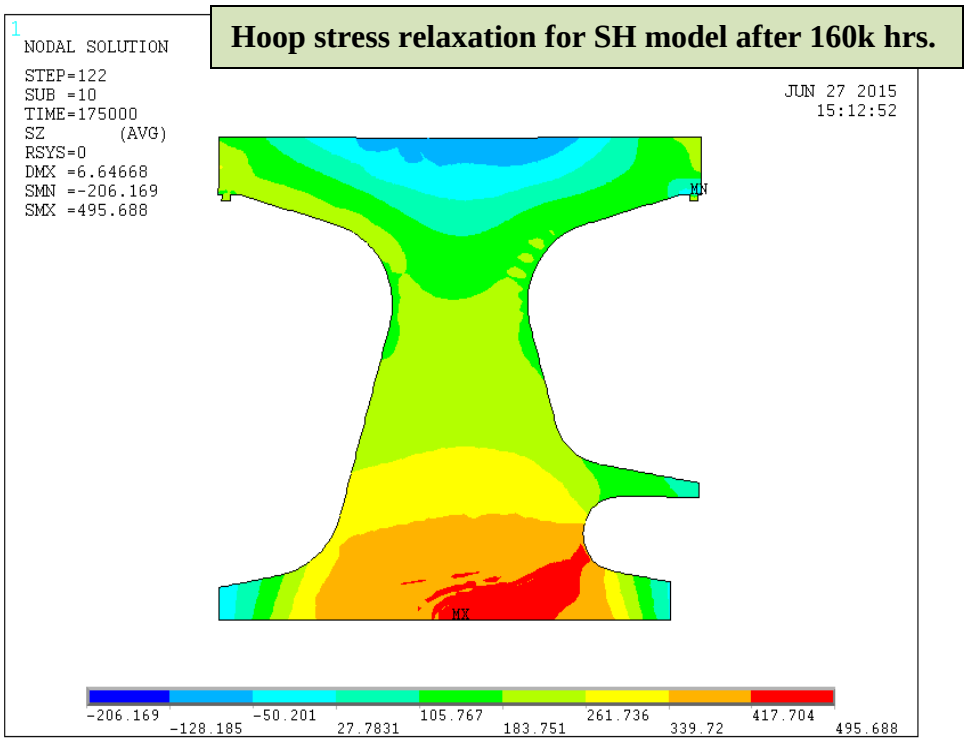

Figure 5.13 : Hoop stress distribution model at constant temp. for Strain hardening model after 160k hours.

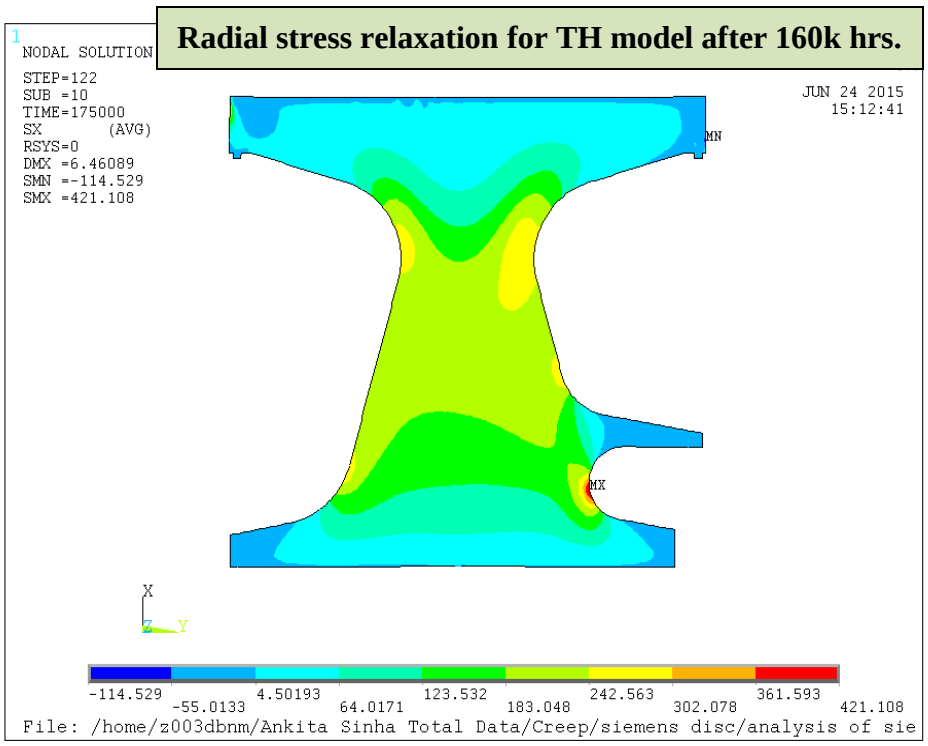

Figure 5.14 : Radial stress distribution model at constant temp. for Time Hardening model after 160k hours.

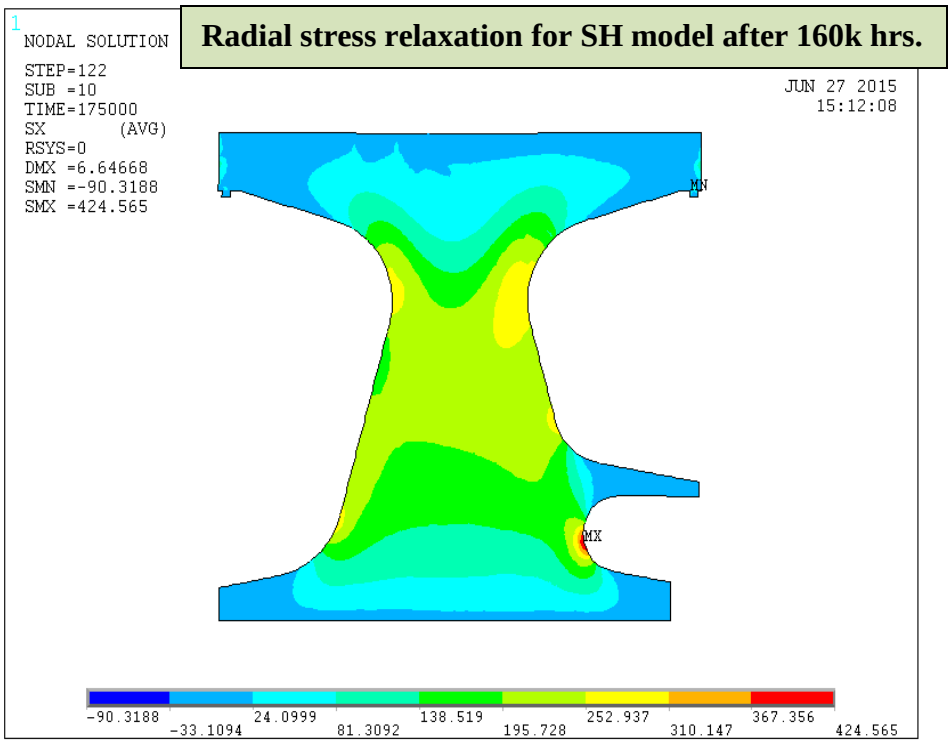

Figure 5.15 : Radial stress distribution model at constant temp. for Strain Hardening model after 160k hours.

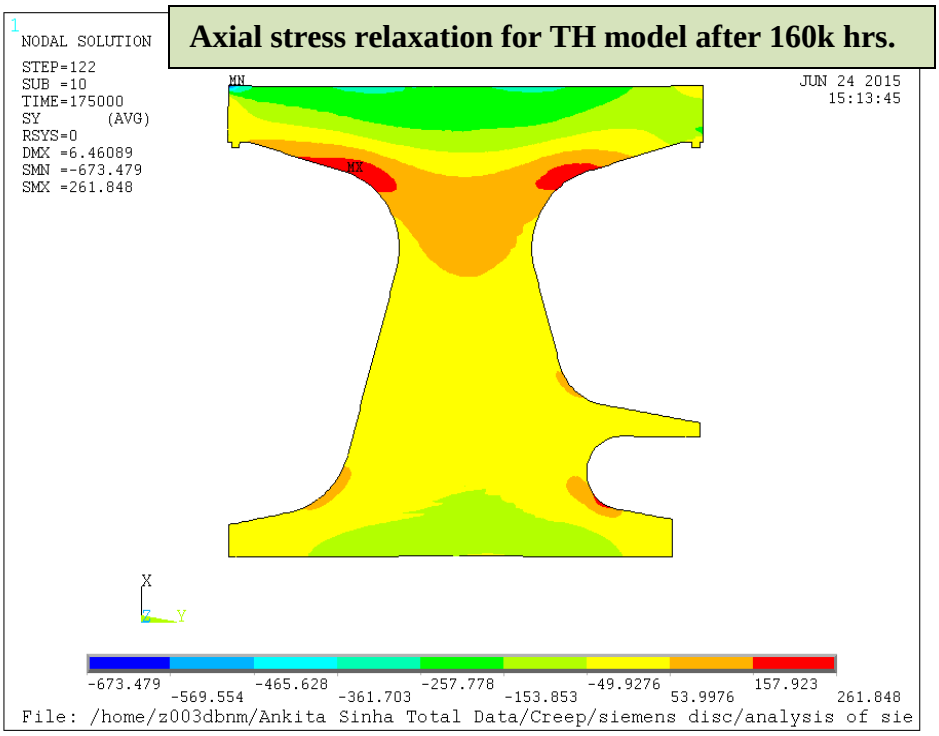

Figure 5.16 : Axial stress distribution model at constant temp. for Time Hardening model after 160k hours.

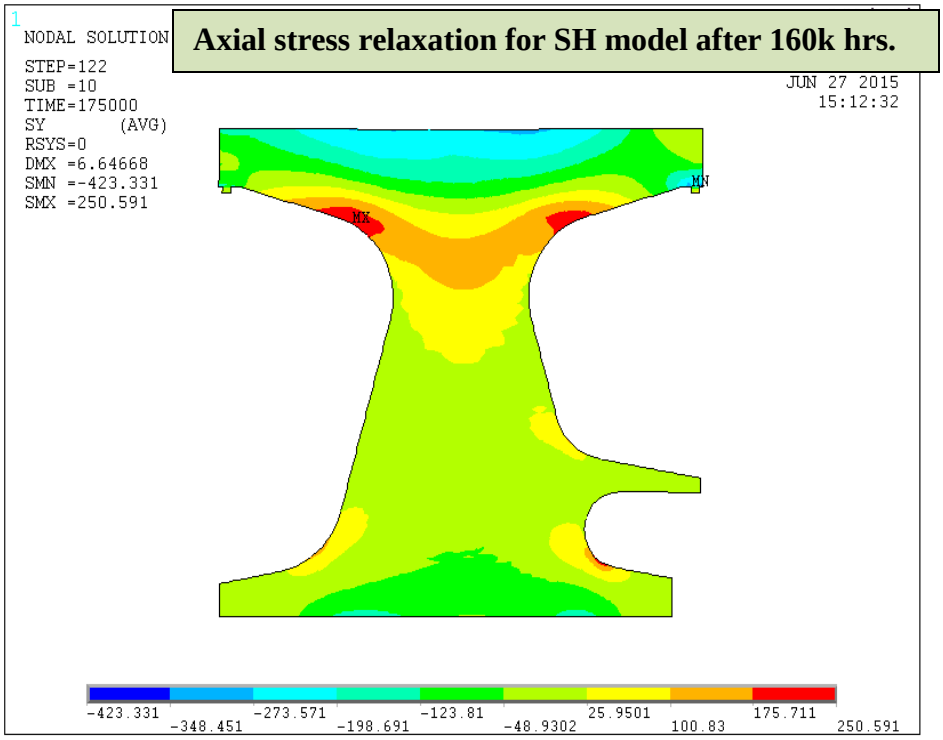

Figure 5.17: Axial stress distribution model at constant temp. for Strain Hardening model after 160k hours.

5.4.1.2 Creep Strain in Terms of Axial and Radial Distortion

Creep strain results the distortion of the disc in different directions. The equivalent creep strain is shown in figure 5.18 for time hardening creep model and for strain hardening creep model, it is shown in fig. 5.19. The analysis has been done for 160k hours. With the current loading condition disc tries to grow radially, So creep is estimated here in terms of axial shortening and radial lengthening with time. The radial elongation and axial shortening because of creep is shown here for the better understanding. Primary zone and secondary zone are correctly captured as shown in the figure 5.20 and 5.21. For initial few years, major creep distortion happens which shows the primary region or transition phase of creep curve. Secondary region has been captured just after primary region where creep rate is almost constant. ANSYS can't predict creep failure region i.e. tertiary region and this can also be seen in the graph shown below. Time hardening model and strain hardening model have different behaviour as shown in figure as they follow different characteristics passed from the start of the test at every current point.

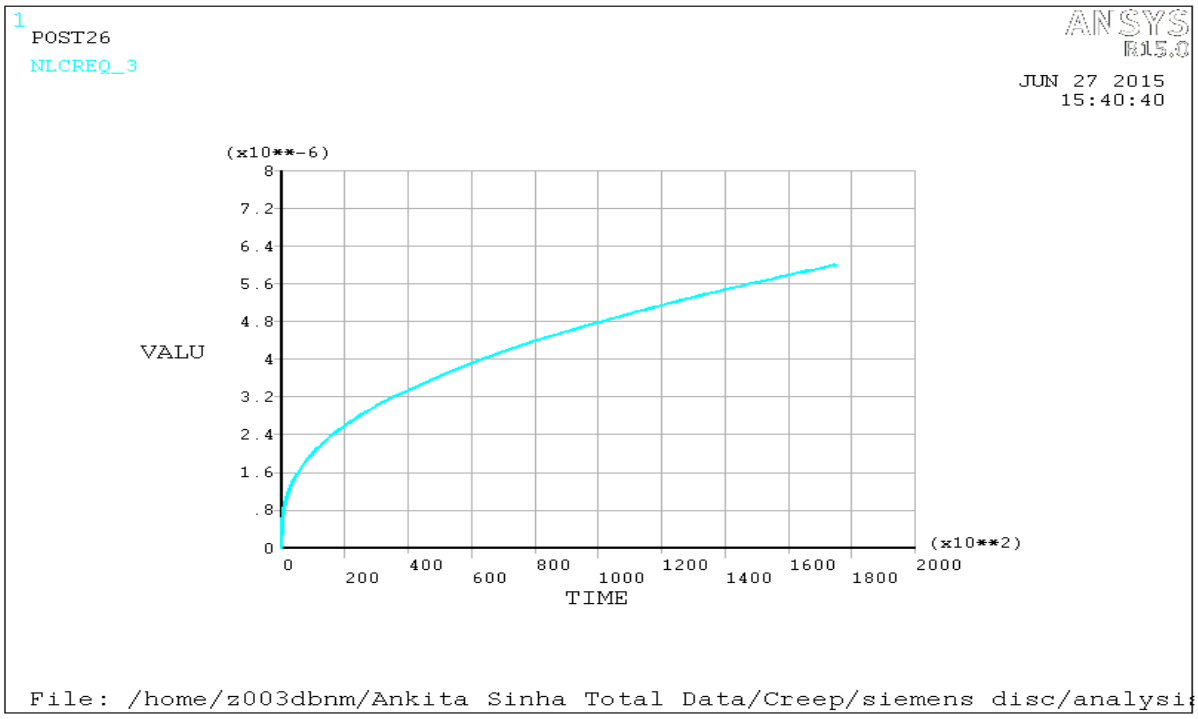

Fig. 5.18: Eqv. Creep strain variation with temperature at radially upmost nodal point of disc for Time Hardening model

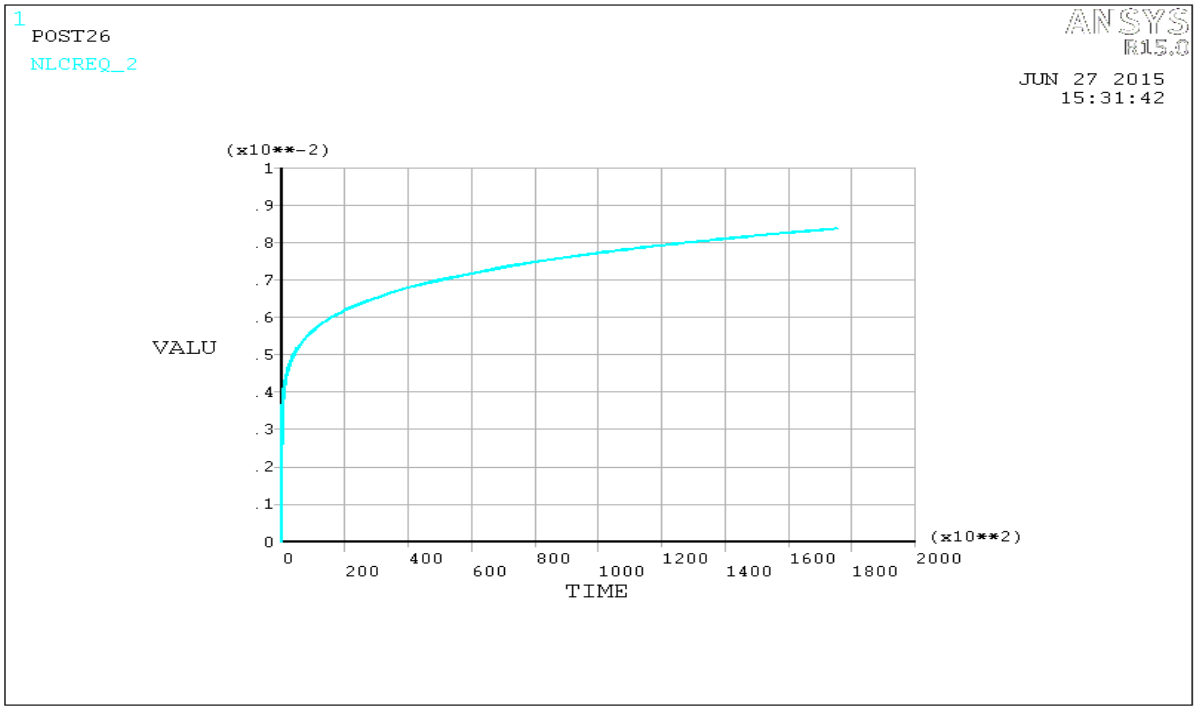

Fig. 5.19: Eqv. Creep strain variation with temperature at radially upmost nodal point of disc for Strain Hardening model

The above shown figure5.18 and figure 5.19 represent equivalent creep strain at the radial upmost point of disc. The radial elongation and axial compression of time hardening model and strain hardening model are calculated by taking data of displacement at different nodal points from ANSYS postprocessing.

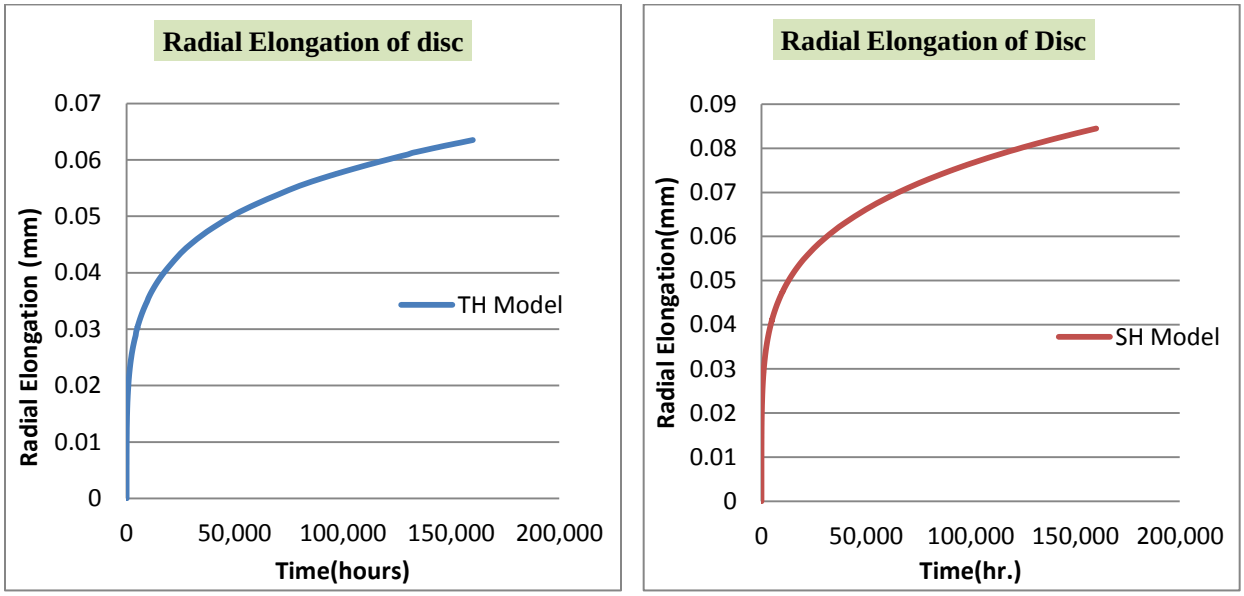

Fig. 5.20 : Final radial elongation of disc at radially upmost nodal point in time hardening model and strain hardening model after 160k hours.

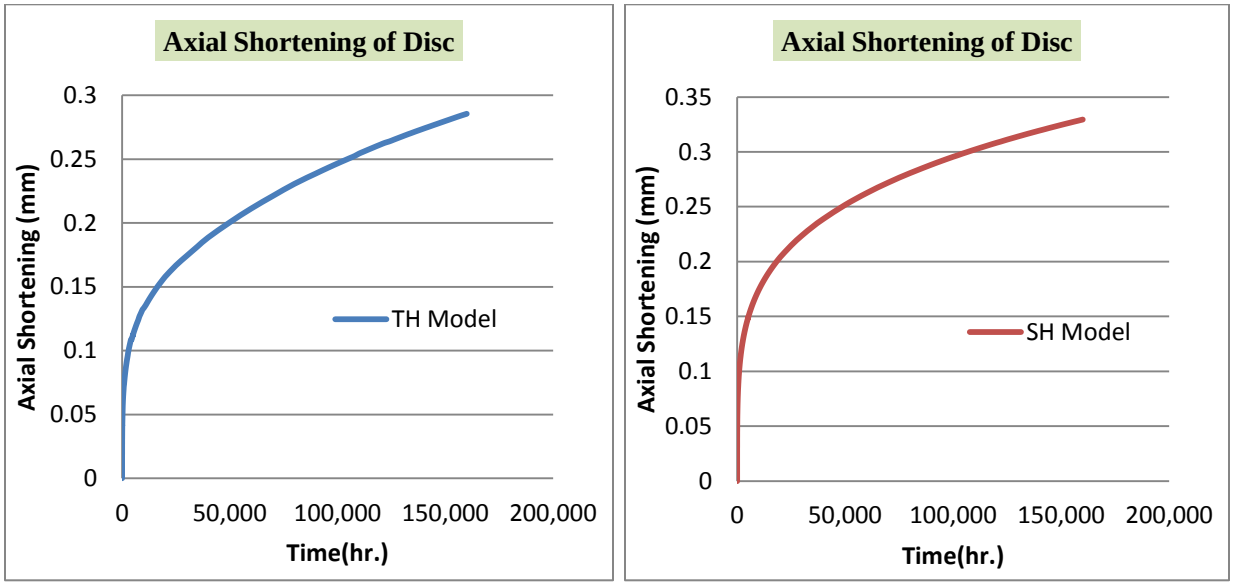

Figure 5.21: Axial Compression of Disc in Time Hardening model and Strain hardening model after 160k hours.

5.4.1.3 Comparisons of Estimated Results

The present work of creep strain of disc for time hardening model and strain hardening model in terms of radial elongation and axial shortening at constant ambient temperature 32^0C are compared. The comparisons are done with both of the model are shown in figure 5.22 and 5.23 for 160k hours. Here, it is clear that strain hardening gives over predicted result and time hardening model is more constrained. This paper work is more concerned about the creep analysis at variable ambient temperature; even though it can be seen that strain hardening mathematical model gives different results than time hardening. Radial elongation in case of strain hardening exceeded by 0.02 mm while axial shortening has increased by approx. 0.04 mm.

Hence, it can be concluded that time hardening creep mathematical model is more constrained that strain hardening even at constant ambient temperature 32^0C and it can lead the failure of disc before the time.

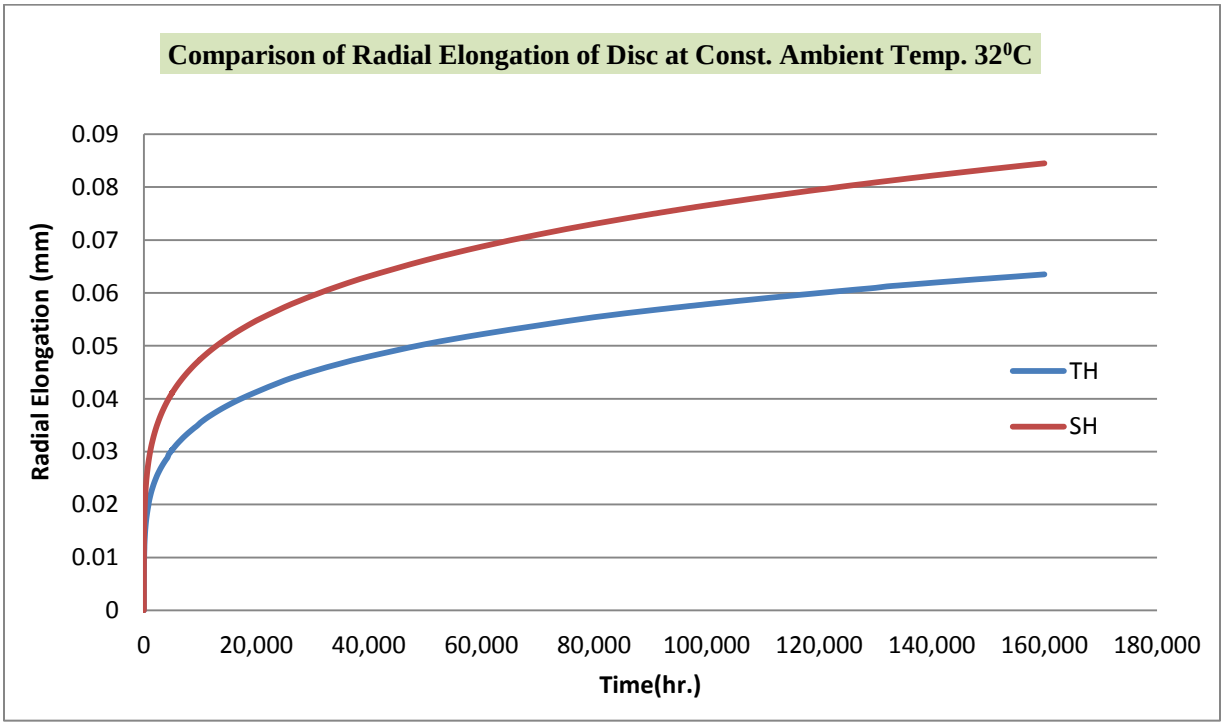

Figure 5.22: Comparison of Radial Elongation of disc at constant ambient temp. 32^0C for Time Hardening and Strain Hardening model after 160k hrs.

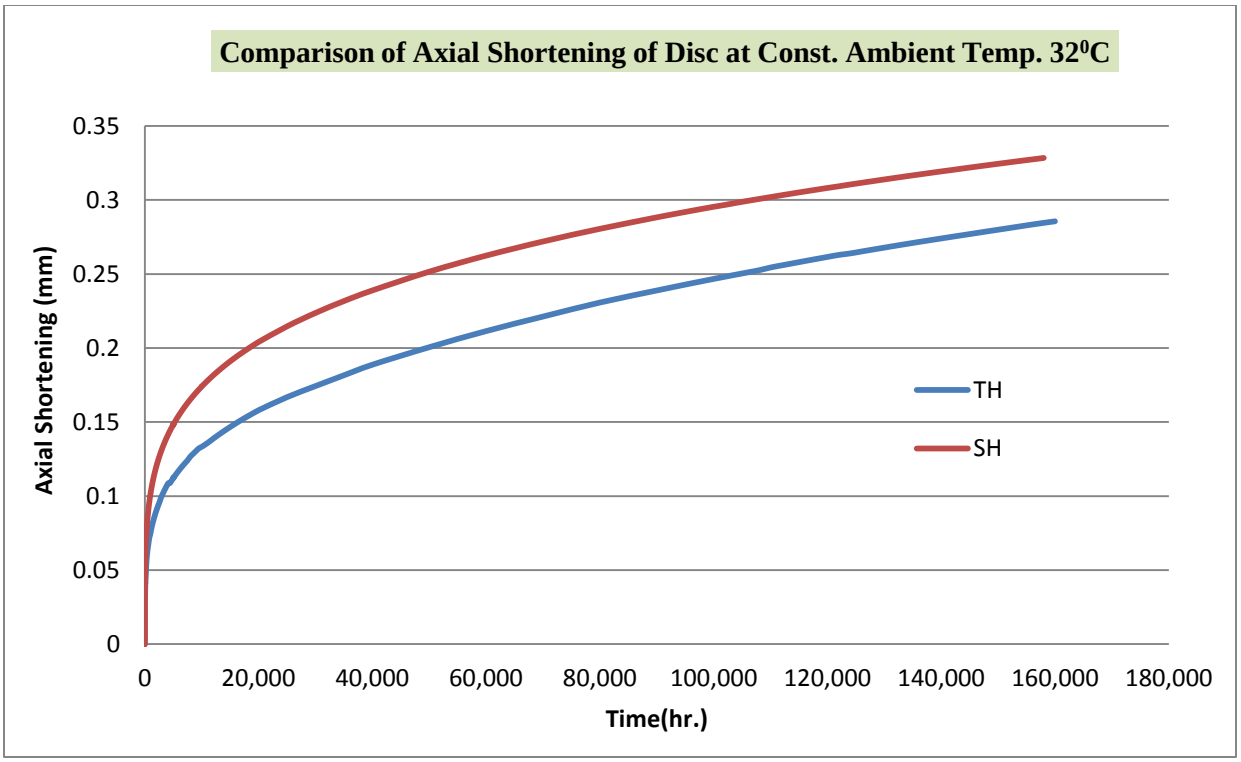

Figure 5.23: Comparison of Axial Shortening of disc at constant ambient temp. 32^0C for Time Hardening and Strain Hardening model after 160k hrs.

5.4.2 Creep of Disc at Variable Ambient Temperature

In this present section, variable ambient temperature has been taken while calculating creep strain instead of constant temperature. The disc temperature profile along the radial direction is varied monthly with time along the year as shown in figure 5.5. If we see the actual case of gas turbine working process, the temperature of disc will vary with time because of the variation in ambient temperature conditions. Sometimes ambient temperature goes down and sometimes it increases because of the geographical conditions. It is also known that creep will be higher in maximum temperature zone area. Sometime considering average ambient temperature as constant throughout GT life span does not lead into correct creep prediction. So to study the variations in result due to varying ambient condition, one hot condition temperature data of city Abu Halifa (Kuwait) throughout the year has taken. The graph is showing clearly how the temperature is varying throughout the year. Twelve temperature profiles are given as an input in structural analysis. This calculation has been done by considering only time hardening creep mathematical model first then strain hardening. This calculation has been done for 160K hour's standard GT life span in which component has to intact with regard to creep distortion. The yearly average temperature of data taken is calculated as 35^0c which is more than 32^0c which was taken as the standard constant average ambient temperature for previous analysis. Further, comparisons have also done in next part of the chapter.

5.4.2.1 Stress Distribution

The stress produced in this analysis at variable ambient temperature condition is different from the analysis done at constant temperature condition. This analysis has also been done for 160k hours. Max hoop stress after 160K hours of operation is 464 MPa in the present case while in constant ambient condition it was 455 MPa. Radial stress and axial stress is also less than previous calculations. So better understanding is required for hot ambient condition where average data is little higher than 32^0c.

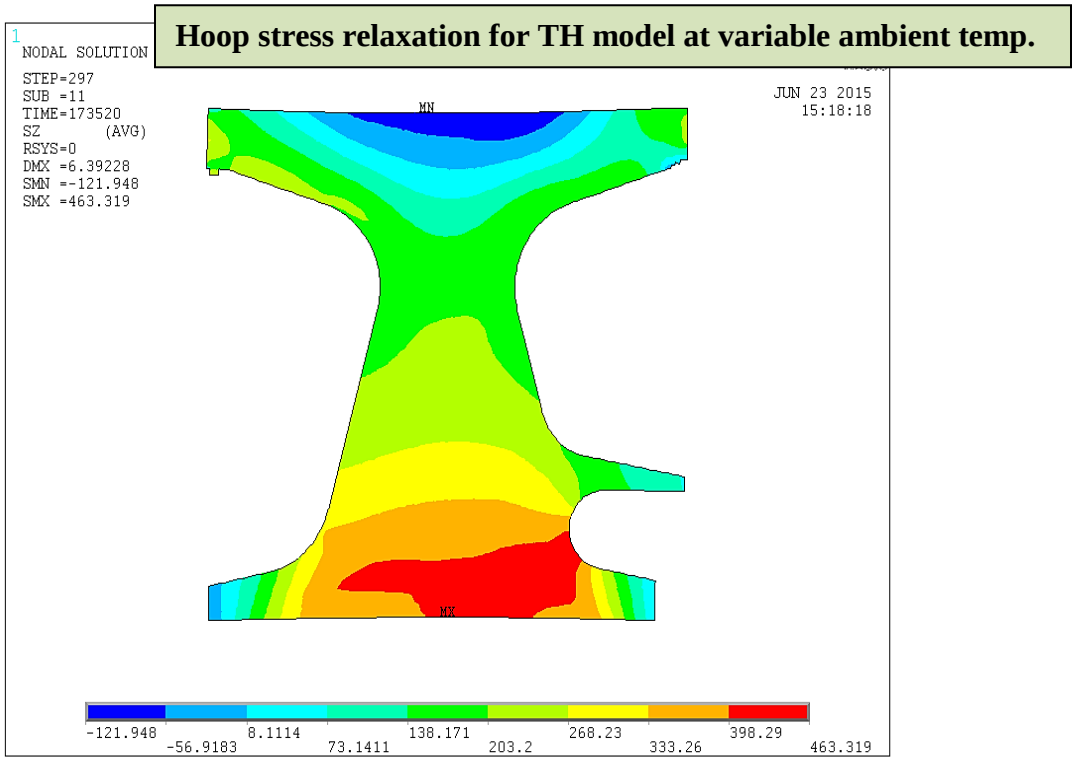

Figure 5.24: Hoop stress distribution of disc at variable ambient temp. for Time Hardening model after 160k hrs.

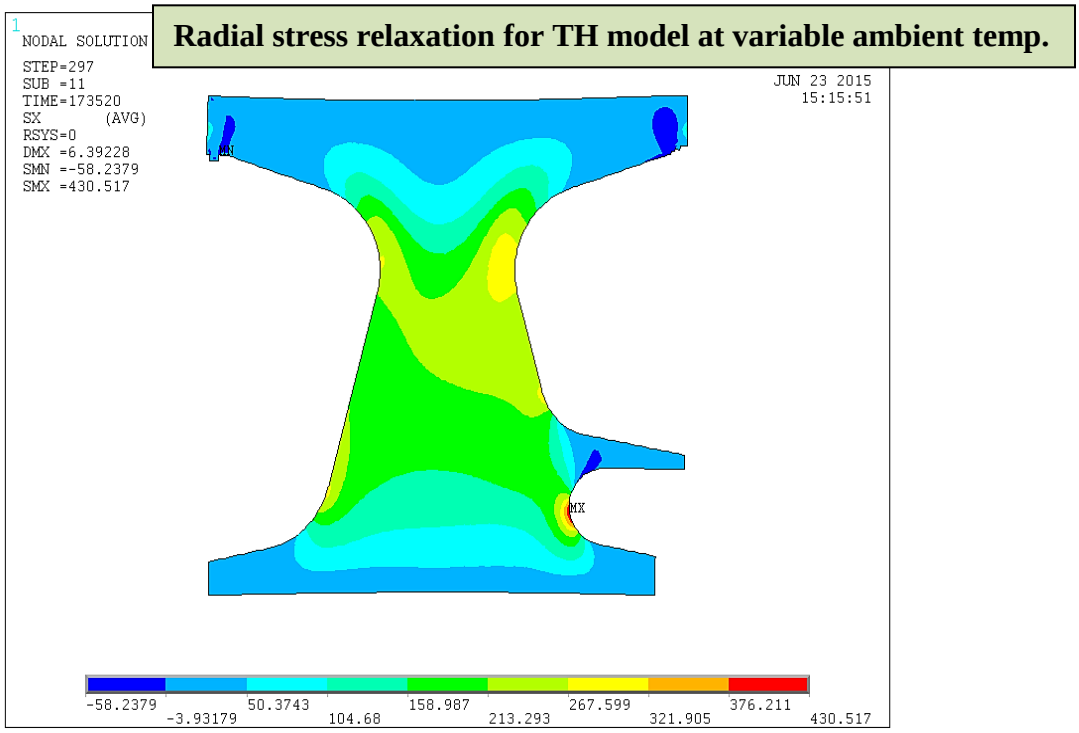

Figure 5.25: Radial stress distribution of disc at variable ambient temp. for Time Hardening model after 160k hrs.

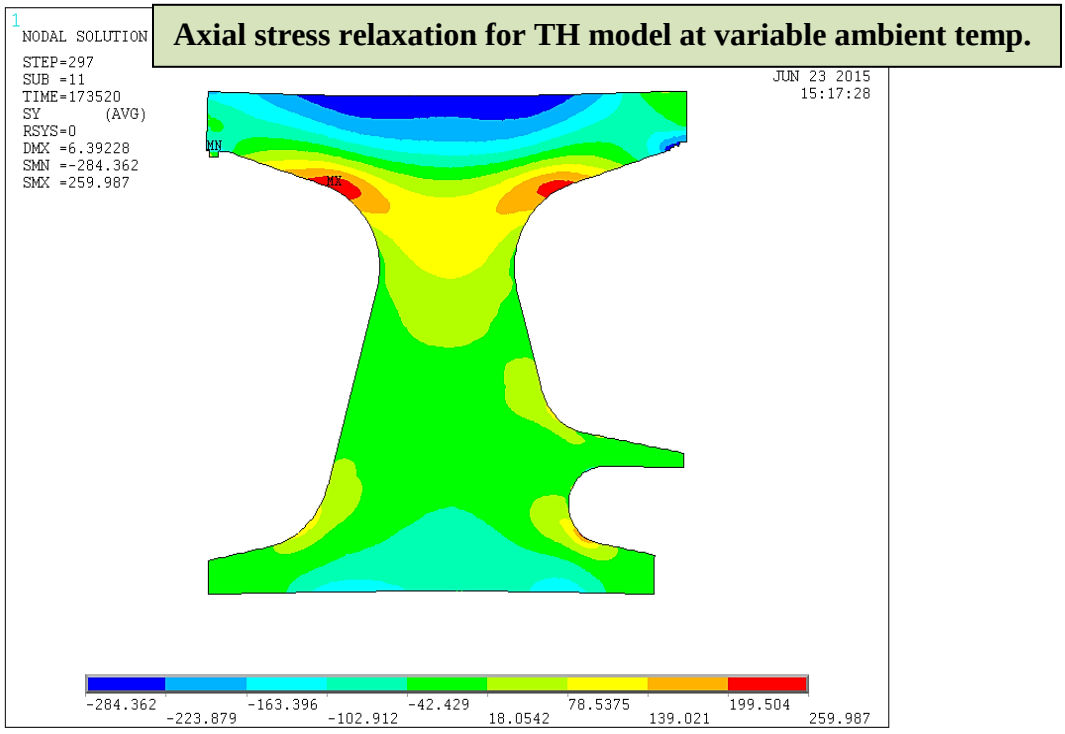

Figure 5.26: Axial stress distribution of disc at variable ambient temp. for Time Hardening model after 160k hrs.

5.4.2.2 Creep Strain in Terms of Axial and Radial Distortion

Since temperature is varying over the year, the results came out is very different from the previous analysis. In fact, creep strain is also varying maximum to minimum with time according to the temperature. Radial and axial distortion is also come out in a sinusoidal manner because of monthly varying temperature. This analysis is also done for 160 hours. The equivalent creep strain at radially upmost nodal point is almost 3 mm after 160k hours in this case as shown in fig. 5.27 which was almost 6 mm in the case of constant ambient temperature.

In figure 5.28 and 5.29, radial elongation and axial compression are shown at variable ambient temperature condition. The maximum radial elongation is calculated as 0.34 mm while axial compression is calculated as 0.45 mm.

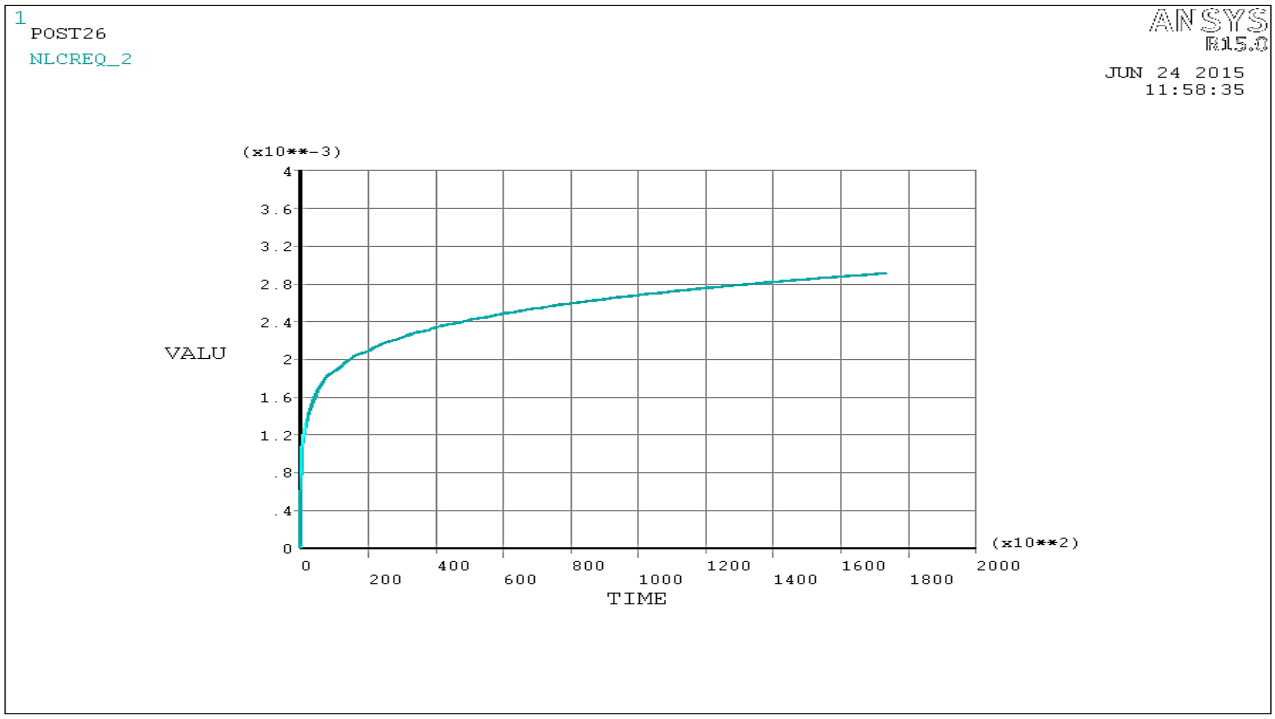

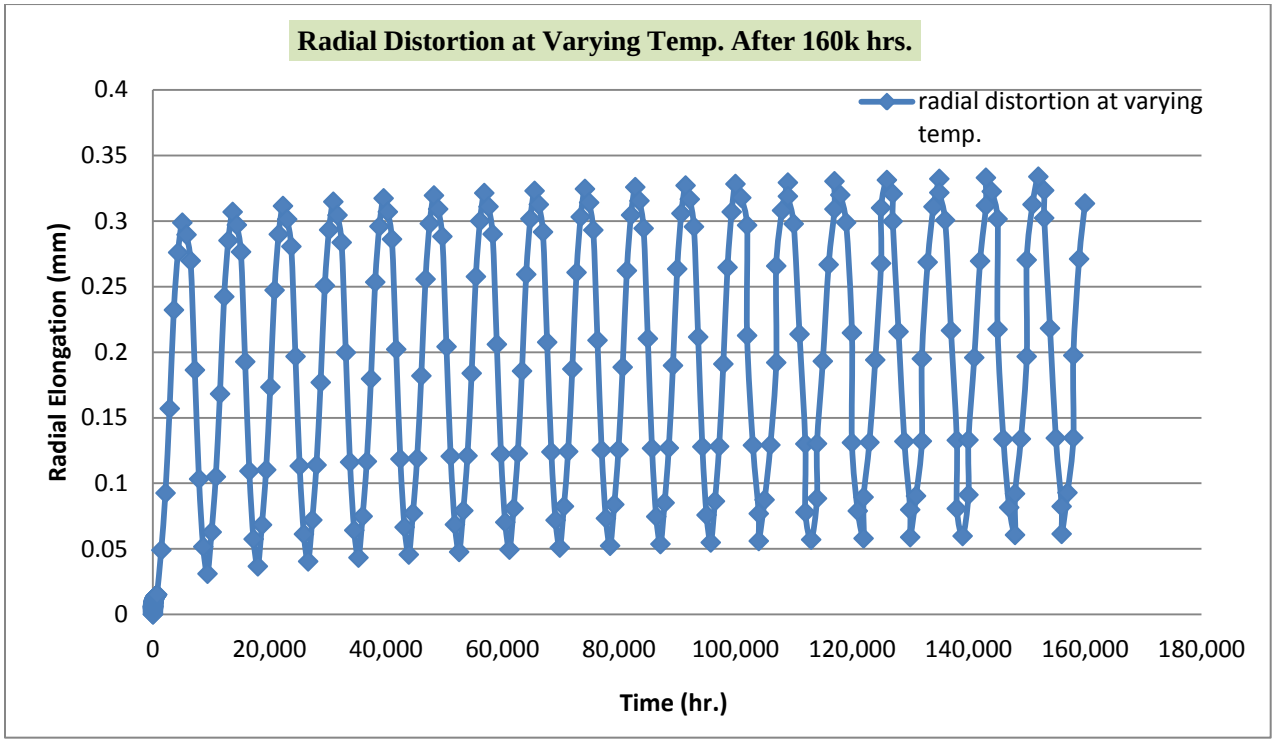

Fig. 5.28: Radial elongation of rotor disc at varying ambient temperature after 160k hours.

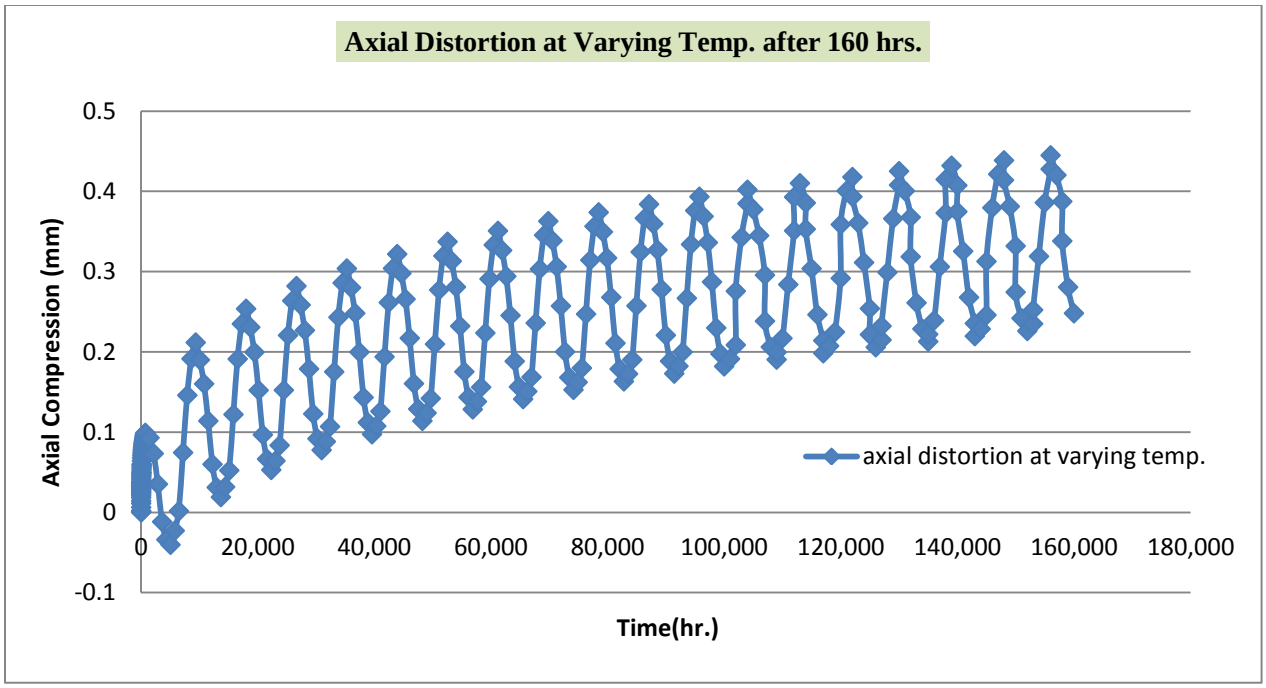

Figure 5.29: Axial distortion of rotor disc at varying ambient temperature after 160k hrs.

5.4.3 Comparisons of Estimated Results at Const. Ambient Condition and Variable Ambient Condition

Comparisons of estimated results have given good outcome. It is clear from the fig. 5.30 that axial displacement at constant ambient temperature and at variable ambient temperature will move with the same proportion. At constant ambient condition, the maximum distortion will rise about 0.3mm while at variable ambient condition; the maximum distortion will vary from 0.25 to 0.45mm. This may lead to distortion in rotor section. The constant ambient temperature taken is 32^0c while the average temperature of data taken from city Abu Halifa (Kuwait) is almost 35^0c. So, graph at constant temperature did not pass through the mid-point of variable temperature curve. Apart from this, disc will distort in a cyclic manner because of cyclic temperature variation throughout the year. Due of these process, shortening will occur in the axial direction of disc and it will lead to dynamic instability and clearance issue between rotor and stator part of GT. Hence, the simulation of axial shortening and radial elongation at 32^0C constant average temperature will give less value but actually it would be higher in reality. If we see fig. 5.31, we will find that radial displacement of disc variation with time at constant ambient temperature is exactly equal to the minimum radial displacement of disc at variable ambient conditions with time which is almost equal to 0.06mm. the maximum radial displacement calculated at variable ambient conditions is 0.34mm which is very high value than at constant temperature. Hence this

condition will lead the rotor disc touch to the casing part which should be the limiting criteria in gas turbine rotor.

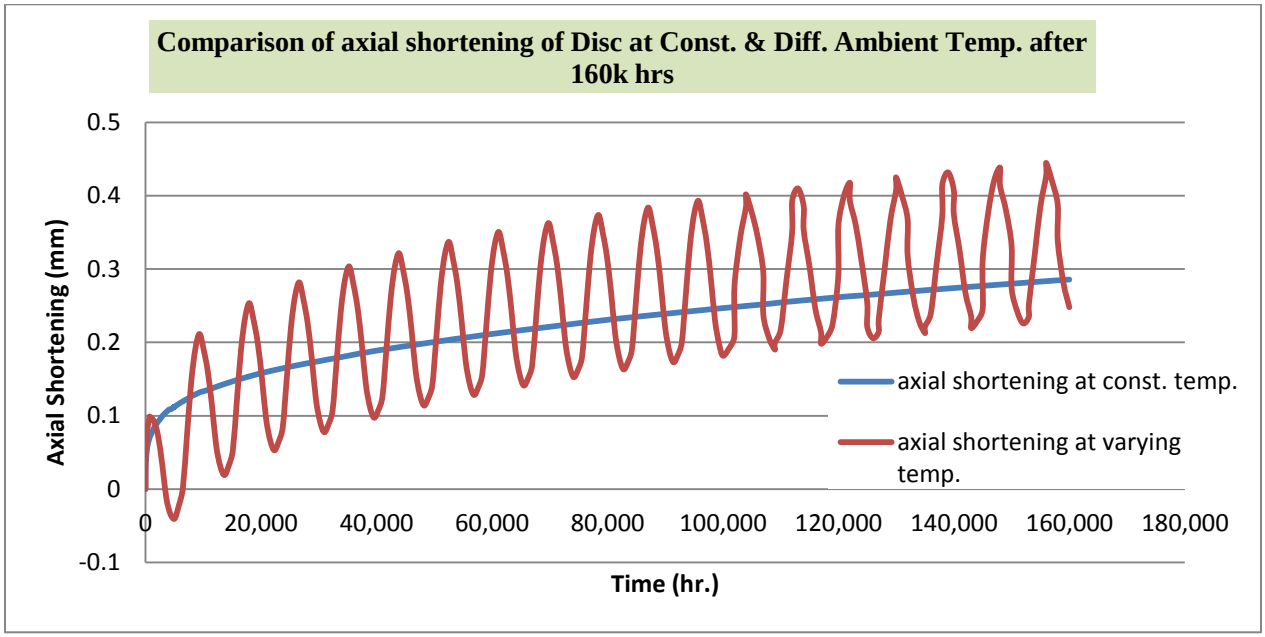

Fig. 5.30: Comparison of axial shortening of disc at const. ambient temp. 32^0C and at variable ambient temp. for Time Hardening model after 160k hrs.

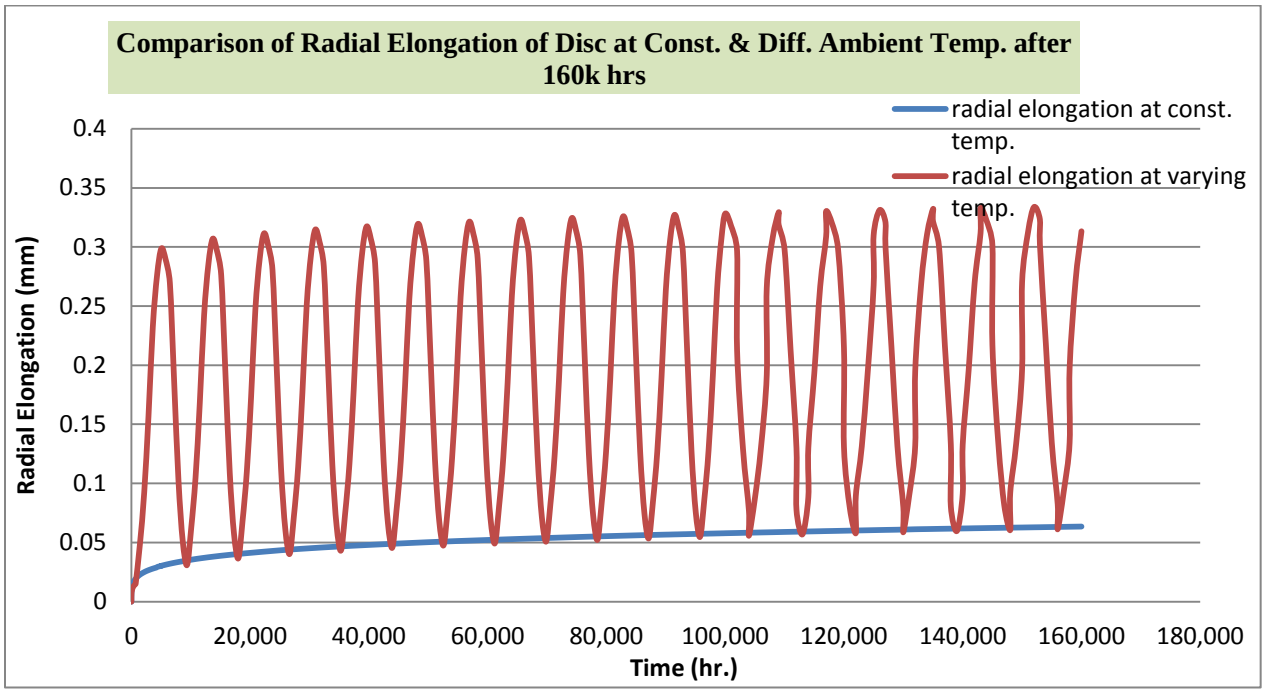

Fig. 5.31: Comparison of radial elongation of disc at const. ambient temp. 32^0C and at variable ambient temp. for Time Hardening model after 160k hrs.

5.4.4 Creep Estimation of Disc at Variable Temperature and pressure

During the study of related journals [17], we come to the point that if stress will increase or decrease after sometimes, cumulative creep strain will also differ in both of the models. Though, strain hardening will give more creep strain than time hardening with increasing stress; in power industries like gas turbine, axial pressure which hold all disc together will decrease with respect to time during the process. So in this part of work, analysis is done at variable ambient temperature and pressure. Here, it is assumed that pressure is reducing each year by one unit. ANSYS APDL coding for 160k hours has been done for analysis. For comparison purpose, time hardening model is also analyzed with varying temperature and pressure. Salient graphs are drawn for comparison.

5.4.4.1 Stress Distribution

Results of stress relaxation for time hardening as well as strain hardening model are clearly shown in figure 5.32 to 5.37. Here, difference of relaxation in hoop stress, radial stress and axial stress can be clearly predicted through all the figures shown below. Maximum hoop stress in case of strain hardening model is 496.4 MPa while it is approx. 462 MPa in case of time hardening model which is much lesser value. Radial stress and axial stress relaxation are predicting a little less value in case of strain hardening model than time hardening model. This analysis is also being done for 160k hours like before. ANSYS APDL coding has been written for this analysis at variable ambient temperature and pressure.

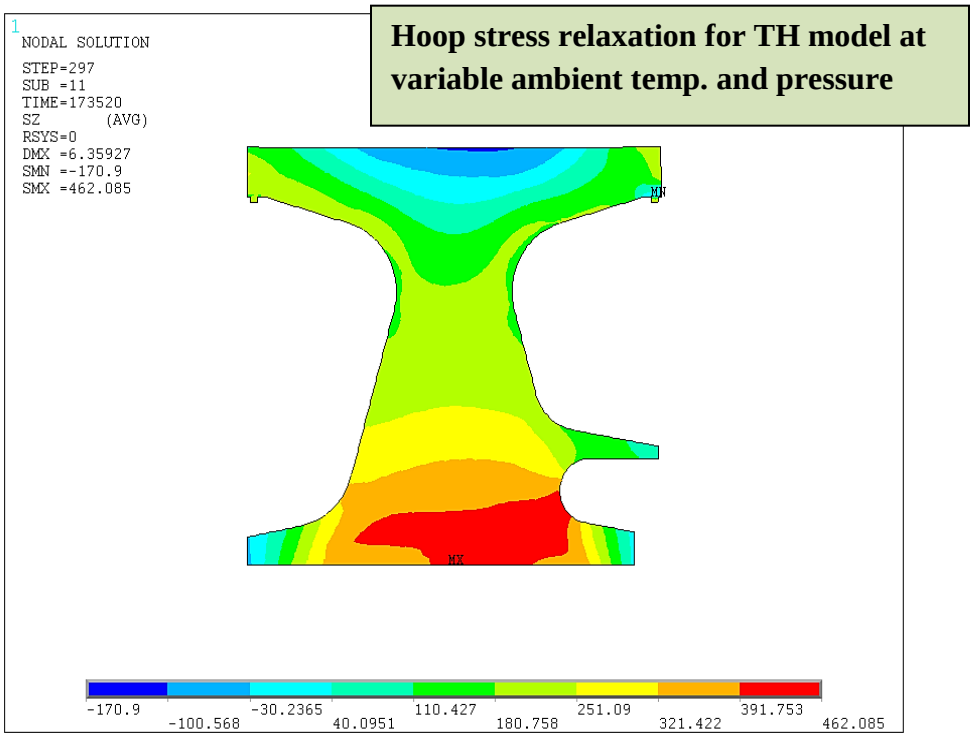

Fig. 5.32: Hoop stress of disc at variable ambient temp. and pressure for Time Hardening model after 160k hours.

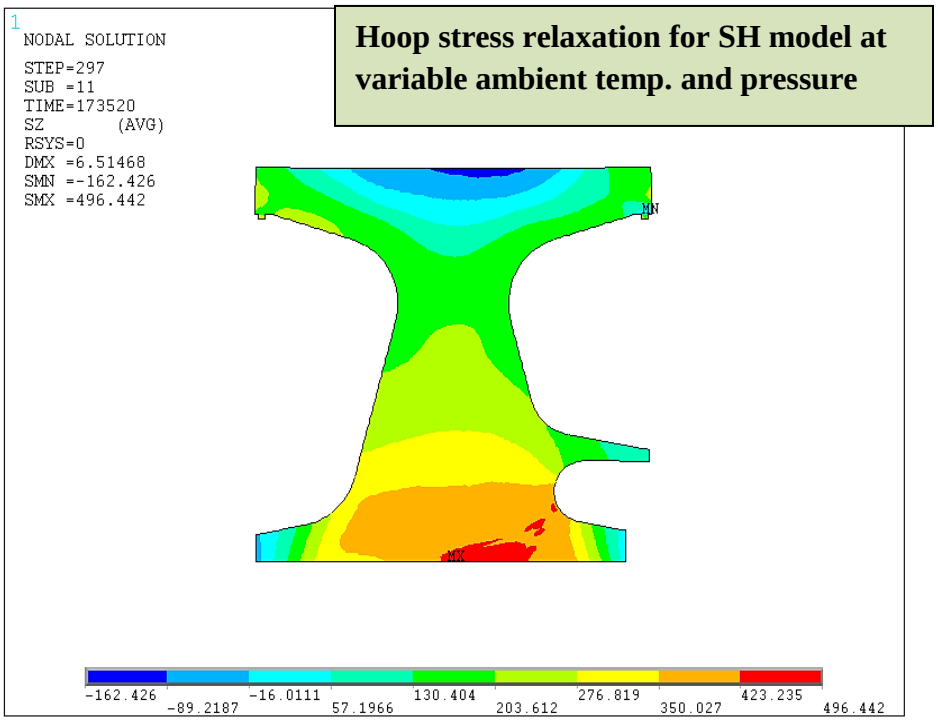

Fig. 5.33: Hoop stress of disc at variable ambient temp. and pressure for Strain Hardening model after 160k hrs.

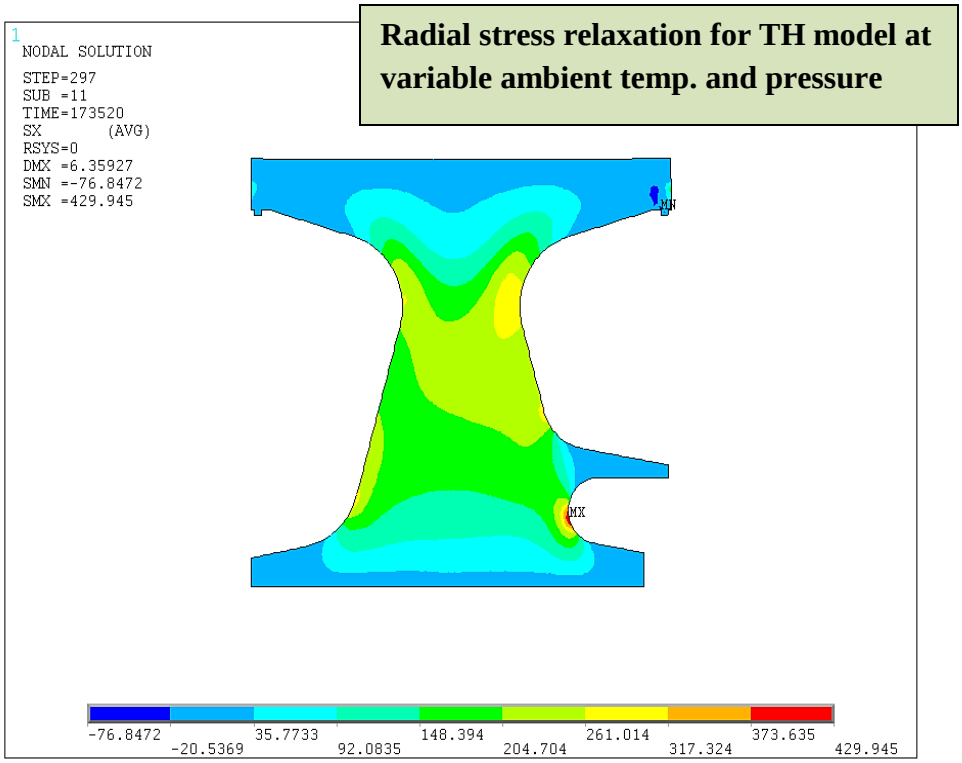

Fig. 5.34: Radial stress of disc at variable ambient temp. and pressure for Time Hardening model after 160k hrs.

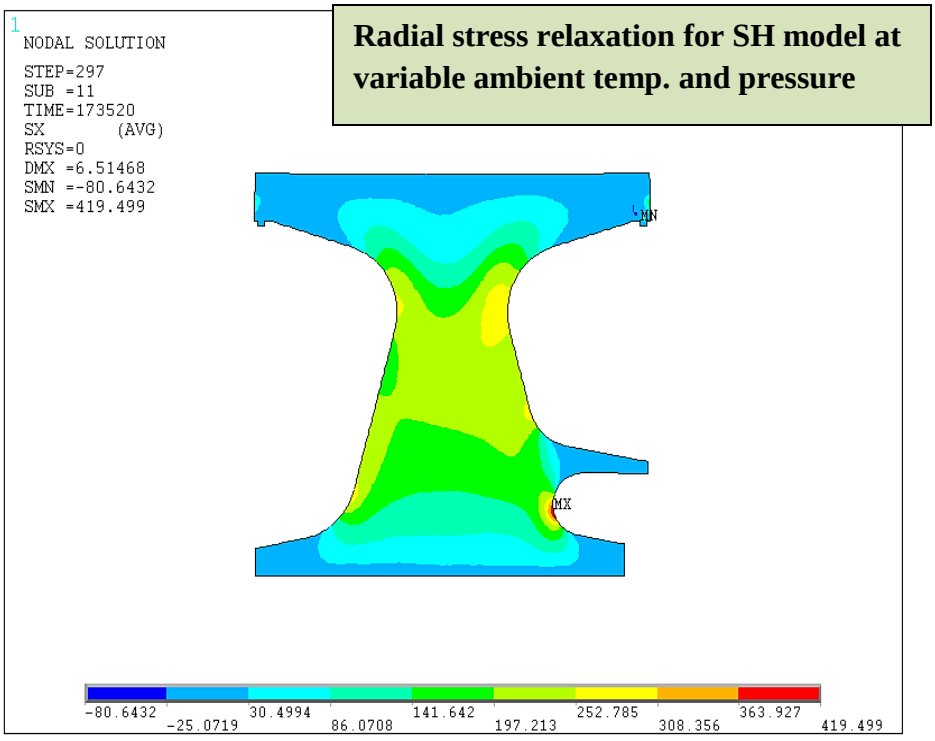

Fig. 5.35: Radial stress of disc at variable ambient temp. and pressure for Strain Hardening model after 160k hrs.

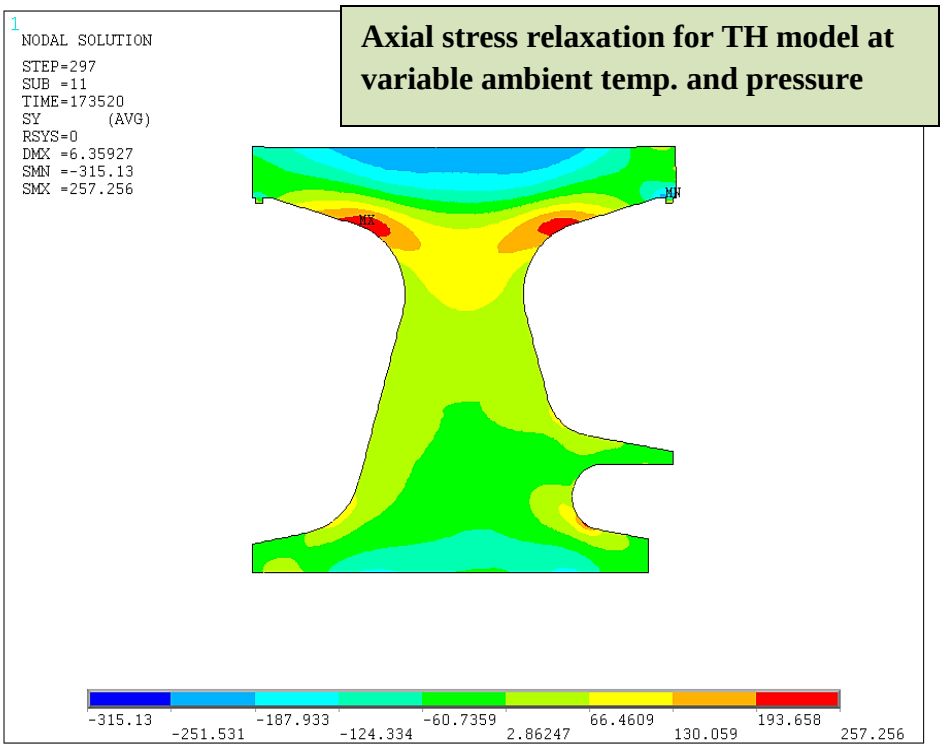

Fig. 5.36: Axial stress of disc at variable ambient temp. and pressure for Time Hardening model after 160k hrs.

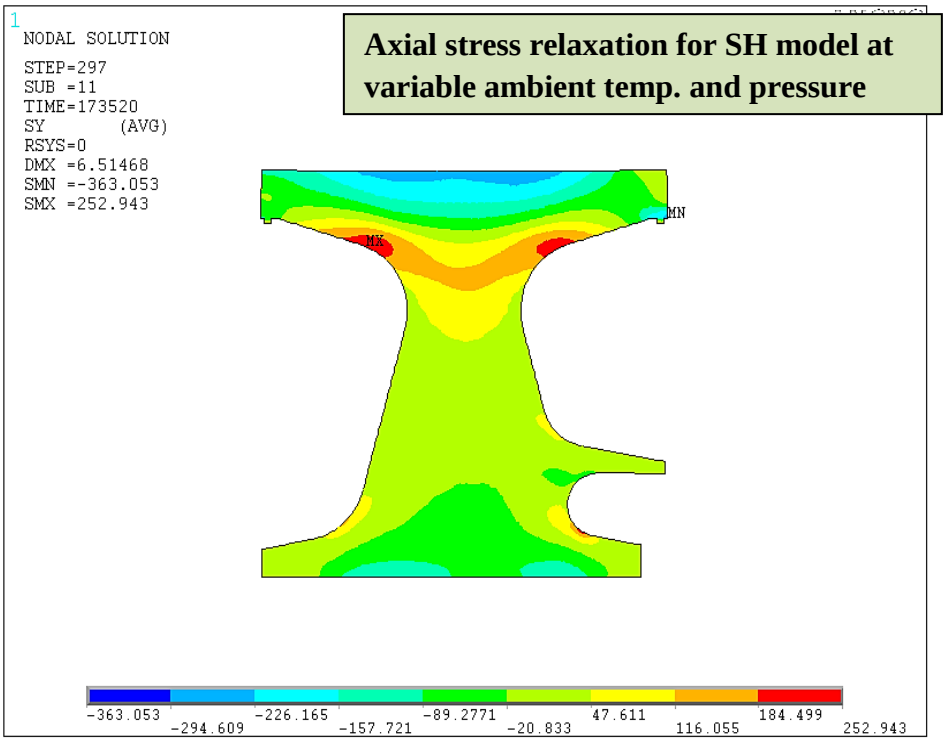

Fig. 5.37: Axial stress of disc at variable ambient temp. and pressure for Strain Hardening model after 160k hrs.

5.4.4.2 Comparisons of Creep Strain in Terms of Axial and Radial Distortion

Creep strain in terms of axial compression (shortening) and radial elongation is discussed here with the comparison graph as shown below in figure 5.38 and 5.39. It is clearly shown that the strain hardening model is over predicting the results than time hardening model. The radial elongation of strain hardening model is almost 0.025 mm more than time hardening model while the axial shortening increased in case of strain hardening model by 0.05 mm. It is quite clear that the analysis predicted by time hardening model will give conservative results. This may lead the failure of GT rotor disc. Hence, there is a need to further investigate creep analysis method with more rigorous analysis and better understanding is required for strain hardening model.

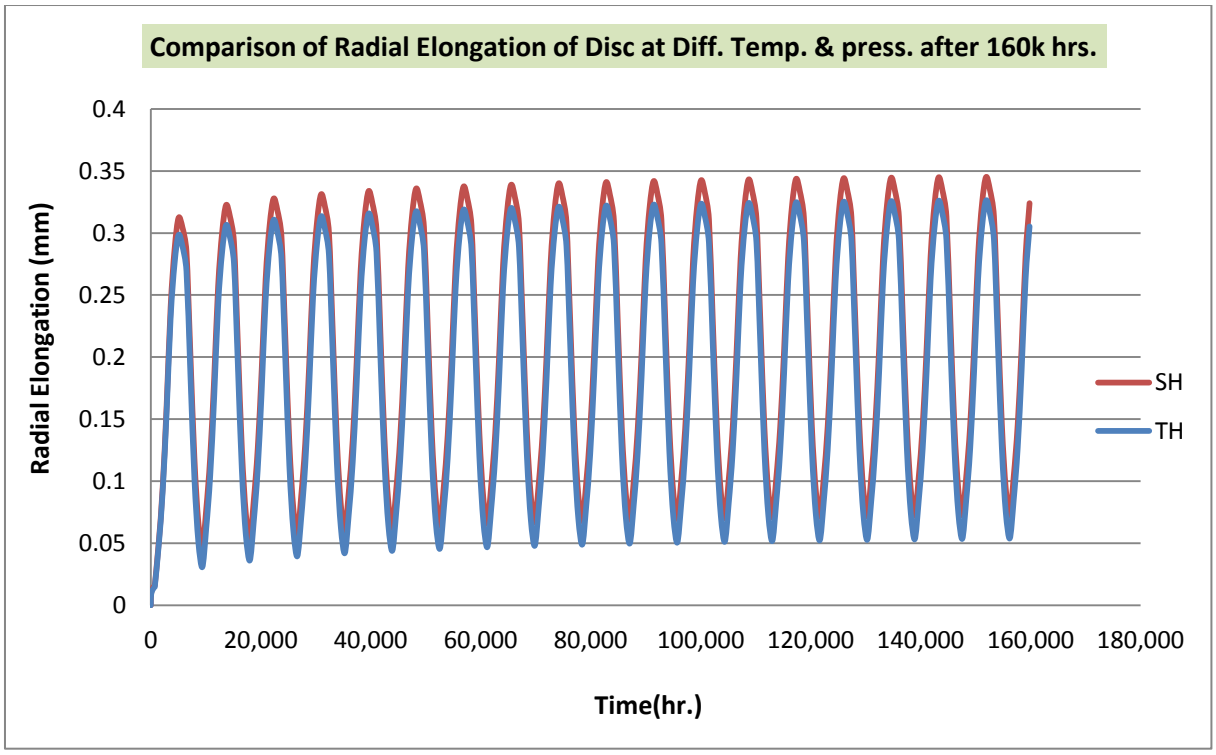

Fig. 5.38: Comparison of Radial Elongation of disc for Time Hardening and Strain Hardening model at variable ambient temperature and pressure

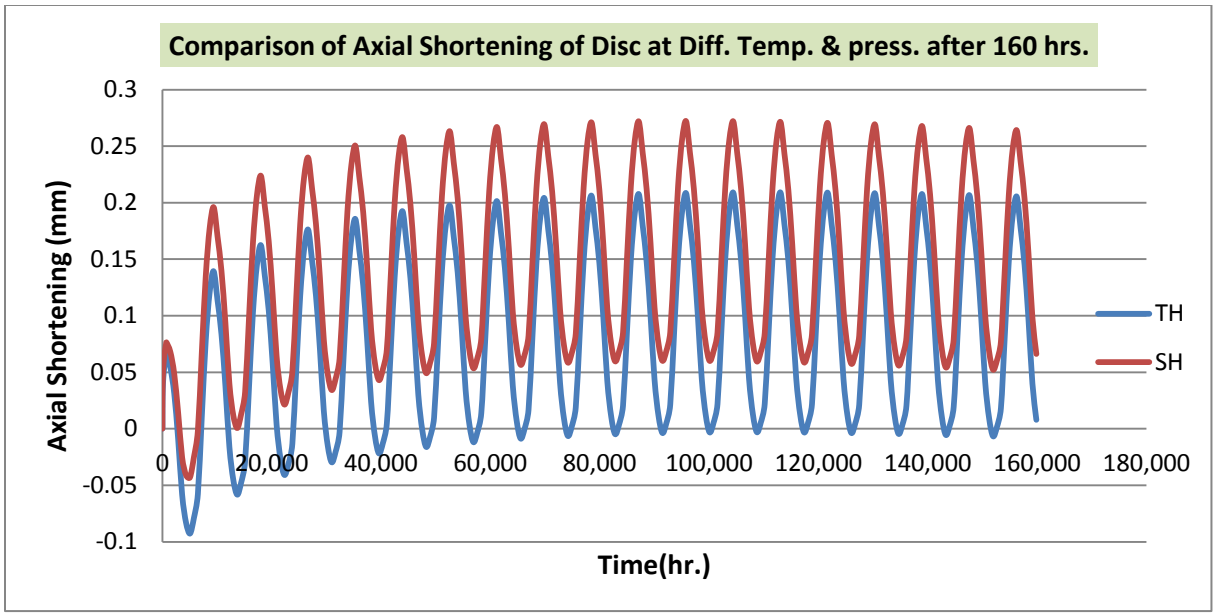

Fig. 5.39: Comparison of Axial Shortening of disc for Time Hardening and Strain Hardening model at variable ambient temperature and pressure

5.5 Summary on Creep Estimation of Disc

In this work, creep estimation results for disc presents below the combustion chamber region are presented. This disc location is chosen based on maximum temperature region. Initially benchmarking problem has been calculated for ease of understanding creep methodology. Only two dimensional analyses are performed in all cases to simplify modeling procedure. ANSYS APDL code has been developed to introduce temperature variations every month for almost twenty years, so that any user can understand every section of analysis with required dimensions. Pressure has also taken as variable during the analysis in every year. Two mathematical models have taken for the creep analysis; time hardening creep mathematical model and strain hardening creep mathematical model.

Firstly, thermal analysis has been done on disc according to the given data. This will give the nodal temperature at every node of disc. Creep material properties, loads and boundary conditions are applied along with the nodal temperature profile for structural analysis of disc. Stresses are calculated for both of the mathematical model. Creep strain in terms of axial shortening and radial elongation are calculated at constant ambient temperature and for different ambient conditions.

Here, no experimental data has been used to compare with ANSYS results because creep data is not available in research papers for long range of time. Hence to validate with previous research paper, localized creep strain is calculated at the top nodal point of disc for both of the mathematical models. The results have given a good agreement with the published paper [17] which states that equivalent creep strain results same for time hardening model as well as strain hardening model at constant stress. Here, constant ambient temperature is taken as 32^0C which is average temperature across the glove for hot ambient condition while for variable temperature; a data which vary at every month in a year has been taken from city Abu Halifa (Kuwait) for hot ambient condition. The average of variable temperature data gives 35^0C. So, creep graph at constant temperature did not pass through the mid-point of variable temperature curve as shown in fig. 5.17 and 5.18. Disc will distort in a cyclic manner because of cyclic temperature variation throughout the year. Due of these processes, shortening will occur in the axial direction of disc and it will lead to dynamic instability and clearance issue between rotor and stator part of GT. Hence, the simulation of axial shortening and radial elongation at 32^0C constant average

temperature will give less value but actually it would be higher in reality. During the analysis, it is also proved that strain hardening model gives over predicted result while time hardening model gives more constrained results at constant ambient temperature as well as at variable ambient conditions.

Chapter 6

Conclusions and Scope for Future Work

6.1 Conclusions

Present work focused on the creep estimation of gas turbine rotor discs using numerical technique. The following conclusions and recommendations are made from the present investigation.

1. Strain hardening and time hardening creep mathematical model give almost equal cumulative creep strain at same stress and temperature condition at same nodal point. Hence, ANSYS proves experimental result as well as theoretical calculations of several research papers.
2. Creep strains obtained from experimental data generally compare for less no. of hours because it is not possible to observe creep data for almost twenty years. In this case, numerical technique is coming out to be the best method to calculate creep data with good accuracy.
3. ANSYS APDL provides curve fitting to determine our creep material behavior i.e. extracting creep coefficients of different mathematical model from the experimental data. Thirteen creep models are available, along with the tools to generate and fit derived coefficients of experimental test data.
4. Creep deformation continues until the material fails because of creep rupture and there is a limited clearance between rotor part and casing. So, creep analysis is a must criterion in gas turbine rotor disc. It is found that axial shortening and redial elongation will be more at variable ambient conditions than at constant average temperature for the same creep mathematical model. Hence this condition will lead the rotor disc touch to the casing part which should be the limiting criteria in gas turbine rotor analysis.
5. Present study shows the difference with actual analysis results of Siemens Ltd. which considered constant average ambient temperature as 32^0C. If we talk about the actual data of temperature for hot ambient condition, it varies from place to place. The yearly average temperature of data taken is calculated as 35^0c for hot ambient condition which is

more than constant average temperature 32^0C. Hence, the simulation of axial shortening and radial elongation at 32^0C constant average temperature will give less value but actually it would be higher in reality.

6. Stresses produced in case of strain hardening model is more than time hardening model. Hoop stress is obtained as 496 MPa in strain hardening model while 462 MPa in case of time hardening model. This will give less value of axial and redial strain through strain hardening model. So time hardening model is more constrained to use creep strain than strain hardening analysis. These concepts are also stated in the related journals that strain hardening is considered to be more accurate while time hardening formulation is easier to use; strain hardening model follows the current stress and accumulated creep strain while time hardening model follows the current stress and on the time passed from the start of the test.
7. To find creep mathematical model coefficients, experimental data is needed and it consumes more time and cost. One can easily derive strain hardening coefficients analytically if time hardening coefficients are known.
8. Present study shows that strain hardening model can be used in analysis of gas turbine rotor disc because of the significant good changing in axial and radial strain. This analysis will give less component cost.
9. If someone wants to calculate creep life with Larsen Millar parameter, one has to consider creep property in analysis. Otherwise creep life will be calculated at less stress value which will give less creep strain.

6.2 Scope for Future Work

1. Temperature data for hot ambient condition during the creep analysis of GT rotor disc should be taken as variable since it gives over predicted results compare to data taken at constant average temperature.
2. Application of creep might offer an opportunity to extend the use of combined hardening mathematical model in analysis. Because, it includes primary zone as well as secondary zone. Results of strain hardening or time hardening can be compared with combined time hardening.

3. Validation of ANSYS creep estimation can be done with analytical solutions.
4. Time hardening model is easier to use while the strain hardening is considered to be more accurate. In this work, strain hardening creep mathematical model is used to calculate creep strain in gas turbine rotor disc analysis. This result can be taken as future reference.

References

1. ANSYS Mechanical APDL Technical Manual.
2. Ashby, M.F.," *A first report on deformation-mechanism maps.* Acta Metallurgica" (pre 1990), 1972.
3. Frost, H.J. and M.F. Ashby, "*A Second Report on Deformation-Mechanism Maps*", Division of Applied Physics, Harvard University, 1973.
4. Kraus, H.,"*Creep Analysis*", John Wiley & Sons, Inc., New York, N.Y, 1980.
5. Bailey, R.W. "*The utilization of creep test data in engineering de sign*", Proc. I. Mech. E.131, 1935, Norton bailey, in Robinson, D. N., Binienda, W. K., and Ruggles, M. B., 2003.
6. Finnie, I., Heller, W.R., "*Creep of engineering materials*", McGraw-Hill Book Co. Inc., New York, 1959.
7. http://www.ansys.com/Resource+Library/Demos/Creep+Curve+Fitting
8. Kelvin-Voigt creep model, cube.case.edu/ EMAC403/ EAMC403_ Mechanical% 20Models.pdf
9. J. Betten, "*Creep Mechanics"* Springer-Verlag, Berlin, 2005.
10. ''*Creep of polymer matrix composites. I: Norton/Bailey creep law for transverse isotropy*'' *J. Eng. Mech.*, 129, 3, 310–317,2003.
11. Norton, F.N., "*The Creep of Steel at High Temperature"*, McGraw-Hill, 1929.
12. Granacher, J., Möhlig, H., Schwienheer, M. & Berger, C., "*Creep equation for high temperature materials*", *Proc. 7th Intern. Conf. on Creep and Fatigue at Elevated Temperatures (Creep 7)*, 3-8/6/01, NRIM, Tsukuba, 2001.
13. Arya, V. K. and Bhatnagar, N. S., "*Creep analysis of rotating",*1979.
14. K. Gupta, M. R. Haider, "*Creep Life Estimation of Low Pressure Reaction Turbine Blade*" Institute of Engineering & Technology-DAVV, Indore, India.
15. Michael E. Kassner, Marı´a-Teresa Pe´rez-Prado "*Fundamentals of Creep in Metals and Alloys*" Department of Physical Metallurgy, Centro Nacional de Investigaciones Metalu´rgicas (CENIM), Madrid, Spain, 2004
16. C. Bailey, Y. D. Fryer, M. Cross, P. Chow, "*ÔPredicting the deformation of castings in moulds using a control*".
17. "*Primary Creep Under Non-constant Load*", Solved with COMSOL Multiphysics 4.3

18. Barindra Singh " *Creep Deformation and Stress Analysis in Rotating Disc of Composite Material*" Thapar University, India
19. "*Creep Behavior of the Inconel 718 Superalloy*", 10.4028/www.scientific.net/DDF.
20. Boris Vasilyev "*Prediction of the Kinetics of the 3D Stress-Strain State of High-Temperature Gas Turbine Blades with Limited Experimental Data*" Central Institute of Aviation Motors (CIAM), Moscow, Russia
21. S.A. Hosseini Kordkheili*, M. Livani "*Thermoelastic creep analysis of a functionally graded various thickness rotating disk with temperature-dependent material properties*" Center of Excellence in Aerospace Systems, Aerospace Engineering Department, Sharif University of Technology, Azadi Ave., Tehran, Iran
22. J. C Levy, I. I. Barodi *"A Comparative Study of Extrapolation Methods for Creep Data at Small Strains*" The City University, London.
23. A. S. Makunte, R. B. N "*Analysis of Turbine Disc for Creep Life*" International Journal of Mechanical Engg. And Robotic Researchs, India.
24. M. N. Faridani "*Classification and Probabilistic Model Development for Creep Failures of Structurs: Study of X-70 Carbon Steel and 7075-T6 Aluminum Alloys*", University of Maryland, 2012.
25. Fredrik Forsberg**, "***Probabilistic Assessment of Failure Risk in Gas Turbine Discs*" Linkoping University.
26. Anderade, E.N. Da.; *TheViscous flow in metals and allied phenomena,* Proc. Roy. Soc., 1914.
27. Prandtl, L.," *Proceedings of the first international conference on applied mechanics*", Delft, The Netherlands, p.43, 1924.
28. Norton, F.H., "*Creep of steel at high temperatures*", McGraw-Hill Book Co. Inc. 1929 Modified Norton model.
29. Weaver, S.H.,"*The creep curve and stability of steels at constant stress and temperature*", Transe. ASME,58, 745, 1936.
30. Soderberg**,** C.R., "*The interpretation of creep tests for machine design*", Trans. ASME,58, 735, 1936.
31. Nadai, A., "*The influence of time upon creep. The Hyperbolic Sine creep law*", Stephan Timoshenko Anniversary Volume, Macmillan Company, New York, 1938.

32. De Lacombe, J., "*A method of representing creep curves*", Rev. Metal. 36, 178.
33. Karen M. B. Taminger, "*Analysis of creep behavior and parametric models for 2124 AL and 2124 AL + SICW composite*", Virginia Polytechnic Institute, Virginia, 1999.
34. Orthotropic discs, "*Nuclear Engineering and Design*", Bhatnagar, N. S., and Arya, V. K. On the constitutive equations of the orthotropic theory of creep. Journal of Physical Society of Japan, 4.
35. E. Ashati, Abdullahi Abu, "*Investigation into the Effects of Operating Conditions and Design Parameters on the Creep Life of High Pressure Turbine Blades in a Stationary Gas Turbine Engine*" Cranfield University ,Cranfield, Bedford MK43 0AL, UK.
36. Eshati, S., Abdul Gha_r, F. M., Laskaridis, P. and Li, Y. G., "*Impact of Operating Conditions and Design Parameters on Gas Turbine Hot Section Creep Life*", Proceedings of ASME Turbo Expo 2010: Power for Land, Sea and Air, GT2010{ 22334, June 14{18, Glasgow, UK, 2010.
37. Guenette, G. R., Pappas, G. and Epstein, A. H., "*The Inuence of Non Uniform Spanwise Inlet Temperature on Turbine Rotor Heat Transfer*", AGARD Heat Transfer and Cooling in Gas Turbine, Antalya, Turkey, 1993.
38. O. C. Zienkiewicz,"T*he Finite Element Method"*, MacGraw Hill, London, 1977. F.R. Larson, J. Miller, Trans. ASME 74, 1952.
39. A.M. Wahl, "*Analysis of creep in rotating discs based on tresea criterion and associated flow rule*", *Jr. Appl. Mech*., 23, 1956.
40. S. Sharma, "*Elastic-plastic Transition of Non-Homogeneous Thick walled Circular Cylinder under internal Pressure*", Def. Sc. Journal, Vol. 54(2), 2004.
41. S.K. Gupta, Pankaj, "*Creep Transition in a Thin Rotating Disc with rigid inclusion*", Def. Sc. Journal, 57(2), 2007.
42. Sanjeev Sharma, "*Creep Transition in Non-homogeneous thick-walled rotating cylinder*", Accepted for Publication in Def. Sci. Journal.
43. *Gas Turbine World 2000-2001 Handbook* , Volume 21, Pequot Publication.
44. Sukhvindar Kaur Bhatti, Shyamala Kumari, M. L. Neelapu, C. Kedarinath, DR. I. N. Niranjan Kumar, "*Transient State Stress Analysis on an Axial Flow Gas Turbine Blade and Disc Using Finite Element Procedure*" Department of Mechanical & Marine Engineering, Andhra University, Visakhapatnam, AP, India.

45. Raghavendra N, Gurudath K P, Dr. Mallikarjunayya C. Math, Chandrashekhar B.,"*Analysis of Creep Life Prediction for Gas Turbine Disc*" Dept. Of Mechanical Engineering, College of BTLIT, Bangalore, India.
46. Mikhail Yakhnis and Robert Zhang "*Analysis of 2D Deformation and Creep Response of Articular Cartilage*".
47. Yang XU, Han YU, Zupei Shen, "*Creep Analysis of Aluminum Alloy Disk Experiment for High Speed Energy Storage Flywheel*" Tsinghua Univ. China.
48. Martin J. Dropik, David H. Johnson, P.E., David E. Roth, P.E. " *Developing an ANSYS Creep Model for Polypropylene from Experimental Data*" Penn State-Erie, Erie, PA, USA.
49. T. Sugahara1a, K. Martinolli1b, D.A.P. Reis1c, C. Moura Neto1d, A.A. Couto2e, F. Piorino Neto3f, M.J.R. Barboza3 "*Creep Behavior of the Inconel 718 Superalloy*"**,** Instituto Tecnológico de Aeronáutica, São José dos Campos-SP, Brazil.
50. N. Ogbonna, N. A. Fleck, A. C. F. Cocks, "*Transient Creep Analysis of Ball Indentation*" University Engg. Department, Cambridge, U.K. 1994.
51. www.ewp.rpi.edu/hartford/~ernesto/F2005/CINVESTAV/Notes/ch6.pdf
52. courses.washington.edu/me354a/chap8.pdf

Appendix

A.1 Different ANSYS Creep Mathematical Models

1	Strain Hardening	$\dot{\varepsilon}_{cr} = C_1\sigma^{C2}\varepsilon_{cr}^{C3}e^{-C4/T}$	$C_1>0$	Primary
2	Time Hardening	$\dot{\varepsilon}_{cr} = C_1\sigma^{C2}t^{C3}e^{-C4/T}$	$C_1>0$	Primary
3	Generalized Exponential	$\dot{\varepsilon}_{cr} = C_1\sigma^{C2}re^{-rt}$, $r = C_5\sigma^{C3}e^{-C4/T}$	$C_1>0$, $C_5>0$	Primary
4	Generalized Graham	$\dot{\varepsilon}_{cr} = C_1\sigma^{C2}(t^{C3} + C_4t^{C5} + C_6t^{C7})e^{-C8/T}$	$C_1>0$	Primary
5	Generalized Blackburn	$\dot{\varepsilon}_{cr} = f(1-e^{-rt}) + gt$ $f = C_1e^{C2\sigma}$, $r = C_3(\sigma/C_4)^{C5}$, $g = C_6e^{C7\sigma}$	$C_1>0$, $C_3>0$, $C_6>0$	Primary
6	Modified Time Hardening	$\varepsilon_{cr} = C_1\sigma^{C2}t^{C3+1}e^{-C4/T}/(C_3+1)$	$C_1>0$	Primary
7	Modified Strain Hardening	$\dot{\varepsilon}_{cr} = \{C_1\sigma^{C2}/[(C_3+1)\varepsilon_{cr}]^{C3}\}^{1/(C3+1)}e^{-C4/T}$	$C_1>0$	Primary
8	Generalized Garofalo	$\dot{\varepsilon}_{cr} = C_1[\sinh(C_2\sigma)]^{C3}e^{-C4/T}$	$C_1>0$	Secondary
9	Exponential form	$\dot{\varepsilon}_{cr} = C_1e^{\sigma/C2}e^{-C3/T}$	$C_1>0$	Secondary
10	Norton	$\dot{\varepsilon}_{cr} = C_1\sigma^{C2}e^{-C3/T}$	$C_1>0$	Secondary
11	Combined Time Hardening	$\varepsilon_{cr} = C_1\sigma^{C2}t^{C3+1}e^{-C4/T}/(C_3+1) + C_5\sigma^{C6}te^{-C7/T}$	$C_1>0$, $C_5>0$	Primary + Secondary
12	Rational polynomial	$\dot{\varepsilon}_{cr} = C_1\frac{\partial\varepsilon_c}{\partial t}$, $\varepsilon_c = \frac{cpt}{1+pt} + \dot{\varepsilon}_m t$ $\dot{\varepsilon}_m = C_2 10^{C9\sigma}\sigma^{C4}$ $c = C_7\dot{\varepsilon}_m^{C8}\sigma^{C9}$, $p = C_{10}\dot{\varepsilon}_m^{C11}\sigma^{C12}$	$C_2>0$	Primary + Secondary
13	Generalized Time Hardening	$\varepsilon_{cr} = f\,t^r\,e^{-C6/T}$ $f = C_1\sigma + C_2\sigma^2 + C_3\sigma^3$ $r = C_4 + C_5\sigma$		Primary
100	---	User Creep	---	---

A.2 Text File of Creep Experimental Results

A.2.1

```
/seqv,400
/temp,350
/1,creq
/2,dcreq
3.50E-14   3.1852E-15
6.29E-14   2.794E-15
8.69E-14   2.4008E-15
1.09E-13   2.1864E-15
1.29E-13   2.0296E-15
1.48E-13   1.9123E-15
1.66E-13   1.8205E-15
1.84E-13   1.7447E-15
2.01E-13   1.6812E-15
2.17E-13   1.6265E-15
2.48E-13   1.556E-15
2.78E-13   1.4809E-15
3.06E-13   1.4192E-15
3.33E-13   1.3675E-15
3.60E-13   1.323E-15
4.82E-13   1.2175E-15
5.38E-13   1.127E-15
5.92E-13   1.0801E-15
```

A.2.2

```
/seqv,400
/temp,400
/1,creq
/2,dcreq
1.80E-08   1.6594E-09
3.28E-08   1.47977E-09
4.57E-08   1.2965E-09
5.77E-08   1.19487E-09
6.89E-08   1.11969E-09
7.95E-08   1.06307E-09
8.97E-08   1.01834E-09
9.95E-08   9.8127E-10
1.09E-07   9.4996E-10
1.18E-07   9.229E-10
1.36E-07   8.879E-10
1.53E-07   8.503E-10
1.69E-07   8.1935E-10
1.85E-07   7.9315E-10
2.01E-07   7.706E-10
2.72E-07   7.1657E-10
3.06E-07   6.6978E-10
3.38E-07   6.4538E-10
```

A.2.3

```
/seqv,400
/temp,450
/1,creq
/2,dcreq
1.66E-05   1.49744E-06
2.96E-05   1.29557E-06
4.05E-05   1.09182E-06
5.03E-05   9.8063E-07
5.93E-05   8.9917E-07
6.77E-05   8.3826E-07
7.56E-05   7.9039E-07
8.31E-05   7.5092E-07
9.03E-05   7.177E-07
9.72E-05   6.8913E-07
1.10E-04   6.5221E-07
1.22E-04   6.1285E-07
1.34E-04   5.8045E-07
1.45E-04   5.5325E-07
1.56E-04   5.2985E-07
2.03E-04   4.7434E-07
2.24E-04   4.2668E-07
2.45E-04   4.0202E-07
```

A.2.4

```
/seqv,400
/temp,500
/1,creq
/2,dcreq
4.88E-04   3.85301E-05
7.89E-04   3.01342E-05
1.01E-03   2.25531E-05
1.20E-03   0.000018872
1.37E-03   0.000016381
1.51E-03   0.000014634
1.65E-03   0.000013328
1.77E-03   0.000012298
1.88E-03   0.000011461
1.99E-03   0.000010767
2.19E-03   0.000009902
2.37E-03   9.017E-06
2.54E-03   8.3205E-06
2.69E-03   7.756E-06
2.84E-03   7.2875E-06
3.46E-03   6.2362E-06
3.73E-03   5.3862E-06
3.98E-03   0.000004972
```

A.3 Calculation of Strain Hardening Creep Model Coefficients at Different Temperature

Power Law (Norton-Bailey Law)

$$\varepsilon_c = A\sigma^n t^m \quad \text{..... (1)}$$

If we solve this equation in rate form, we get

$$\dot{\varepsilon_c} = mA\sigma^n t^{m-1} \quad \text{..... (2)}$$

ANSYS Equation of Time Hardening Creep Mathematical Model

$$\dot{\varepsilon_c} = C_1\sigma^{C_2} t^{C_3} e^{-C_4/T}$$

Neglecting temperature dependency i.e. $C_4 = 0$,

$$\dot{\varepsilon_c} = C_1\sigma^{C_2} t^{C_3} \quad \text{..... (3)}$$

Equating equation (2) and (3), we get

$$m = 1 + C_3$$

$$n = C_2$$

$$A = \frac{C_1}{C_3 + 1}$$

Again from equation (1),

$$t = \frac{\varepsilon_c}{A\sigma^n}^{1/m}$$

So, equation (2) will become as,

$$\dot{\varepsilon_c} = mA\sigma^n \frac{\varepsilon_c^{\frac{1}{m}-1}}{A^{\frac{1}{m}-1}\sigma^{\frac{n}{m}-1}} = A^{1/m}\, m\sigma^{n/m}\varepsilon_c^{\,m-1/m}$$

Hence, the Time hardening creep coefficients can be changed into Strain hardening creep coefficients as follows as,

$$D_1 = A^{1/m}\, m = \left(\frac{C_1}{C_3+1}\right)^{1/C_3+1} (C_3+1)$$

$$D_2 = {}^{n}/_{m} = {}^{C_2}/_{C_3+1}$$

$$D_3 = \frac{m-1}{m} = \frac{C_3}{C_3+1}$$

Where ANSYS Equation of Strain Hardening Creep Mathematical Model represents as,

$$\dot{\varepsilon}_c = D_1 \sigma^{D_2} t^{D_3} e^{-D_4/T}$$